DISSERTATION

TRANSPORT VELOCITIES OF BEDLOAD PARTICLES IN ROUGH OPEN CHANNEL FLOWS

Submitted by

Bounthanh Bounvilay

Department of Civil Engineering

In partial fulfillment of the requirements

For the Degree of Doctor of Philosophy

Colorado State University

Fort Collins, Colorado

Spring 2003

ProQuest Information and Learning Company
300 North Zeeb Road
P.O. Box 1346
Ann Arbor, MI 48106-1346

COLORADO STATE UNIVERSITY

November 12, 2002

WE HEREBY RECOMMEND THAT THE DISSERTATION PREPARED UNDER OUR SUPERVISION BY **BOUNTHANH BOUNVILAY** ENTITLED **TRANSPORT VELOCITIES OF BEDLOAD PARTICLES IN ROUGH OPEN CHANNEL FLOWS** BE ACCEPTED AS FULFILLING IN PART REQUIREMENTS FOR THE DEGREE OF DOCTOR OF PHILOSOPHY

Committee on Graduate Work

Advisor

Department Head

ABSTRACT OF DISSERTATION

TRANSPORT VELOCITIES OF BEDLOAD PARTICLES IN ROUGH OPEN CHANNEL FLOWS

This dissertation aims at defining the bedload particle velocity in smooth and rough open channels as a function of the following variables: bed slope S_f, flow depth y, viscosity of the fluid ν, particle size d_s, bed roughness k_s, particle specific gravity G, and gravitational acceleration *g*.

Sets of aluminum plates were placed on the bottom of an experimental plexiglass-tilting flume, with trapezoidal cross-section, to form a smooth bed. A layer of sand or gravel was glued onto aluminum plates to form bed roughness. Bedload particles used in the experiments were stainless steel ball bearings, glass marbles, and natural quartz particles. The experiments were performed to provide 529 average bedload particle velocities. The analysis of the laboratory measurements showed that: (1) for a smooth bed ($k_s = 0$), the rolling bedload particle velocity V_p increases with particle sizes d_s; (2) for a rough bed ($k_s > 0$), particle velocity decreases with particle density G, thus lighter particles move faster than heavier ones; and on a very rough boundary V_p decreases with particle sizes; (3) bedload particles move at values of the Shields parameter $\tau_{*ds} = u_*^2/(G-1)gd_s$ below the critical Shields parameter value of $\tau_{*dsc} = 0.047$; (4) few of the observed particles moved at values of Shields roughness parameter $\tau_{*ks} = u_*^2/(G-1)gk_s$ less than 0.01; (5) particles are observed to move at values of the Shields roughness parameter 0.01

$< \tau_{*ks} < 0.15$; (6) the ratio of particle velocity V_p to mean flow velocity u_f lies in the range of 0.2 to 0.9, while Kalinske (1942) suggested 0.9 to 1.0; and (7) the ratio of particle velocity V_p to shear velocity u_* lies in the range of 2.5 to 12.5, compared to the values cited in the literature $6.0 < V_p/u_* < 14.3$.

New methods for predicting transport velocity of bedload particles in rough and smooth open channels are examined. Two approaches for transport velocities of bedload particles were considered. The first approach combines dimensional analysis and regression analysis to define bedload particle velocity as a power function of the Shields parameter τ_{*ds}, boundary relative roughness k_s/d_s, dimensionless particle diameter d_*, and excess specific gravity (G-1). The second approach considers the transport velocity of a single particle on a smooth bed. The reduction in particle velocity due to bed roughness is then examined through a theoretical and empirical analysis. Results show that the bedload particle velocity on smooth beds is approximately equal to the flow at the center of the particle; and the bed roughness gradually decreases the transport velocity of the rolling bedload particles. Comparatively, The first approach gives satisfactory results, except when k_s equals 0, then V_p goes to ∞; and when k_s is large, V_p does not stop (unbounded); for the second approach $V_p = V_{pmax}$ when k_s equals 0, and when V_p equals 0 (no motion), then k_s follows the criteria a and b described in Chapter 5 (section 5.4).

The analysis shows that the proposed formula, Eq. (5.34) provides much better predictions than the existing formulas. The discrepancy ratio distributions using Eq. (5.34) are normally distributed and have higher density (close to perfect agreement) than all other formulas. In addition, the proposed formula, Eq. (5.34) is also verified with the

devastating flood of the Avila Mountain in Venezuela in December 1999. The results give realistic estimates of particle velocities.

Bounthanh Bounvilay
Civil Engineering Department
Colorado State University
Fort Collins, CO 80523
Spring 2003

ACKNOWLEDGMENTS

I would like to express my gratitude to Prof. Pierre Y. Julien, for his inspiration, guidance, encouragement, friendship and financial support during the course of this work. Working with him has been a rewarding and enjoyable experience.

I also wish to express my appreciation to the members of my committee, Prof. Maurice L. Albertson, Dr. Deborah J. Anthony, Dr. Brian P. Bledsoe, and Dr. Daniel Gessler, for their valuable comments and review of this dissertation.

Special appreciation is extended to H.E. Mr. P. Leuangkhamma, Dr. S. Mangnomek (MOE), Duane Smith, Dr. R. Thaemert, Dr. M. Giger, Dr. H. Coowar, Prof. C. Loukides for their help and encouragement. Also, a great deal of thanks is due to Prof. R. Kersten, Dr. M. Chopra, Dr. N. D. Hoan, Dr. F. Nnadi, D. Mowry (UCF), Prof. P. K. Nam, Prof. N. D. Lieu (DHTL), Dr. R. Simmons, Nurse Sharon (Center for Gastroenterology), Dr. R. Risma (HHS), M. Hallett (ISS), L. Howard (CE), Dr. K. Bunte, Dr. J. Guo, M. Casey, R. Rojas, C. Leon (ERC), R. Slosson, P. Schei, D. Marsh, T. Tochtrop, K. Flowers (Smith Geotechnical), T. Pong, K. Phanouvong, S. Akalin, H. Hussain, J. Noh for their encouragement and friendship.

Finally, my deepest gratitude goes to my parents, my brothers and sisters, Khone-Lien, Bi-Ngan, Que-Teo, Noi, Sone, Minh-Nang, Bou, chi Lann, chi Noi, chi Binh (Bouavanh) my aunts and uncles mo Phu, di Duc, cau Be, mo Gai, di Nho, duong Thiene, cau Gai, mo Be, di Hone, duong Duong, bac Bay, bac Tu, bac Nghia, co Ly, co Huong, co Ngoc, co Nga, di Meo, Ama (Pakse), co Phuong, bac Dong, bac Phuong, co The, chu

Ly, bac Quy, anh Ngoc (Hanoi), co Lan, co Quy (BL), my nieces and nephews, Ni, Na, Nu, Piu, Sam, Ky, Kay, Big, Be, Cho, and my friends Hoa (Pakse) and Ha (Hanoi) for their continual support and encouragement throughout this research.

To my Grant parents, Parents, Brothers and Sisters,
Nieces and Nephews, and aunt Hoang Thi Duc

TABLE OF CONTENTS

LIST OF FIGURES

LIST OF TABLES

LIST OF SYMBOLS

Symbol	Description
A	area of the stream cross-section (m^2), $A = ½ (T_w + B_w)y$;
b	constant parameter;
B_w	width of the plate, which also defined the bottom width of the channel (mm);
c	constant parameter;
c_c	$\rho/4\mu$ (s/m^2);
C_D	drag coefficient;
C_L	lift coefficient;
c_a, c_b, c_d, c_e	constant parameters;
c_α	proportionality constant;
c_μ	sliding friction coefficient;
d_s	diameter of the rolling particles (mm);
d_*	dimensionless particle diameter, $d_* = d_s\left[\frac{(G-1)g}{\nu^2}\right]^{1/3}$;
f	collision coefficient;
F_D	drag force;
F_L	lift force;
F_f	friction force;
F_N	support force of the plane;
Fr	Froude number;
g	gravitational acceleration (m/s^2);

G specific gravity of the particles;

H energy grade line elevation (m) at the two point gages;

$H_{u.s.} = y_{u.s.} + (S_o \Delta X) + (V_{u.s.})^2/2g$;

$H_{d.s.} = y_{u.s.} + (V_{u.s.})^2/2g$;

k_s bed roughness, average diameter of the particles of gravel glued to the plates (see Table 3.1), in mm;

m constant parameter;

m_μ static friction coefficient;

n number of trials for each particle (between 15 and 21 trials per particle type and size);

n_a $(0.014 k_s/u_*)^{0.26}$;

n_μ bulk friction coefficient;

P wetted perimeter of the stream cross-section (mm);

$$P = B_w + 2\sqrt{y^2 + \left(\tfrac{1}{2}(T_w - B_w)\right)^2};$$

Q flow rate in liters/s, $Q = 6.45632$ (manometer reading / 12)$^{0.503}$;

Re Reynolds number;

Re_* Shear Reynolds number;

R_h hydraulic radius of the stream cross-section (m), $R_h = A/P$;

R_i discrepancy ratio (%);

S_f friction slope $\Delta H / \Delta X$;

S_o bed slope (m/m);

T_{avg} average water temperature in ^oC (measured at start and end of each run);

T_w top width of the channel (mm); measured at each point gage along the flume;

u_c critical velocity (m/s);

u_f average stream flow velocity (m/s); $u_f = Q/A$;

u_1 flow velocity at the height of the particle center (m/s);

u_{1c} critical velocity at the threshold motion (m/s);

u_* Shear velocity (m/s), $u_* = \sqrt{gR_hS_f}$;

u_{*c} critical shear velocity (m/s);

V_p average velocity over n trials for each particle (mm/s);

w settling velocity of the rolling particles (m/s);

W_s submerged weight of the sphere;

y flow depth in mm (measured at three location with point gages);

y/k_s relative submergence, ratio of average stream depth to bed roughness;

ΔX distance between two point gages in the test section (1.62 m);

ΔH energy loss or head loss (m) between the two point gages; $H_{u.s}-H_{d.s.}$;

ν kinematic viscosity in mm^2/s or $m^2/s \times 10^{-6}$;

$\nu = 0.0003625\ (T_{avg})^2 - 0.038775\ (T_{avg}) + 1.6345$;

δ laminar sub-layer thickness (m), $\delta = 11.6\frac{\nu}{u_*}\times 10^{-6}$ if ν in mm^2/s;

σ standard deviation of particle velocities (m/s);

ΔB roughness function;

ΔB_c	calculated rough ness function;
τ	mean bed shear stress (kg/m^2);
τ_c	shear stress at threshold of motion (kg/m^2);
τ_{oc}	critical bed shear stress required for the particle to roll (kg/m^2);
τ_{*ds}	Shields parameter;
τ_{*ks}	Shields roughness parameter;
ρ_s	particle density (kg-sec^2/m^4);
ρ_f	fluid density (kg-sec^2/m^4);
θ	bed slope angle;
μ	dynamic viscosity of water (kg-sec/m^2);
ν	kinematic viscosity (m^2/s);
τ_o	bed shear stress (kg/m^2);
$\tan\alpha$	dynamic friction coefficient;
α, β, χ	particle velocity coefficients;
Pump setting	for major adjustment of the flow (slow, medium, fast);
Valve setting	for fine adjustment of the flow;
Reach length	length of test section (2000 mm);
Slope reading	reading of vertical displacement (mm) for a ruler attached to the flume near the upstream end, the ruler is 7145 mm upstream of the pivot point of at flume support;
Manometer readings	manometer height in inches of water to compute flow rates;
u.s.	upstream -- generally refer to the position of the upstream point gage in the test section;

d.s.	downstream – generally refer to the position of the downstream point gage in the test section;
$V_{u.s.}$	average flow velocity at the upstream point gage;
$V_{d.s.}$	average flow velocity at the downstream point gage;

CHAPTER 1

INTRODUCTION

1.1. PROBLEM STATEMENT

The study of rolling bedload particle velocity in rough open channel flows is a basic subject in the field of river mechanics and sediment transport. This study aims at the determination of the velocity of rolling bedload particles in rough open channel flows.

1.2. BACKGROUND

Three major approaches for the study of bedload transport are often found in the literature: (1) deterministic approach; (2) empirical approach; and (3) statistical-mechanical approach. The deterministic approach, which is based on some physical laws, studies the relation between bedload transport rates and the corresponding stream power, flow momentum, or other flow properties. The results are expressed in terms of average

flow conditions. A representative of this type of work is the Bagnold stream power function (Chien and Wan, 1983). The empirical approach relates measured bedload rates with their corresponding flow conditions. The results of many observations provide the basis for engineering applications, but sometimes give conflicting estimates when applied to rivers. The statistical-mechanical approach proposed by Einstein (1950), is a combination of the above two approaches. It considers both flow stochastic and deterministic properties of particle motion. The Einstein bedload function (Einstein 1950) shows that individual particle mechanics is one important aspect in this type of approach. Since bedload particle movement can be divided into rolling, sliding and saltation, this proposed research concentrates on the rolling motion, i.e., the motion of a single particle rolling over a rough open channel bed. The primary interest of this research has been to quantitatively examine the velocity of individual particles moving as rolling bedload on rough beds.

1.3. OBJECTIVES

The specific objectives address in this study are: (1) to compile a large database including observed bedload particle velocity measurements on smooth and rough beds; (2) to analyze the database using existing bedload particle velocity formulas; (3) to develop new functions that computes bedload particle velocity in rough open channel flows using dimensional and regression analysis, and theoretical analysis; (4) to determine threshold conditions; and (5) to test the new functions with laboratory measurements and select the best function for field applications representative of very large floods.

1.4. METHODS

To achieve the objective, an extensive compilation of existing laboratory measurements at CSU and other laboratory data from literature has been done. The theoretical and empirical analyses have been studied, and new theoretical and empirical equations were developed and tested with a database including data from Meland and Norrman (1966), Fernandez Luque and van Beek (1976), Steidtmann (1982), Bridge and Dominic (1984), CSU (1995), and Bigillon (2001).

1.5. OUTLINE

This dissertation includes 7 chapters. Chapter 1 briefly introduces the subject and states the objective. Chapter 2 includes a literature review, presented as a highlight of a few of the major papers written on the particle velocity approximations. Chapter 3 describes the CSU experimental set-up and data analysis. Chapter 4 provides a dimensional and regression analyses and testing of empirical formulas. Chapter 5 describes the theoretical development leading to a particle velocity formula. Chapter 6 describes laboratory and field applications of the proposed formulas. Finally, Chapter 7 summarizes the main results of this research.

CHAPTER 2

LITERATURE REVIEW

The purpose of this chapter is to review the pertinent information available from experimental studies on this subject. This material is presented as a highlight of a few of the major papers written on the bedload particle velocity on smooth and rough beds.

2.1. EARLIER STUDIES

Krumbein (1942) studied the effect of particle shape on sediment transportation with experiments conducted in flumes. Krumbein related the observed behavior to the settling velocities of particles. His experiments were confined to the bed movement of single particles of different shapes, over a hydraulically smooth bed, for turbulent flow conditions. Through dimensional analysis, Krumbein determined a relationship between sphericity and the ratio of particle velocity to mean flow velocity, V_p / u_f, as a function

of the Froude number. Krumbein noticed that the curves followed an exponential type of equation, and proposed:

$$\frac{V_p}{u_f} = \left(\frac{V_p}{u_f}\right)_0 \left(1 - \exp(-bFr)\right) \tag{2.1}$$

where: V_p = particle velocity (m/s); u_f = mean flow velocity (m/s); b = constant; Fr = Froude number. In a discussion of Krumbein's paper, Kalinske (1942) noted that all of Krumbein's experiments were made at a constant flow depth of 131 mm, which allowed the Froude number to be written as a function of mean flow velocity:

$$Fr = \frac{u_f}{\sqrt{9.81 \times 0.131}} = 0.88 u_f$$

For the case of spheres, Eq. (2.1) can then be written as:

$$\frac{V_p}{u_f} = 0.88\left[1 - \exp(-1.85 u_f)\right] \tag{2.2}$$

Therefore, Krumbein's equation is not more than a plot of V_p / u_f vs. u_f. He did not make any attempts either to correlate against variables other than Fr, or to find a physical basis for his empirical equation. Moreover, the nominal diameter of all particles tested was kept constant, so that size effects were not taken into account. Finally, even though the flow was turbulent, all of Krumbein's experiments were done over a smooth bed, and therefore have less applicability to real world situations.

Kalinske (1942) reported that the Froude number Fr has no physical significance in regard to the movement of particles on the bed. Kalinske proposed that the particle

velocity V_p should be equal, or at least proportional to $u'-u_c$. where: u' = the velocity of the fluid acting on the particle (m/s); u_c = critical velocity for that particle. As u' is proportional to u_f, Kalinske obtained the following expression

$$V_p = c_a\left(u_f - u_c\right) \tag{2.3}$$

where: c_a = constant; u_f = mean flow velocity (m/s); V_p = particle velocity (m/s); u_c = critical velocity (m/s). Kalinske applied his model to Krumbein's data and found the best agreement for $0.9 < c_a < 1.0$. No mention is made regarding how to obtain the critical velocity for a given particle.

Ippen and Verma (1955) analyzed the motion of small spheres over beds of different roughness in flume experiments, for turbulent flow conditions. Upon plotting the ratio u_f / V_p against the Reynolds number, Re, they found that after a transition of variable length (proportional to grain density), u_f / V_p reached an ultimate value that remained constant over a wide range of Re and that the particle velocity increased directly with size, and attributed this to the fact that larger particles protrude into higher velocities than smaller ones. Assuming that the nearly constant ratio u_f / V_p is governed by the following variables: (G -1), k_s / d_s, and $1/S$, they obtained the following equation as a best fit to the data:

$$\frac{u_f}{V_p} = 1 + \frac{1}{12}(G-1)\left(\frac{k_s}{d_s}\right)\left(\frac{1}{\sqrt{S}}\right) \tag{2.4}$$

where: G = the specific gravity of grains; d_s = particle size (mm); k_s = roughness size (mm); S = energy grade line; Eq. (2.4) is explicitly dependent on the particle size, and shows an increase in particle velocity with size. From the definition of shear velocity u_* and mean bed shear stress τ_o:

$$u_* = \sqrt{\frac{\tau_o}{\rho}} \tag{2.5}$$

$$\tau_o = \gamma h S \tag{2.6}$$

one can obtain:

$$S = \frac{u_*^2}{gh} \tag{2.7}$$

and replacing Eq. (2.7) into Eq. (2.4) leads to:

$$\frac{u_f}{V_p} = 1 + c_b \left(\frac{k_s}{d_s}\right)\left(\frac{1}{u_*}\right) \tag{2.8}$$

where: $c_b = \frac{1}{12}(G-1)\sqrt{gh}$, a constant for a given flow depth and grain material (m/s); u_* = shear velocity (m/s); V_p = particle velocity (m/s); u_f = mean flow velocity (m/s); Eq. (2.8) clearly shows that particle velocity is directly related to both particle size and shear velocity, while inversely related to roughness size.

Meland and Norrman (1966) represent the most complete up-to-date approach to generate information about single grain transport velocities. Most recent theoretical papers on sediment transport rates rely heavily on Meland and Norrman for data in order

to validate their models. Meland and Norrman investigated the interactive effects of water velocity, bed roughness, and particle size on the transport rate of single particles over rough beds by turbulent flows, keeping particle shape, density and bed packing constant. Meland and Norrman used glass beads only, rolling on top of a bed made from the same beads. Upon analyzing their results, in which particle velocity is plotted against particle size for different values of shear velocity, it can be clearly seen that, for a given bed roughness and shear velocity, larger particles move faster than smaller ones, as concluded by Ippen and Verma (1955). Meland and Norrman give two main reasons for this behavior: First, larger particles ride higher off the bed, being thus exposed to the greater velocities; and second, the rolling resistance decreases when the ratio of particle size to roughness size is increased. They also found that the influence of size upon transport velocity decreases with increasing shear velocity and with decreasing bed roughness size. In other words, at high shear velocities and small bed roughness, the particle velocity tends to be constant with size.

$$\frac{V_p}{k_s^{\,m}} = a_m u_* \frac{d_s^{\,n_a}}{k_s} - b_m \tag{2.9}$$

where: u_* = shear velocity (m/s); V_p = particle velocity (m/s); k_s = roughness size (mm); $m = 0.75$; $n_a = \left(\frac{0.014 k_s}{u_*}\right)^{0.26}$; a_m = 7.05; and b_m = 5.1. This empirical equation applies only to Meland and Norrman's experiments; the constants appearing in the equation are of no particular importance. V_p is directly related to u_* and d_s, and inversely related to k_s. In other words, V_p is directly related to the ratio k_s / d_s of particle size, i.e., larger particles roll easier than smaller ones over a given bed, or a given particle rolls more

easily over a smooth than a rough bed. They also observed that transport velocities were lower on beds of loosely packed glass beads than in corresponding fixed, solid beds. This effect was most noticeable at high transport stages, and decreased, or was even reversed for low shear velocities. Eq. (2.9) gives a better results when applied the constants $a_m = 4$, and $b_m = 5.8$ (see Figs. 2.1 and 2.2).

Parson (1972) reported measurements on the rates of travel of several sizes of sand grains and glass beads in laminar sheet flow (i.e., overland flow) at different discharges and slopes, over a smooth bed. Parson found that particles moving in contact with the bed (i.e., rolling and sliding motion) travel at speeds approximately one-half the velocity of water in unobstructed flow, at a distance from the bed equal to the radius of a sphere of equal volume. For some tests with a large number of grains thrown at the same time, Parson overlooked a significant difference in speed. For glass beads, he found good agreement with the following equation:

$$V_p = \frac{\tau_o d_s}{4\mu}\left(1 - \frac{\tau_{oc}}{\tau_o}\right) \tag{2.10}$$

where: V_p = particle velocity (m/s); μ = fluid dynamic viscosity (kg-s/m^2); d_s = grain diameter (mm); τ_o = bed shear stress (kg/m^2); τ_{oc} = critical bed shear stress required for the glass beads to roll (kg/m^2). Using Eq. (2.5), one can express τ_o and τ_{oc} as:

$$\tau_o = \rho u_*^2 \tag{2.11}$$

$$\tau_{oc} = \rho u_{*_c}^2 \tag{2.12}$$

replacing (2.11) and (2.12) into Eq. (2.10), and defining $c_c = \frac{\rho}{4\mu}$ (s/m^2), results in:

$$V_p = c_c d_s \left(u_*^2 - u_{*c}^2\right) \tag{2.13}$$

where: u_* = shear velocity (m/s); u_{*c} = critical velocity (m/s). Eq. (2.13) not only shows that V_p depends directly on d_s, but also that V_p is proportional to the difference between a velocity and a critical velocity. In this case, it is shear velocity squared.

Ikeda (1971) made a theoretical analysis of the mechanics of the motion of a single spherical grain rolling on the bed, by considering the four main forces acting on the particle: drag, lift, gravity and friction with the bed. The resulting equation is as follows:

$$\frac{V_p}{u_*} = \frac{u_f}{u_*} - \left[\frac{4}{3} c_\mu \frac{(G-1)}{\left(c_\mu C_L + C_D\right)} \frac{g d_s}{u_*^2}\right]^{1/2} \tag{2.14}$$

where: V_p = particle velocity (m/s); u_* = shear velocity (m/s); u_f = fluid velocity at the center of the spherical grain (m/s); c_μ = sliding friction coefficient; G = particle specific gravity; g = gravitational acceleration (m/s^2); C_D and C_L = the drag and lift coefficients respectively; However, Ikeda did not give a method to specify the values of c_μ, C_D and C_L, which makes this formula inapplicable in practice. Besides, Ikeda assumed that the particle velocity is always behind the fluid velocity. This is not true for the case of steep slopes at very low fluid velocities.

Francis (1973) studied the motion of solitary grains along the bed of a flume. Francis' investigation was limited to particles moving over a fixed-plane bed made out of particles of the same type as those being transported, and he did not consider the effects

of grain size relative to roughness size. Francis found a satisfactory correlation between V_p (m/s) and the particle settling velocity, w (m/s). He also found a considerable difference in V_p for grains of different shapes. Specifically, he concluded that rounded particles always roll faster than angular ones.

The effect of grain size on V_p was always accounted for by using the regression with w, but shape effects could not be reduced. Francis performed the experiments with spherical particles traveling over a bed consisting of cylinders of the same diameter as the grains laid perpendicular to the flow. In this case, spherical particles traveled faster than any natural grains. Finally, he observed marked grains moving in the company of many other grains, in order to test the applicability of results derived from single grain experiments. In this case, speed was reduced 5% on average below that corresponding to solitary grains. This effect was most noticeable for low transport stages, and disappeared altogether for very high shear velocities.

Fernandez Luque and van Beek (1976) used a different approach than the one in previous studies, by using a loose bed for all of their experiments. They measured particle velocities as a function of bed shear stress in a closed-flow rectangular flume. The measured grains were scoured from the bed and then rolled on top of it. The average transport velocity of particles, which were saltating, or even in suspension, for most of the time was found to be equal to the average fluid velocity for turbulent flow without bed load at about three particle diameters above the bed surface minus a constant proportional to u_{*_c}, as shown below:

$$V_p = c\left(u_* - 0.7u_{*_c}\right) \tag{2.15}$$

where: u_{*_c} = critical shear velocity at Shields condition for entrainment (m/s); V_p = particle velocity (m/s); u_* = shear velocity (m/s) and c = constant (11.5). Eq. (2.15) is valid over a wide range of slopes. The form of this equation is quite misleading, since it seems that V_p will decrease with size (because u_{*_c} is higher for larger particles), but this is not the case because the points through which the equation was plotted correspond to all different experiments. Thus, in Eq. (2.15), u_* is also a function of size; because in experiments with larger particles, larger shear velocities were required not only to entrain grains, but also to keep them moving. As in Francis (1973), the particles were rolling on top of a bed made from the same material, so that the effect of size cannot be described.

Romanovskiy (1977) not only shows his own experimental results, but he also discusses previous approaches to the problem of modeling grain transport velocity. In particular, he presents Goncharov's (1938) empirical equation:

$$V_p = u_1 - u_{1c} \tag{2.16}$$

where: V_p = particle velocity (m/s); u_1 = flow velocity at the height of the particle center (m/s); u_{1c} = critical value at the threshold of motion (m/s). Assuming a logarithmic velocity profile, it is possible to relate u_1 to the mean flow velocity, u_f, through a constant, so that one obtains:

$$V_p = c_a\left(u_f - u_c\right) \tag{2.17}$$

where: c_a = constant; u_f = mean flow velocity (m/s); u_c = critical velocity (m/s). This is identical to Kalinske' Eq. (2.3). One considers the shear velocity as:

$$u_* = \sqrt{\frac{f}{8}} u_f \tag{2.18}$$

where: f = Darcy-Weisbach coefficient; u_* = shear velocity (m/s); we can write Eqs. (2.3) and (2.17) in terms of shear velocities:

$$V_p = c(u_* - u_{*_c}) \tag{2.19}$$

where: $c = (f/8)^{1/2}$, which is assumed constant; u_{*_c} = critical shear velocity (m/s). The later equation is quite similar to the form of Fernandez Luque and van Beek's (1976) Eq. (2.15). Romanovskiy (1977) made a simplified analysis of the forces acting on a rolling grain and proposed:

$$V_p = c_e \left(u_f - u_c \sqrt{\frac{\tan\alpha}{m_\mu}} \right) \tag{2.20}$$

where: $\tan\alpha$= dynamic friction coefficient; m_μ = static friction coefficient; u_f = mean flow velocity (m/s); c_e = constant; u_c = critical velocity (m/s). For a particle at repose, $\tan\alpha = m_\mu$; and if u_f is allowed to increase slowly from zero, at a certain velocity $u_f = u_c$, the particle will be entrained. From his experimental work he concluded that the form of Eq. (2.20) adequately represents the data.

Abbott and Francis (1977) continued the investigations reported by Francis (1973). More experiments were carried out and the following equation was found to represent all data sets with very low scatter:

$$V_p = c(u_* - u_{*_c}) \tag{2.21}$$

where: u_* = shear velocity (m/s); u_{*_c} = critical shear velocity (m/s); and c = constant parameter ($13.5 < c < 14.5$); A particle riding on top of the bed has a far lower threshold of motion than one nested into it. Abbott and Francis obtained u_{*_c}, based on actual measurements of overriding grains. Thus, instead of using Shields' criterion, the critical shear velocity was derived assuming a Shields parameter value of $\theta_o = 0.02$.

Bridge and Dominic (1984) made an extensive analysis of bed load grain transport velocity data in order to calibrate their proposed physically based model to estimate sediment transport rates. On theoretical grounds they showed that:

$$V_p = c(u_* - u_{*_c}) \tag{2.22}$$

where: $cu_{*_c} = w\sqrt{\tan\alpha}$; w = the settling velocity of particles (m/s); $\tan\alpha$ = dynamic friction coefficient; $6 < c < 14.3$; u_* = shear velocity (m/s); u_{*_c} = critical shear velocity (m/s); Application of this model to the existing data sets on single grain transport velocities yielded good results.

Wiberg and Smith (1987) developed an expression for the critical shear stress in non-cohesive sediment derived from the balance of forces on individual particles at the surface of a bed. The resulting equation, for a given grain size and density, depends on near bed drag force, the lift force to drag force ratio, and the particle angle of repose. Calculated values of the critical shear stress for uniformly sized sediment correspond closely to those determined from Shields' diagram. The initial motion problem for mixed grain sizes additionally depends on the relative protrusion of the grains into the flow and the particle angle of repose. The latter decreases when the diameter of a moving grain, d_s,

is larger than the length scale of the bed roughness, k_s $(d_s / k_s > 1)$, and increases when $d_s / k_s < 1$, producing a corresponding decrease or increase in critical shear stress. Using the Miller and Byrne (1966) experimental relationship between d_s / k_s, and particle angle of repose, which is consistent with Shields' definition of initial motion, Wiberg and Smith obtain results that are in good agreement with the available experimental critical shear stress data for heterogeneous beds. Wiberg and Smith used a physically based model of bedload sediment transport and data sets from Francis (1973), Fernandez Luque and van Beek (1976) and Abbott and Francis (1977) to derive the semi-empirical equation:

$$\frac{V_p}{u_*} = 4.2 \frac{\left[\frac{(\tau - \tau_c)}{\tau_c}\right]^{1/2}}{\left(\frac{\tau}{\tau_c}\right)} + 2.4 \qquad (2.23)$$

where: τ = mean bed shear stress (kg/m^2); τ_c = shear stress at threshold of motion (kg/m^2); V_p = particle velocity (m/s); and u_* = shear velocity (m/s).

Jan (1992) addressed the relative contribution of the stresses developed in granular fluid flows (viscosity, collision and friction stresses). Jan determined how much each of the examined stresses contributed to the total stress acting on a rolling sphere. Experiments were conducted for the steady movement of a sphere rolling down smooth and rough inclines in air, water and salad oil. An equation was derived expressing the velocity of a sphere rolling down a roughened incline without acceleration or deceleration based on the principle of conservation of momentum. Jan 's average terminal velocity V_p was derived as the following:

$$V_p = \sqrt{\frac{(\rho_s - \rho_f) g d_s (\sin\theta - n_\mu \cos\theta)}{f_c \rho_s + \frac{3}{4} C_D \rho_f}} \tag{2.24}$$

where: ρ_s, ρ_f = particle and fluid densities (kg-s^2/m^4); C_D = drag coefficient; θ= bed slope angle; d_s = particle diameter (mm); g = gravitational acceleration (m/s^2); f_c = collision coefficient (0.667); and n_μ = bulk friction coefficient (0.13). Both f and n_μ were determined via regression analysis using experiment data. Jan' experiments were performed for situations where the tested particle was identical to those comprising the roughness over which it rolled. Roughness particles were tightly spaced in a single layer on a smooth wooden bed of a tilting flume. Several conclusions were made as a result of the experiments and analysis. First, velocity is independent of rolling particle density. Second, collision stresses increase with increased bed inclination. Third, side wall friction from particles interacting with the side boundaries of the flume is negligible.

Meier (1995) completed the literature review on the existing formulas of transport velocity, in which he analyzed seventeen equations. Most of the equations can be written in the following form:

$$V_p = c_\alpha (u_* - u_{*c}) \tag{2.25}$$

where: V_p = particle velocity (m/s); u_* = shear velocity (m/s); u_{*c} = critical shear velocity (m/s); and c_α = proportionality constant. The differences between various investigators is how they correlate c_α and u_{*c} with the flow parameters. A shortcoming of this type of equation is that it does not apply for a steep bed slope.

Steidtmann (1982) conducted an experiment to assess the effects of size and density, with sand-size spheres of two densities being transported and deposited under controlled flume conditions. Observations on the motion of discrete particles show that grains smaller than bed roughness grains move continuously and have the same transport velocities regardless of density. For grains near and slightly larger than the roughness, movement is intermittent; and, for a given size, heavy particles move more slowly than light particles. For grains much larger than bed roughness grains, movement is continuous over the rough surface, and light and heavy grains have nearly the same transport velocities. Steidtmann's analysis of bulk sediment deposited from plane-bed transport, show that the size and proportion of heavy grains decrease and that of light grains increase with distance transported. For ripple bed transport, the size relations between associated light and heavy grains remains essentially unchanged with transport distance and the proportion of light and heavy grains is extremely variable. The results suggest that size-density sorting in plane-bed transport is a function of the transportability identified in the discrete grain studies but that sorting in ripple-bed transport is related to deposition on, and recycling through, the bed forms.

Bigillon (2001) conducted an experiment in a tilted, narrow, glass-sided channel, 2m in length and 20 cm in height. The channel inclination ranged from 0° to 12°. Two types of spherical particles were used in the experiments: glass beads and steel beads, the particle density was 2500 and 7750 kg/m^3 respectively. The water supply at the channel entrance was controlled by an electromagnetic flow meter provided by Krohne (France). The flow depth was a few particle diameters. Most of the time, channel slope was in excess of 1°, the water flow regime was supercritical, that is the Froude number exceeded

unity. The channel bed was made up of regularly juxtaposed half-cylinders of equal size. Bigillon selected three sizes of cylinder: their radius are 1.5 mm, 3 mm, and 4 mm. The motion of mobile beads was recorded using the Pulnix camera. A single particle was dropped from above into the water stream 1 m upstream from the measuring window. Bigillon filmed the motion of the particle with the Pulnix camera. For each flow condition (u_f,θ), the variability of the results was evaluated by repeating the run between three and five times, and only the average value was reported. The standard deviation was low relative to the mean (less than 5%) when the particle rolled. Bigillon noted that, these mean velocities cannot be rigorously assimilated to asymptotic velocities V_p, they provide a reasonable approximation of V_p. Fifty experimental data points were collected and the variability for hydraulic and particle parameters include: the range of shear velocity $u_* = 0.018\text{-}0.038$ m/s, $T_{water} = 20°C$, $\nu_{water} = 1.004\times10^{-6}$ m^2/s, particle diameter d_s = 1.5 mm and 3 mm, G = 2.5 (glass bead) and 7.75 (steel bead), k_s = 1.5 mm and 3 mm, bed slope $S_f = 0.02$ and 0.05, mean flow velocity $u_f = 0.223\text{-}0.492$ m/s, flow depth y = 2.13-28.65 mm, and observed bedload particle velocity $V_{pobs} = 0.076\text{-}0.496$ m/s.

2.2. DATA COMPILATION

A complete set of the experimental and data measurements is provided in Chapter 3. It includes the laboratory data of Meland and Norrman (1966), Fernandez Luque and van Beek (1976), Steidtmann (1982), Bridge and Dominic (1984), CSU (1995), and Bigillon (2001). A summary of this database is given in Table 2.1. It is comprised of 6 data sets containing a total of 1038 data points. These data are limited to the particle sizes

with median diameters in the range of 0.21 to 29.3 mm, bed roughness in the range of 0.19 to 7.76 mm, average flow velocity in the range of 0.22 to 1.00 m/s, shear velocity in the range of 0.0097 to 0.1108 m/s, flow depth in the range of 2.13 to 180 mm, and slope in the range of 0.00073 to 0.05. Details on the variability of hydraulic and bedload particle parameters are given in the appendices. Table 2.2 to 2.4 provides the summary of literature review, including existing equations, data sources and previous and recent studies.

Table 2.1: Variability of Hydraulic and Bedload Particle Parameters

Variables	Existing Experiments Data				Recent Experiments Data	
	Meland and Norrman (1966)	Fernandez Luque and van Beek (1976)	Steidtmann (1982)	Bridge and Dominic (1984)	CSU (1995)	Bigillon (2001)
(1)	(2)	(3)	(4)	(5)	(6)	(7)
Number	120	85	330	77	356	50
S_f	-	-	-	-	0.00073-0.011	0.02-0.05
T (°C)	20	22	18-22	20	17.25-21.5	20
$\nu \times 10^{-6}$ (m^2/s)	1.004	1.26	0.98-1.095	1.004	0.968-1.08	1.004
y (mm)	-	-	180	-	50.3-71.15	2.13-28.65
u_* (m/s)	0.0172-0.1108	0.0122-0.0641	0.0172-0.0277	0.0122-0.0641	0.0097-0.0641	0.018-0.038
u_f (m/s)	0.25-1.0	-	0.29-0.44	-	0.25-0.89	0.22-0.49
k_s (mm)	2.09-7.76	0.9-3.3	0.35	0.19-3.5	1.2-3.4	1.5-3
d_s (mm)	2.09-7.76	0.9-3.3	0.21-1.25	0.19-3.5	2.4-29.3	1.5-3
d_s/k_s	1.0	1.0	0.6-3.57	1.0	2.02-24.4	1.0
Shape of Particles	Spherical	Angular	Spherical	Spherical Angular	Spherical Angular	spherical

Table 2.2: Summary of Literature Review

Sources	Equations	Notes
Krumbein (1942)	$\frac{V_p}{u_f} = 0.88\left(1-\exp(-1.85u_f)\right)$	where: V_p = particle velocity; u_f = mean flow velocity; b = constant; Fr = Froude number
Kalinske (1942)	$V_p = c_a\left(u_f - u_c\right)$	where: c_a = constant; u_f = mean flow velocity; V_p = particle velocity; u_c = critical velocity; Kalinske applied his model to Krumbein's data and found the best agreement for $0.9 < c_a < 1.0$
Ippen and Verma (1955)	$\frac{u_f}{V_p} = 1 + c_b\left(\frac{k_s}{d_s}\right)\left(\frac{1}{u_*}\right)$	Where: $c_b = \frac{1}{12}(G-1)\sqrt{gh}$, k_s = roughness size, d_s = grain size, u_* = shear velocity, V_p =particle velocity and u_f = mean flow velocity
Meland and Norrman (1966)	$\frac{V_p}{k_s^{\,m}} = 7.05u_*\frac{d_s^{\,n}}{k_s} - 5.1$	Where: u_* = shear velocity, V_p = particle velocity, k_s = roughness size, m = 0.75 and $n = \left(\frac{0.014k_s}{u_*}\right)^{0.26}$
Ikeda (1971)	$\frac{V_p}{u_*} = \frac{u_f}{u_*} - \left[\frac{4}{3}c_\mu\frac{(G-1)}{\left(c_\mu C_L + C_D\right)}\frac{gd_s}{u_*^2}\right]^{1/2}$	where, V_p = particle velocity, u_* = shear velocity, u_f = fluid velocity

		at the center of the spherical grain, c_μ = sliding friction coefficient, G = the particle specific gravity, g = gravitational acceleration, and C_D and C_L = drag and lift coefficients
Parson (1972)	$V_p = c_c d_s \left(u_*^{\,2} - u_c^{\,2}\right)$	where, u_* = shear velocity, u_c = critical velocity, d_s = grain size and $c_c = \rho/4\mu$.
Fernandez Luque and van Beek (1976)	$V_p = c\left(u_* - 0.7u_{*_c}\right)$	Where: u_{*_c} = critical shear velocity at Shield's condition for entrainment, V_p = particle velocity and u_* = shear velocity, and c = 11.5;
Romanovskiy (1977)	$V_p = c_e\left(u_f - u_c\sqrt{\frac{\tan\alpha}{m_\mu}}\right)$	Where: $\tan\alpha$ = dynamic friction coefficient, m_μ = static friction coefficient, u_f = mean flow velocity, c_e = constant and u_c = critical velocity
Abbott and Francis (1977)	$V_p = c\left(u_* - u_{*_c}\right)$	Where: u_* = shear velocity, u_{*_c} = critical shear velocity and $13.5 < c < 14.3$, c = constant parameter.
Bridge and Dominic (1984)	$V_p = c\left(u_* - u_{*_c}\right)$	$c_h u_{*_c} = w\sqrt{\tan\alpha}$, w = the settling velocity of particles, $\tan\alpha$ = the dynamic coefficient

		friction, 6< c <14.3, u_* = shear velocity and u_{*_c} = critical shear velocity
Wiberg (1987)	$\frac{V_p}{u_*} = 4.2\frac{\left[\frac{(\tau-\tau_c)}{\tau_c}\right]^{1/2}}{\left(\frac{\tau}{\tau_c}\right)} + 2.4$	Where: τ = mean bed shear stress, τ_c = shear stress at threshold of motion, V_p = particle velocity and u_* = shear velocity
Jan (1992)	$V_p = \sqrt{\frac{(\rho_s-\rho_f)gd_s(\sin\theta - n_\mu\cos\theta)}{f\rho_s + \frac{3}{4}C_D\rho_f}}$	Where: ρ_s, ρ_f = particle and fluid density, C_D = drag coefficient, θ= bed slope angle, d_s = particle diameter, g = gravitational acceleration, f = collision coefficient, and n_μ = bulk friction coefficient
Meier (1995)	$V_p = c_\alpha(u_* - u_{*_c})$	Where: V_p = particle velocity, u_* = shear velocity, u_{*_c} = critical shear velocity, and c_α = proportionality constant

Table 2.3: Existing Database

Sources	Number of Data Points	Bed-load Particle Size	Notes
Meland and Norrman (1966)	120	d_s=2.09, 3.15, 3.93, 5.1, 5.95, 7.0 and 7.76mm; k_s=2.09 and 7.76mm	Glass spheres G=2.65
Fernandez Luque and van Beek (1976)	85	d_{walnut}=1.5mm 0.9mm<d_{sand}<1.8mm d_{gravel}=3.3mm $d_{magnetite}$=1.8mm	Walnut, sand (I), sand (II), gravel and magnetite; G=2.64 and 4.58 Shape, density,...
Steidtmann (1982)	330	0.21mm<d_{sand}<1.25mm k_s=0.35mm(Glass sphere)	Sand-size spheres (d_s) Glass spheres (k_s) 154 with G_s=4.5 176 with G_s=2.5
Bridge and Dominic (1984)	77		Glass spheres G=2.56
Wiberg (1987)	115	d_s = 0.35, 0.5, 0.8, 1.5, 2.0, 2.5, 5, 10, 28.6mm	Shape, density,...
Rakoczi (1991)	100	d_{s1}=5-10mm, d_{s2}=10-15mm, d_{s3}=15-20mm; d_{s4}=20-25mm and d_{s5}=25-36mm	Gravel G=2.65
Jan (1992)	158	13.5mm<d_{glass} <24.1mm d_{steel} = 13.5mm d_{golf} = 42.5mm 13.5mm<k_s<42.5mm	Golf, steel balls; water, air and salad oil
CSU (1995)	356	1.57mm<d_{steel}<19.04mm d_{tin}=4.375mm	Glass, natural and steel spherical and angular

		$14.48mm<d_{glass}<29.3mm$ $1.2mm<d_{natural}<13.6mm$ k_s=1.2,1.7,2.4 and 3.4mm	shapes
Bigillon (2001)	50	$1.5mm<d_{steel}<3mm$ $1.5mm<d_{glass}<3mm$ k_s=1.5 and 3mm	Glass and steel spherical shape

Table 2.4: Summary of Previous and Recent Studies

Author	Equation	Data	Particle Size	Particle Shape	Particle Density	Smooth Bed	Rough Bed	Still Fluid	Flowing Fluid
Meland and Norrman (1966)	Yes	Yes	Yes	Spherical			Yes		Yes
Fernandez Luque and van Beek (1976)	Yes	Yes	Yes	Angular	Yes		Yes		Yes
Steidtman (1982)		Yes	Yes	Spherical	Yes	Yes	Yes		Yes
Bridge and Dominic (1984)	Yes	Yes	Yes	Spherical, Angular			Yes		Yes
Wiberg (1987)	Yes	Yes	Yes	Spherical, Angular	Yes		Yes		Yes
Jan (1992)	Yes	Yes	Yes	Spherical	Yes	Yes	Yes	Yes	
CSU (1995)	Yes	Yes	Yes	Spherical, Angular	Yes	Yes	Yes	Yes	Yes
Bigillon (2001)	Yes	Yes	Yes	Spherical	Yes		Yes		Yes

2.3. APPLICATION OF EXISTING METHODS

Figs. 2.1 to 2.6 show the application of the equations of Meland and Norrman (1966), Fernandez Luque and van Beek (1976), and Bridge and Dominic (1984) to their own database. The results show that the equations of Meland and Norrman, Fernandez Luque and van Beek, and Bridge and Dominic predict very well with their own data.

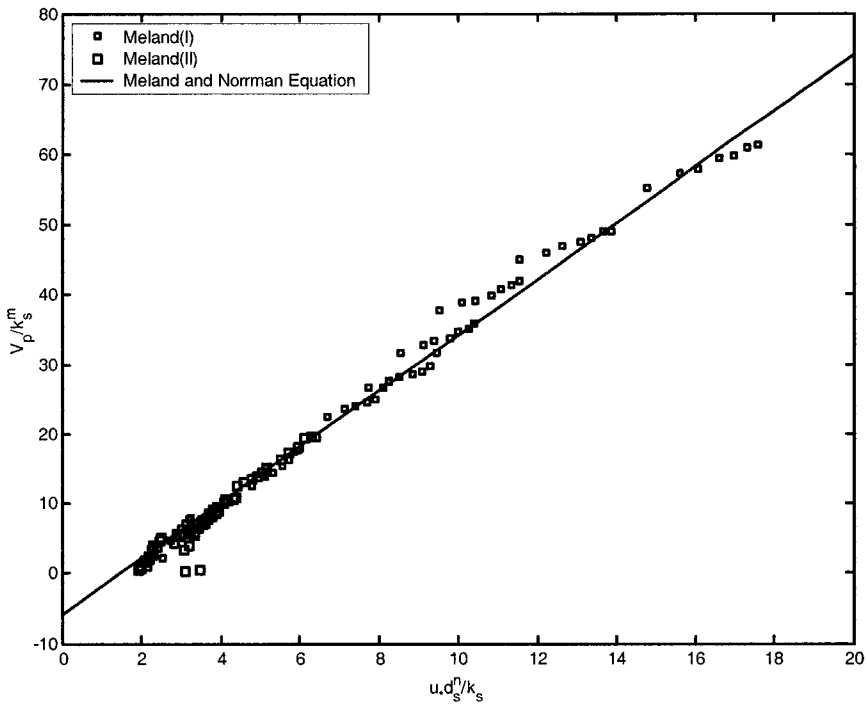

Figure 2.1: V_p/k_s^m vs. $u_*d_s^n/k_s$

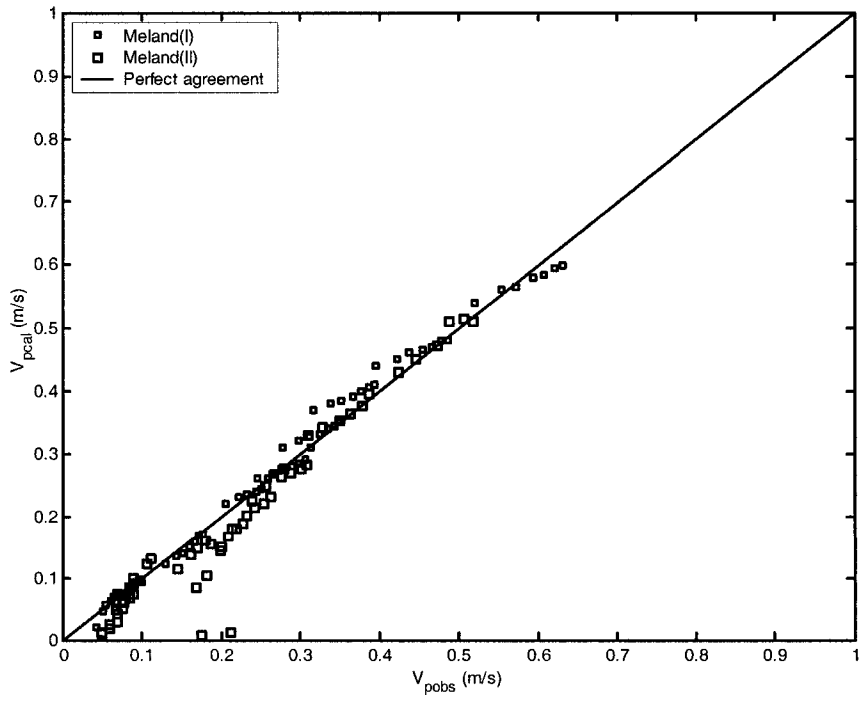

Figure 2.2: Comparison between Calculated and Observed V_p using Eq. (2.9)

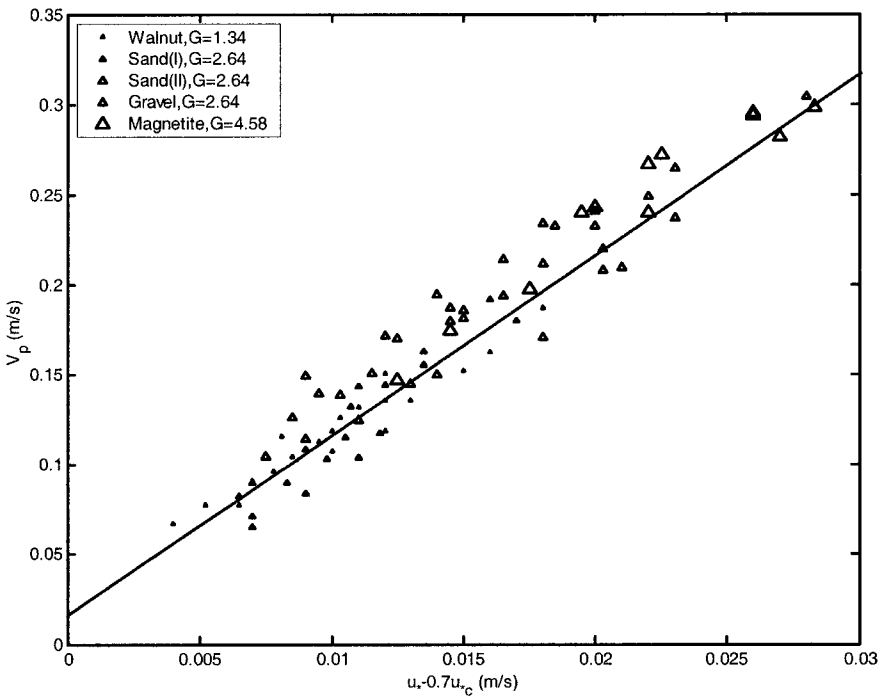

Figure 2.3: V_p vs. (u_*-0.7u_{*c})

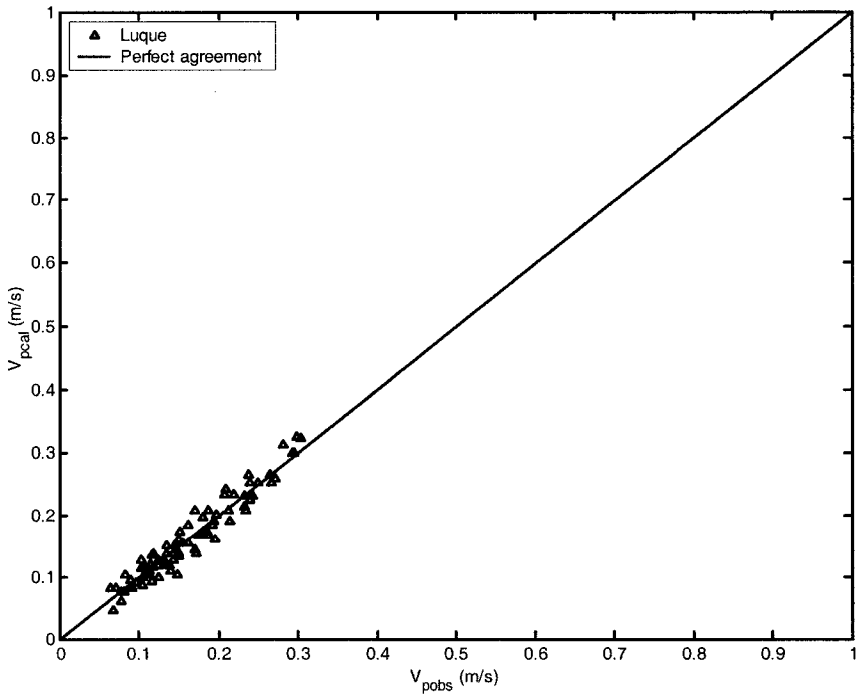

Figure 2.4: Comparison between Calculated and Observed V_p using Eq. (2.15)

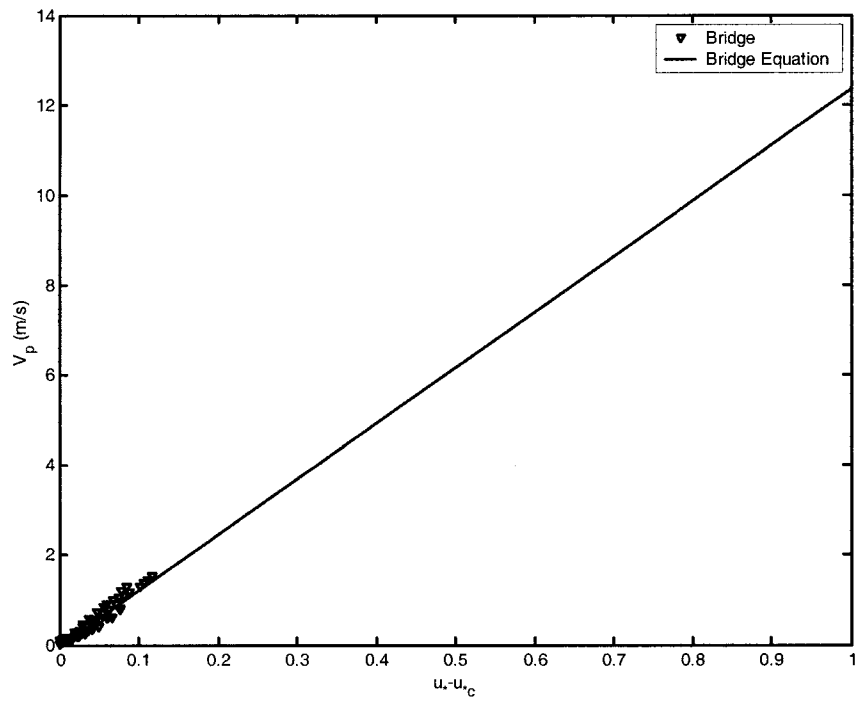

Figure 2.5: V_p vs. (u_*-u_{*c})

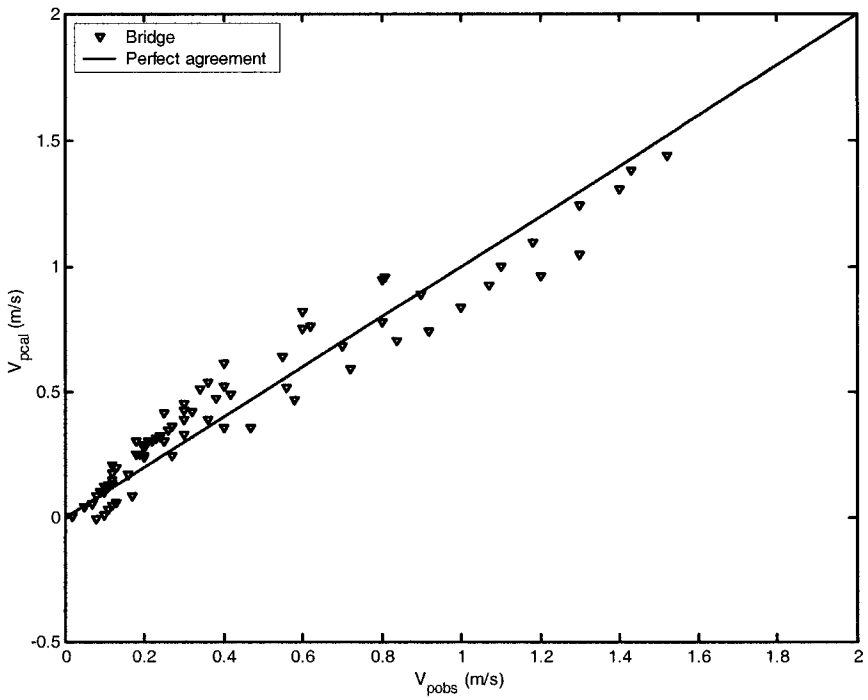

Figure 2.6: Comparison between Calculated and Observed V_p using Eq. (2.22)

2.4. SUMMARY

The existing methods, i.e., Meland and Norrman, Fernandez Luque and van Beek, and Bridge and Dominic compare well with their own data. There is a shortage of laboratory data on particle specific gravity G (density), particle shape, bed roughness k_s, particle size d_s, etc., therefore more extensive physical experiments are needed to cover a greater range of variability for hydraulic and particle parameters.

CHAPTER 3

DATA COMPILATION

Julien, Meier, and Blackard (1995) conducted experiments at the Engineering Research Center (ERC) of Colorado State University on transport velocities of bedload particles in smooth and rough open channel flows. This chapter represents the descriptions of the flume, plates, particles, set up, experiments, and methodology used in the experiments.

3.1. THE FLUME

A 9.77m long plexiglass tilting flume shown in Fig. 3.1, with trapezoidal cross-section was used for the experiment. The bed slope has a range of approximately 0% to 4%, although 1% was the largest slope used (run 18, 20, 28 and 37). The side walls of the flume are adjustable, allowing for the channel cross-section to be varied. In these experiments the side walls were kept fixed at a 3 H to 1 V ratio, in order to minimize

their influence on the flow. A 2 m long test reach near the downstream end of the flume was used to measure particle velocities.

The location of the test reach was chosen by visual inspection as that portion of the flume with most uniform flow conditions. An adjustable weir located at the downstream end of the flume was used in some of the runs to control the test reach water levels. Many runs with higher flow rates were performed with the weir removed as long as the flow was steady and uniform in the test section. The system re-circulated water collected at the downstream end of the flume in a stilling tank with a pump driven by an electric motor.

The motor has three speed settings (slow, medium, and fast) and the return pipe has a valve for fine adjustment of the flow rate. Three point gages were used to measure flow depths. Two gages were located at the beginning and end of the test section, the third was used to record flow depth over the weir. Flow rates were measured using an orifice plate located in the water return pipe. Pressure taps on each side of the construction were connected to two manometers in parallel, with water and mercury as manometric fluids. The mercury manometer was needed for the higher flow rates.

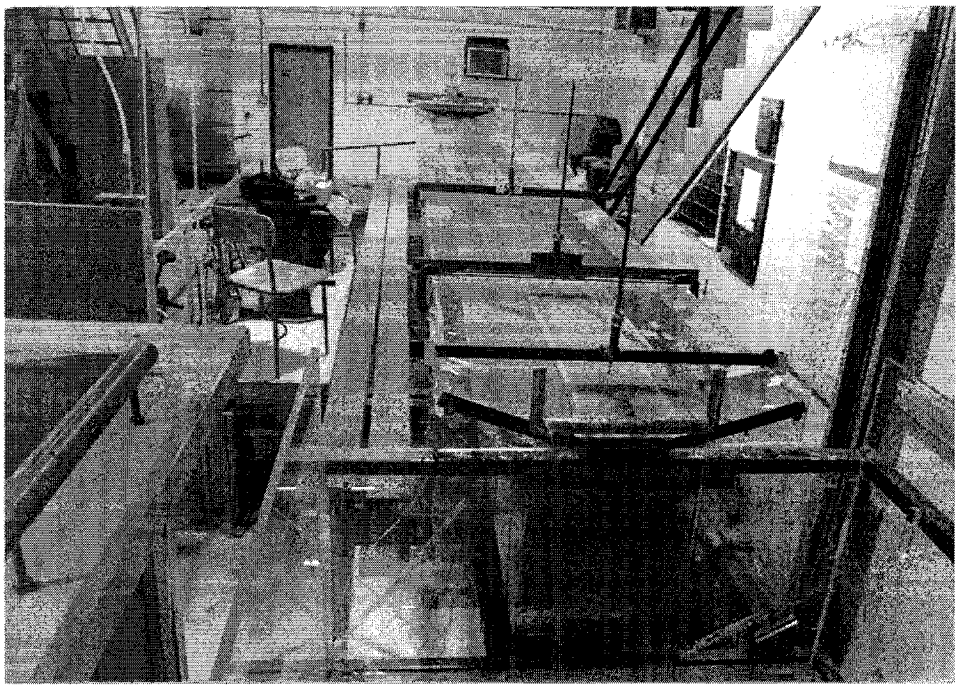

Figure 3.1: Three Point Gages used to Measure Water Depth.

3.2. THE PLATES

Sand or gravel was glued to aluminum plates to achieve various bed roughnesses. Four sets of plates with rounded sand and gravel were used, one set with angular gravel and one smooth aluminum plate (bed roughness k_s=0). Grain sizes used as bed roughness are shown in Table 3.1. Two 12-ft long plates were used for each bed roughness condition. The upstream plate used the same roughness as the downstream plate in order to establish the velocity profile of the stream. The test reach was located over the downstream plate.

Table 3.1: Gravel Gradations for Roughened Plane Surfaces

Sieve Retained (mm)	Sieve Passed (mm)	Bed Roughness (mm)
No gravel	No gravel	0
1.0	1.4	1.2
1.4	2.0	1.7
2.0	2.8	2.4
2.0	2.8	2.4(angular)
2.8	4.0	3.4

Various adhesives were used to bond the sand and gravel to the plates. The first set of plates was produced using a spray lacquer made by Krylon to glue 2.4 mm (angular) gravel particles. This attempt failed as the gravel did not stick to the plates well. A vanish substitute called "EnviroTex Lite pour-on" made by Environmental Technology, Inc. was then used; the particles of gravel adhered much better. A contact cement from DAP was also used. It performed as well as the EnviroTex and the contact cement avoided the difficulty in producing a uniform layer of gravel without having "clumps" on the plates. For the 1.2 mm sand, a waterproof paint was used (Tile Clad II from Sherwin Williams). This held the sand in place very well, although clumping was difficult to prevent with this paint as well.

In the early runs, particles had a tendency to roll off the sides of the plates. To solve this problem extra sand/gravel was glued to the sides, creating small ridges that acted as "guard rails" to keep the particles on the plate. The roughened plates are shown in Fig. 3.2, 3.3, 3.4, 3.5 and 3.6

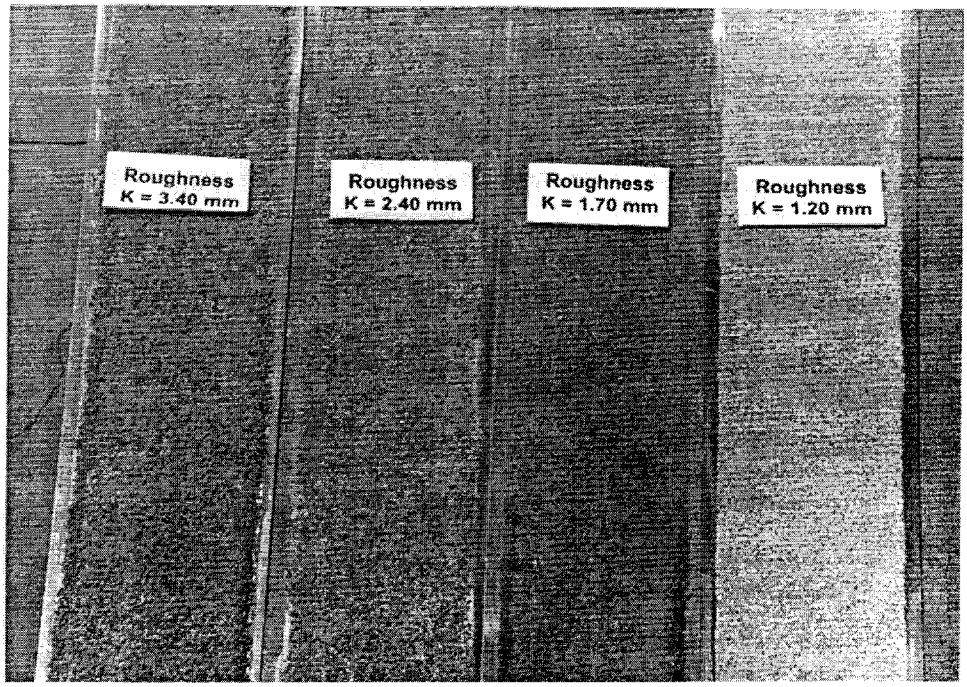

Figure 3.2: Form Roughened Plates

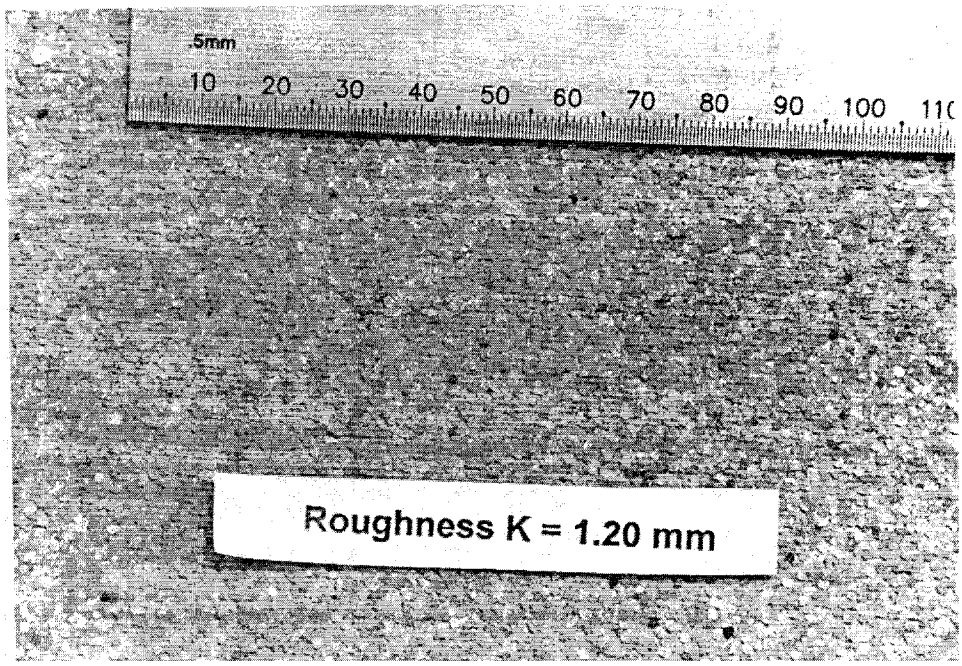

Figure 3.3: Plate at Roughness k_s = 1.2 mm

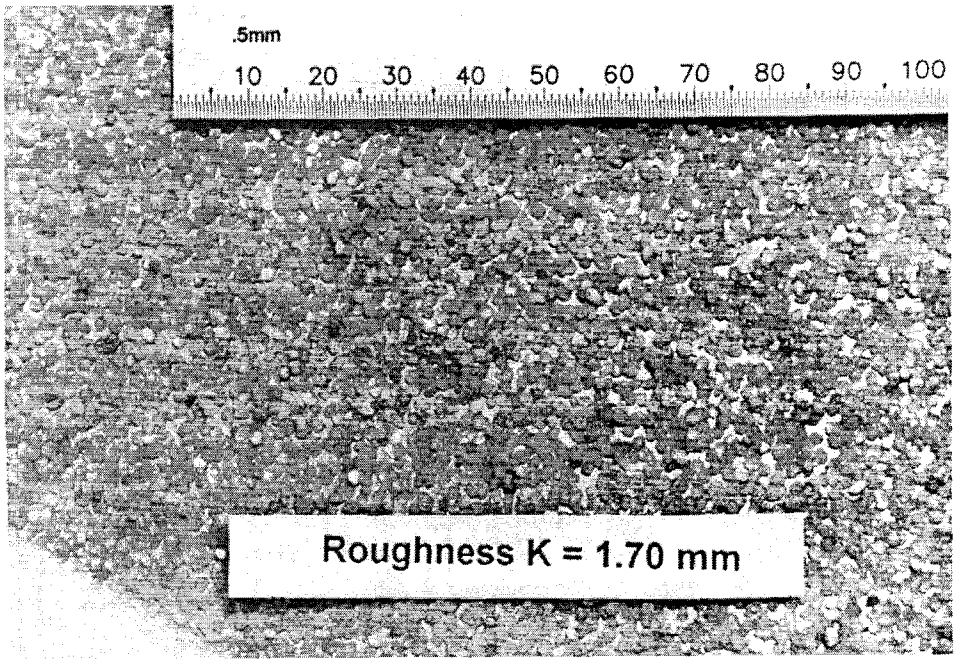

Figure 3.4: Plate at Roughness k_s = 1.7 mm

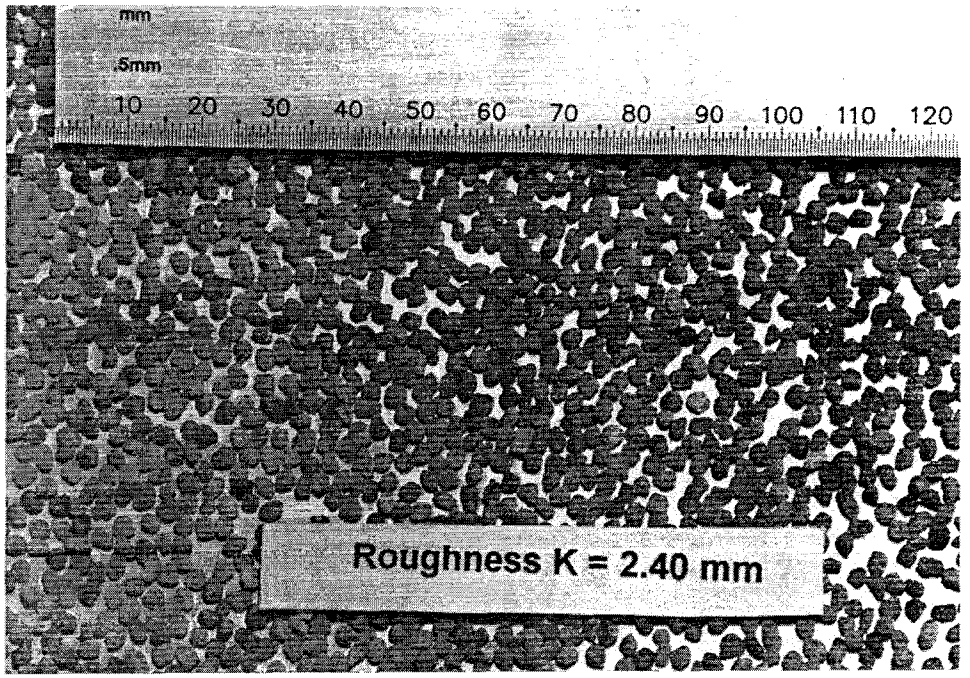

Figure 3.5: Plate at Roughness k_s = 2.4 mm

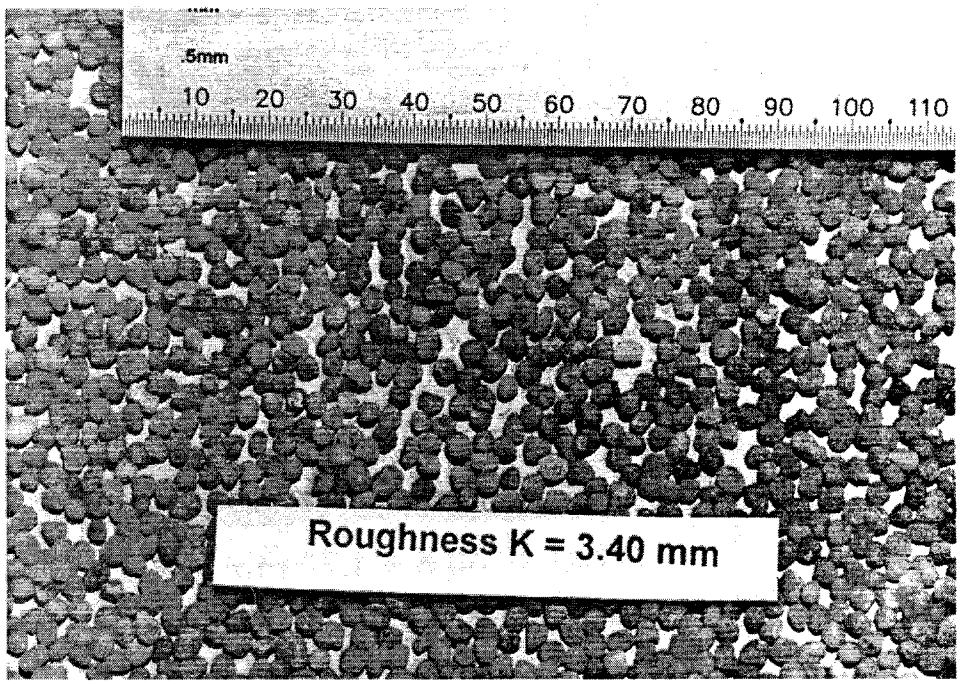

Figure 3.6: Plate at Roughness k_s = 3.4

3.3. THE PARTICLES

Three types of particles were run in the experiment: stainless steel ball bearings, glass marbles and natural quartz particles. The steel ball bearing and glass marbles were used because of their precise spherical shape. Using steel and glass also gave results for particles of two different densities. The quartz particles were used to emulate conditions closer to natural conditions for slope and density, and also to examine the effects of particle angularity.

As can be seen from Fig. 3.7 and Table 3.2, a large number of particle types and diameters were tested. Not all of them moved in every run. For the lower transport rates, most steel particles didn't move at all, or did so only for short distances before halting, because of their high density. The natural particles also rolled very little at low transport

stages, tending to sit on their flatter sides. For the higher transport stages the smaller steel and natural particles simply disappeared when dropped in the water, presumably whisked away in suspension. The glass marbles were the most consistent across all transport stages. Almost every run used all five marbles. Many different particles were used for each size. The particles were sieved and categorized accordingly. For example, the 3.4 mm diameter "particle" was in fact a set of particles, all passing though the 4.00 mm sieve and retained in the 2.8 mm sieve.

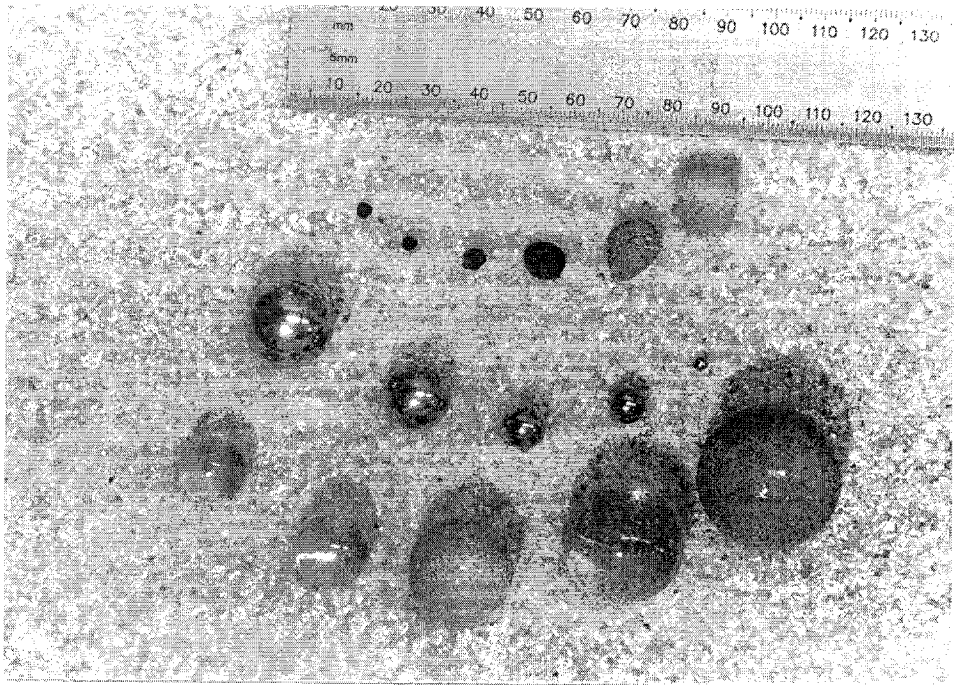

Figure 3.7: Particles used in the Experiment

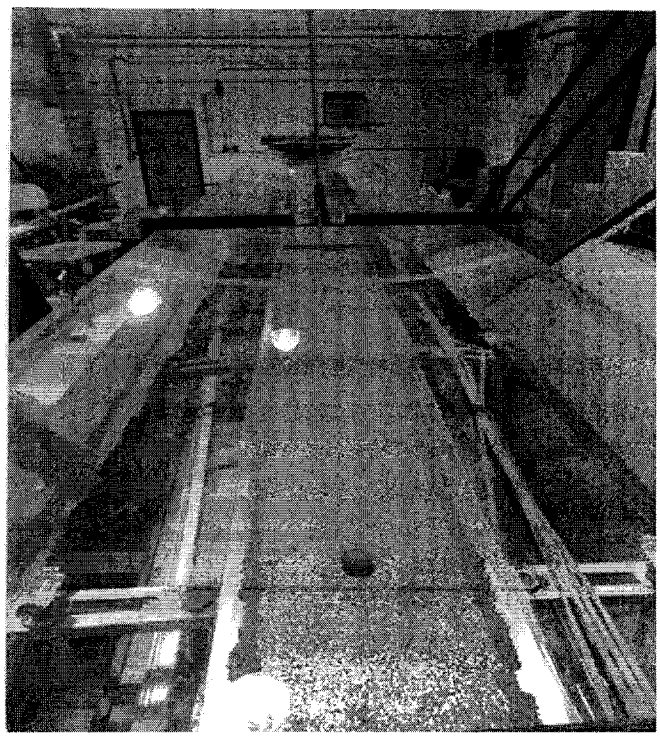

Figure 3.8: The Experiment

Table 3.2: Particle Size used in the Experiments

Type	G	Diameter (mm)	Sieve Retained (mm)	Sieve Passed (mm)
Steel	8.02	19.04		
		15.88		
		14.28		
		9.50		
		7.90		
		6.34		
		4.75		
		3.14		
		1.57		
Glass	2.60	29.30		
		25.17		
		21.70		
		15.97		
		14.48		
Natural	2.65	13.60	11.2	16.0
		9.60	8.0	11.2
		6.80	5.6	8.0
		4.80	4.0	5.6
		3.40	2.8	4.0
		2.40	2.0	2.8
		1.70	1.4	2.0
		1.20	1.0	1.4

3.4. EXPERIMENTAL SET UP

Establishing the desired hydraulic conditions for each run involved setting the bed slope, pump, valve and (optionally) adjusting the weir in order to reach a predetermined value of shear velocity u_*. In general, a bed slope and pump setting were selected, then the valve and weir adjusted until the two point gages in the test section indicated approximately the same flow depth. If the flow depth was too shallow (<50 mm), or if the value of u_* undesirable, bed slope and/or pump setting were changed and the process started over. Adjustments were made until the difference in flow depths between point gages was smaller than 15% of the drop in bed elevation between the point gages (due to the bed slope).

After the hydraulic conditions were set (and recorded) for a given run, the particles were released upstream and their times measured over the 2 m test section. Notes were taken on any non-uniform particle motion, such as surging of particles, suspension or halting. If a particle ran off the plate, that measurement was discarded and repeated. Each particle was run at least 15 times. Hydraulic conditions were measured and recorded at the middle and end of each run, allowing an average over three readings for flow depths, top flow widths, and manometer readings. A total of 49 runs have been completed on plates with six different roughness. For each roughness, a range of values of shear velocity $u_* = (\tau_o/\rho)^{1/2}$ were used in the range where the particles are expected to be in motion and in contact with the bed. A summary of the runs is presented in Tables 3.3 and Table 3.4. One set of plates had no roughness and the experiments for the 2.4 mm gravel were repeated using rounded versus angular material to identify possible differences owing to the angularity of the surface material. Fig. 3.9 Shows a linear relationship

between settling velocity w, and $[(G-1)gd_s]^{1/2}$, the plot indicated that $w \cong 0.9423\ [(G-1)gd_s]^{1/2}$ with $R^2 = 1.0$.

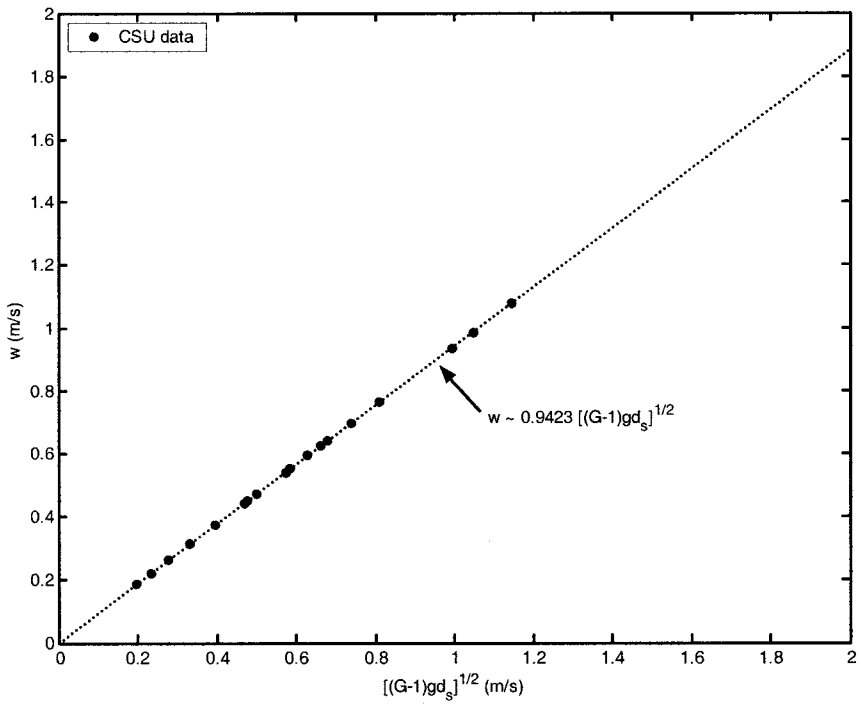

Figure 3.9: w vs. $[(G-1)gd_s]^{1/2}$

Table 3.3: Classification of Experimental Runs

Run Number	u_* (m/s)	Roughness (mm)	Run Number	u_* (m/s)	Roughness (mm)
1	0.0111	0	26	0.0501	3.4 (rounded)
2	0.0176	0	27	0.055	3.4 (rounded)
3	0.016	0	28	0.0625	1.7 (rounded)
4	0.0119	0	29	0.0593	1.7 (rounded)
5	0.0141	0	30	0.0516	1.7 (rounded)
6	0.0152	0	31	0.048	1.7 (rounded)
7	0.0194	0	32	0.0419	1.7 (rounded)
8	0.0249	0	33	0.0359	1.7 (rounded)
9	0.0299	0	34	0.0242	1.7 (rounded)
10	0.0176	0	35	0.0285	1.7 (rounded)
11	0.0356	0	36	0.0186	1.7 (rounded)
12	0.0097	0	37	0.0616	2.4 (rounded)
13	0.0301	2.4 (angular)	38	0.0558	2.4 (rounded)
14	0.0386	2.4 (angular)	39	0.0514	2.4 (rounded)
15	0.025	2.4 (angular)	40	0.0467	2.4 (rounded)
16	0.0339	2.4 (angular)	41	0.0378	2.4 (rounded)
17	0.0506	2.4 (angular)	42	0.0317	2.4 (rounded)
18	0.0641	2.4	43	0.019	2.4 (rounded)
19	0.0424	0	44	0.0248	2.4 (rounded)
20	0.0623	3.4 (rounded)	45	0.019	1.2 (rounded)
21	0.024	3.4 (rounded)	46	0.027	1.2 (rounded)
22	0.0231	3.4 (rounded)	47	0.036	1.2 (rounded)
23	0.0298	3.4 (rounded)	48	0.044	1.2 (rounded)
24	0.0362	3.4 (rounded)	49	0.051	1.2 (rounded)
25	0.0438	3.4 (rounded)			

The voluminous data set in Appendix A provides a substantial compilation of particle velocity information for each size fraction for plane surfaces of different roughnesses and particles of different size, density and angularity.

3.5. PRELIMINARY RESULTS

The data set shows the following overall characteristics: (1) under given hydraulic and surface roughness conditions, coarse particles generally roll faster than fine particles; (2) exceptions to (1) were observed, either when smaller particles were partly in saltation, or when the standard deviation of repeated particle velocity measurements were large compared to the mean velocity; (3) the most convincing results are found on runs 3 and 5 for a smooth plate, and runs 34, 36, and 44 for rough plates; (4) at a given roughness size, particles roll slightly faster on a plane boundary of rounded particles as opposed to angular particles; and (5) as shear velocity u_* increases, the smaller particles enter saltation and tend to move faster than coarse particles.

A plot of particle velocity against particle diameter for a smooth bed ($k_s = 0$) is shown in Fig. 3.10. where larger particles move faster than smaller ones for all values of shear velocity. Larger particles protrude higher into the flow, in regions with higher flow velocities. There are no clear differences in transport velocities for particles of different densities; Fig. 3.11 shows that lighter particles move faster than heavier particles, and particle velocity tends to decrease with the increase of the particle size; for natural particles, the variability of particle velocity with respect to particle size is high, this may

be the effect of particle shape; and for glass particles, larger particles move faster than smaller ones.

Fig 3.12 shows the ratio of particle velocity V_p to shear velocity u_* lies in the range of 2.5 to 12.5; Fig. 3.13 shows, for glass and natural particles (lighter), $V_p \cong 9.14u_*$, and for steel particles (heavier), $V_p \cong 3.94u_*$; Fig. 3.14 shows the variation of particle velocity, V_p against Shields parameter, τ_{*ds}. Fig. 3.15 shows the ratio of particle velocity V_p to mean flow velocity u_f lies in the range of 0.2 to 0.9; Fig. 3.16 shows that spherical particles move faster than angular particles at the same $u_*/[(G-1)gd_s]^{1/2}$.

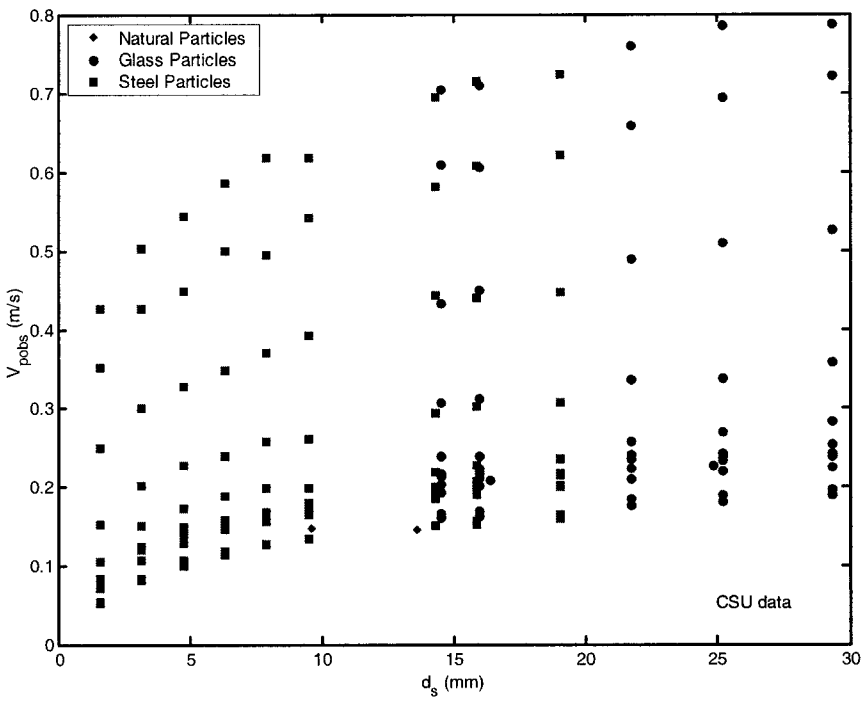

Figure 3.10: V_{pobs} vs d_s for $k_s = 0$

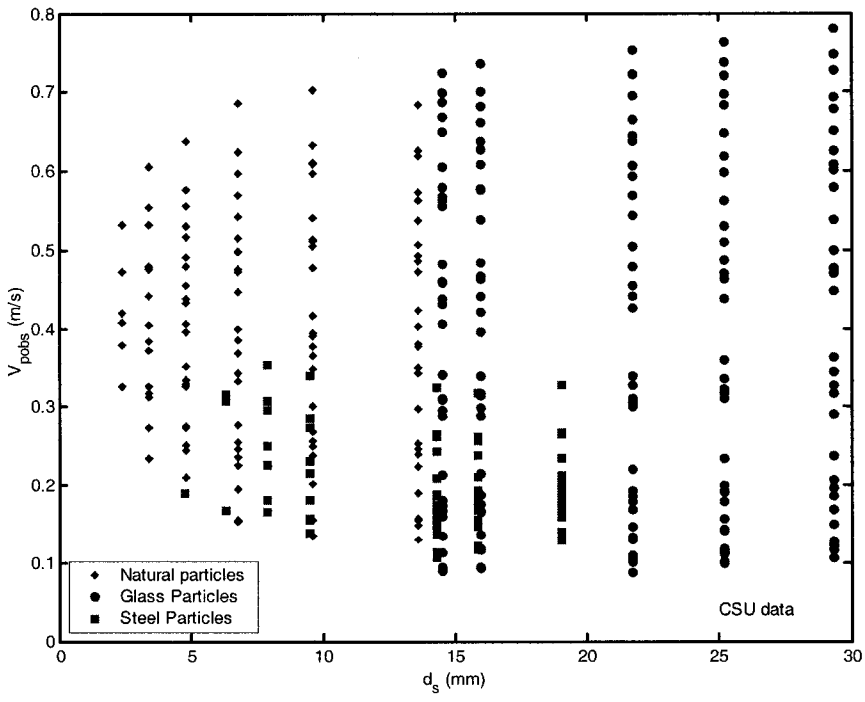

Figure 3.11: V_{pobs} vs d_s for $k_s > 0$

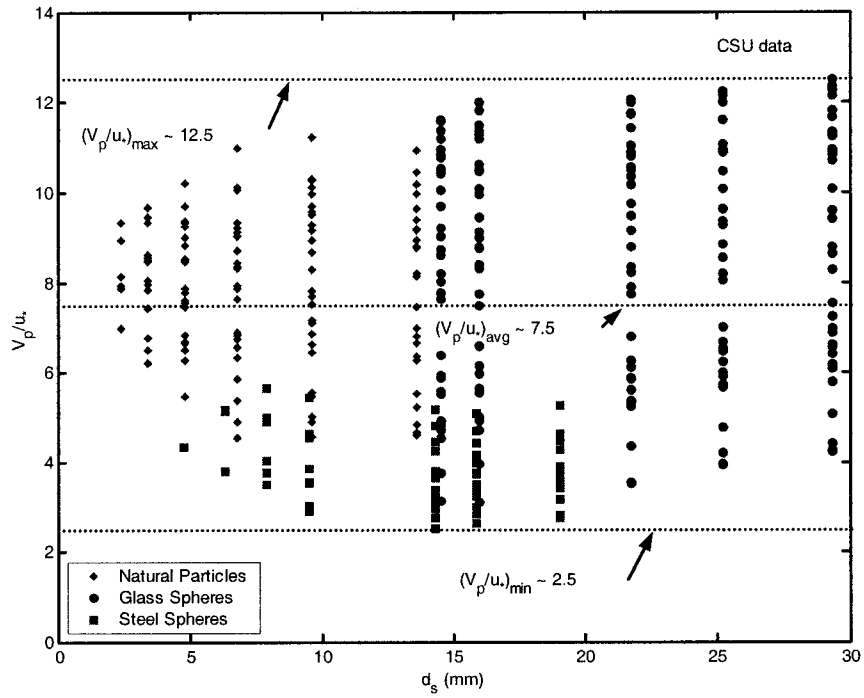

Figure 3.12: V_p/u_* vs d_s

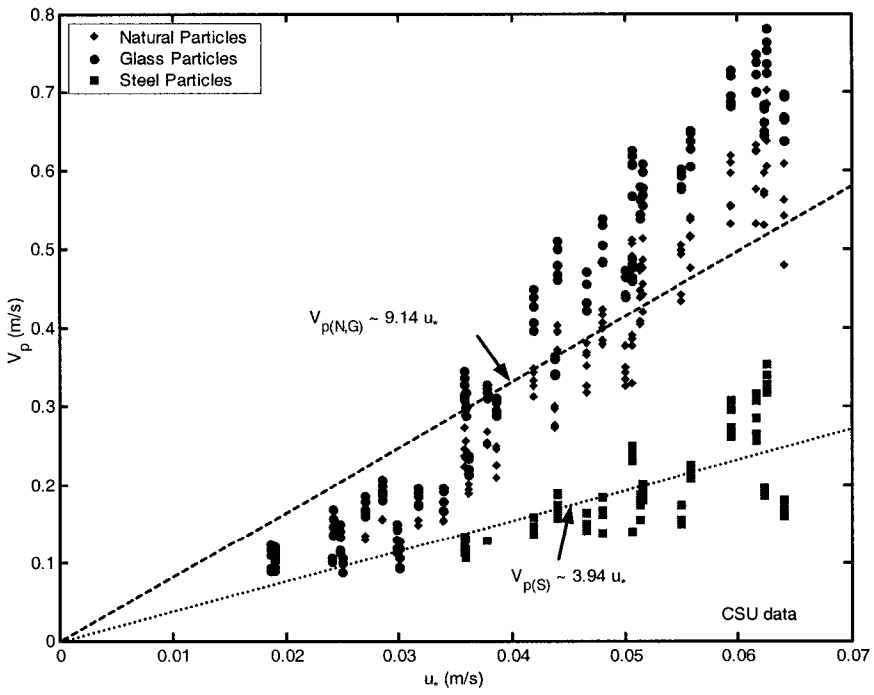

Figure 3.13: V_p vs u_*, a) $V_{p(N,G)} \sim 9.14u_*$, and b) $V_{p(S)} \sim 3.94u_*$

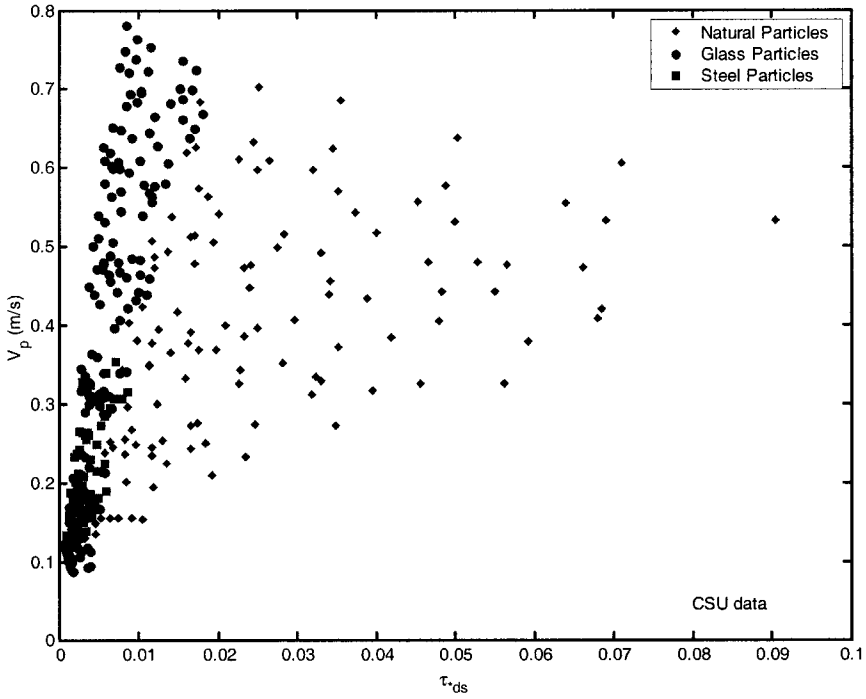

Figure 3.14: V_p vs τ_{*ds}

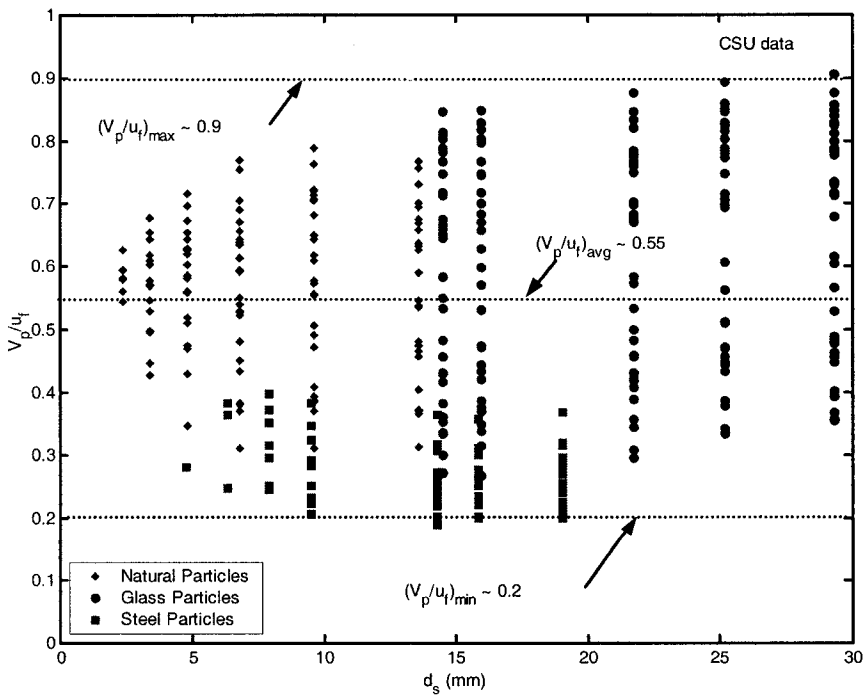

Figure 3.15: V_p/u_f vs d_s

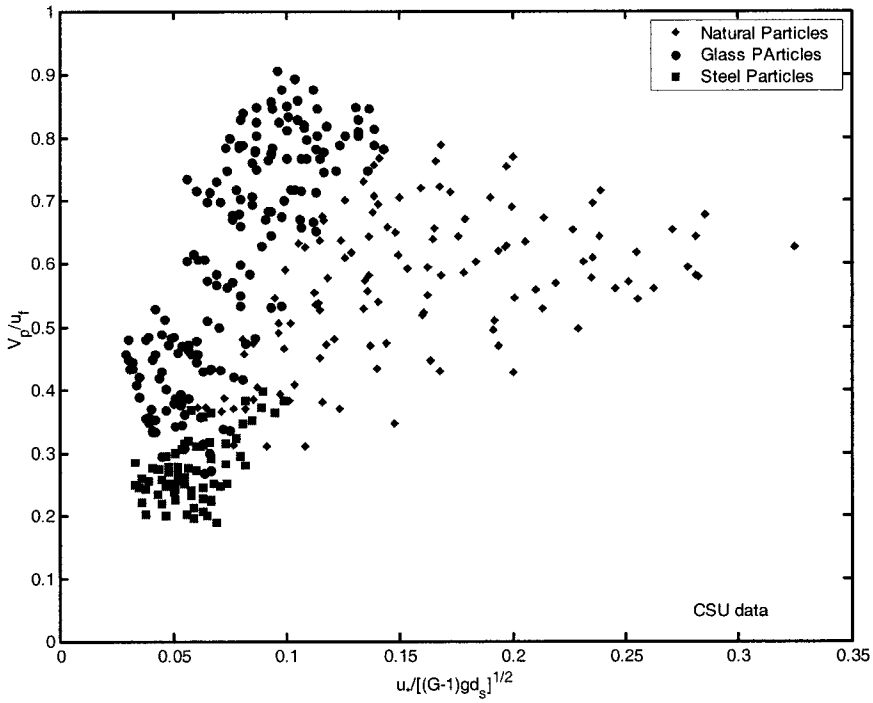

Figure 3.16: V_p/u_f vs $u_*/[(G-1)gd_s]^{1/2}$

From Fig. 3.13, we generated linear equations of the following form, for each bed roughness and particle type:

$$V_p = C_1 + C_2 u_* \tag{3.1}$$

where: C_1 and C_2 are constants, these equations were then reduced to the form of Eq. (2.19) by introducing the absolute value of C_1/C_2 as a new positive constant:

$$V_p = C_2\left(u_* - \left|C_1 / C_2\right|\right) \tag{3.2}$$

where: $c = C_2$ and $\left|C_1/C_2\right| = u_{*c}$. The computed values of c and u_{*c} for different bed roughness and particle types is shown in Table 3.4.

Table 3.4. Computed Values of c and u_{*c} for different k_s and Particle type

Particle Type	k_s (mm)	c	u_{*c} (m/s)	R^2
Natural	0	NA	NA	NA
(G = 2.6)	1.2	15.51	0.0192	0.98
	1.7	14.83	0.0197	0.97
	2.4	14.03	0.0212	0.93
	3.4	14.83	0.0244	0.95
Glass	0	18.61	0.0033	0.94
(G = 2.65)	1.2	16.29	0.0145	0.98
	1.7	15.39	0.0143	0.99
	2.4	15.87	0.0187	0.95
	3.4	16.33	0.0214	0.98
Steel	0	15.08	0.0044	0.85
(G = 8.02)	1.2	7.93	0.0213	0.93
	1.7	8.21	0.0251	0.89
	2.4	5.08	0.0152	0.42
	3.4	4	0.0147	0.77

3.6. STATISTICAL ANALYSIS

In the statistical analysis, the discrepancy method is adopted to indicate the goodness of fit between the calculated and observed results. The discrepancy ratio, R_i

$$R_i = \frac{V_{pcal(i)}}{V_{pobs(i)}} \tag{3.1}$$

in which $V_{pcal(i)}$, $V_{pobs(i)}$ = calculated and observed bedload particle velocity corresponding to data point number in a data set. For a perfect fit, $R_i = 1.0$.

3.7. PARAMETRIC ANALYSIS OF CSU DATA

Fig. 3.17, 3.19, and 3.20 show that $\tau_{*ds}/0.047 \approx 0.01$ ($\tau_{*ds} \approx 0.00047$), when $k_s<d_s$, bedload particles move at values of shear stress below the threshold value given by the Shields diagram, and $\tau_{*ds} = 0.047$ when $d_s = k_s$. Fig. 3.18 shows the values of τ_{*ks} is in the range of 0.01 to 0.15; Fig. 3.20 shows values of $Re_* > 100$; Fig. 3.21 shows $V_p/[(G-1)gd_s]^{1/2} < 2$, then combined with Fig. 3.9, resulted in $V_p/w < 2$, and therefore $V_p < 2w$; and Figs. 3.22 and 3.23 show the values of V_p/u_* is in the range of 2.5 to 12.5, and the threshold value for τ_{*ks} is 0.01; Figs. 3.24 and 3.25 show the values of $u_*/w < 0.5$, which is in agreement with the criterion for bedload sediment transport in Julien (1995, p.187, Figure 10.4).

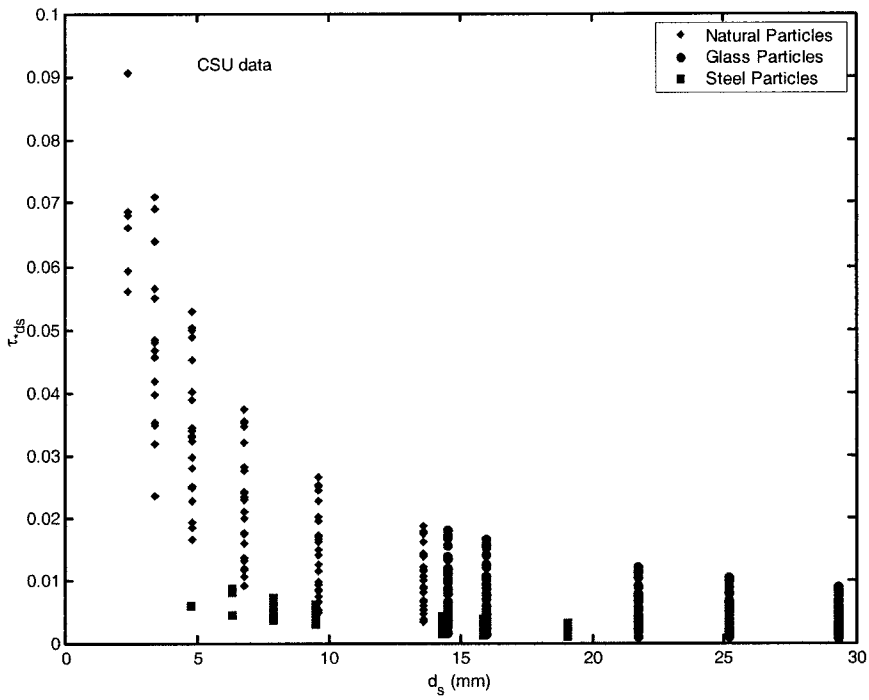

Figure 3.17: τ_{*ds} vs d_s

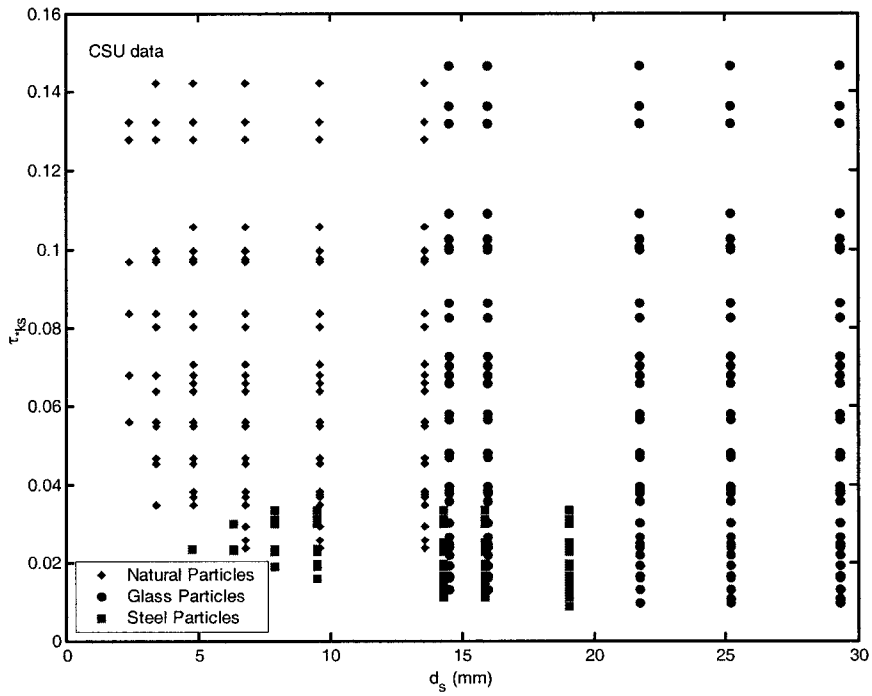

Figure 3.18: τ_{*ks} vs d_s

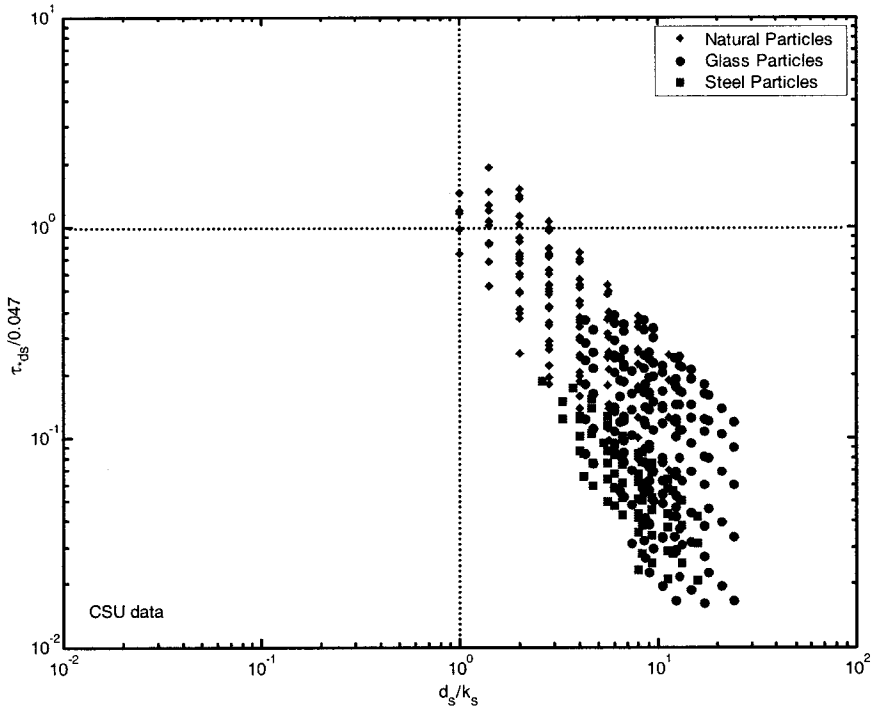

Figure 3.19: $\tau_{*ds}/0.047$ vs d_s/k_s

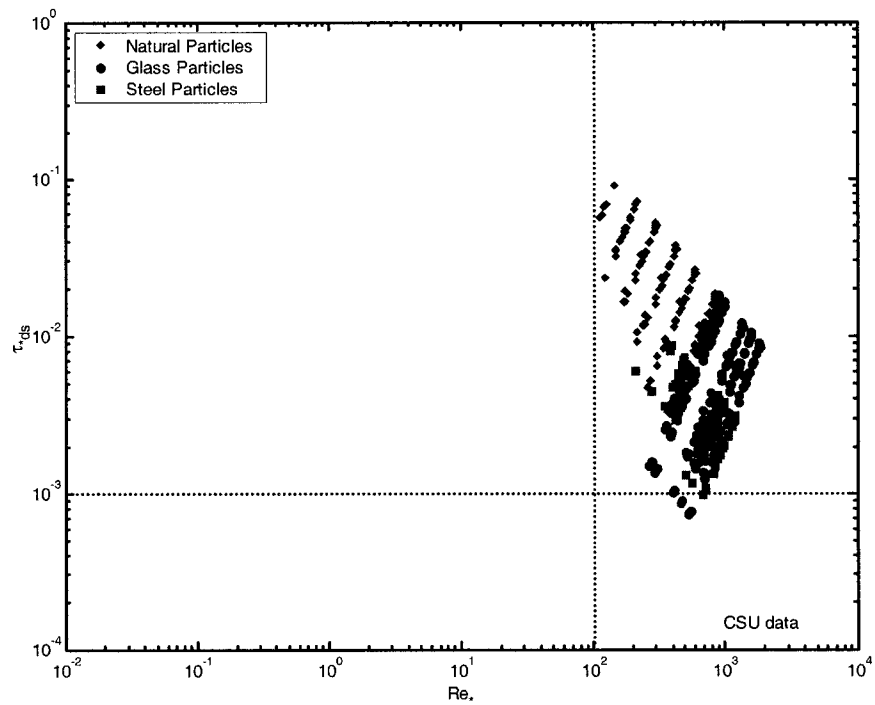

Figure 3.20: τ_{*ds} vs Re_*

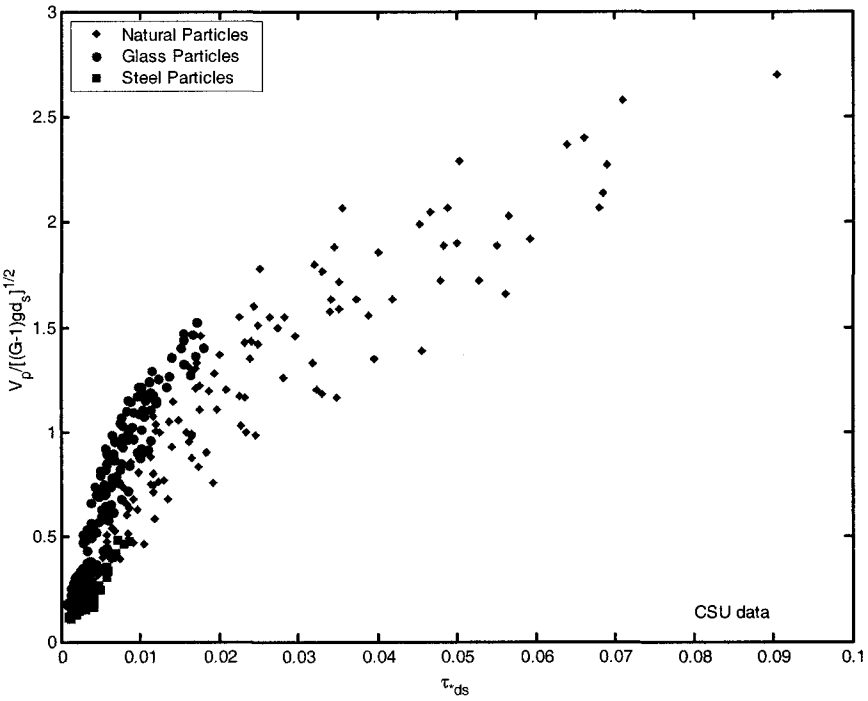

Figure 3.21: $V_p/[(G-1)gd_s]^{1/2}$ vs τ_{*ds}

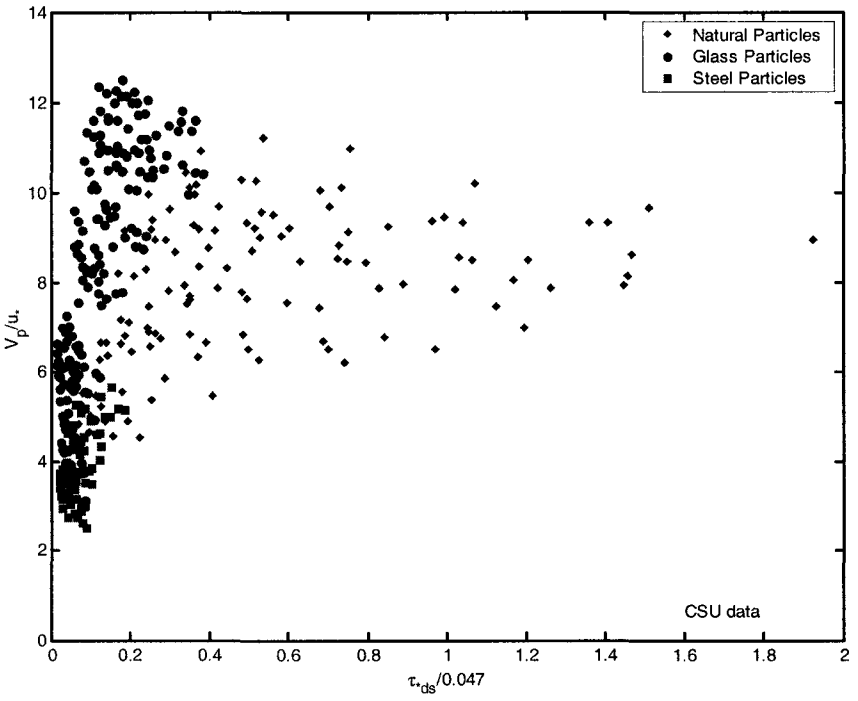

Figure 3.22: V_p/u_* vs $\tau_{*ds}/0.047$

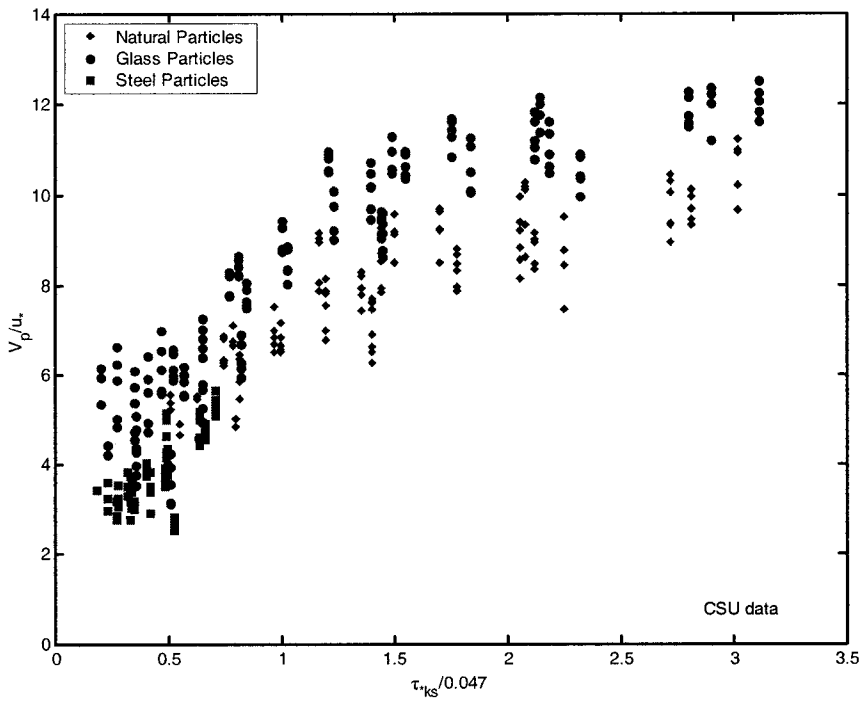

Figure 3.23: V_p/u_* vs $\tau_{*ks}/0.047$

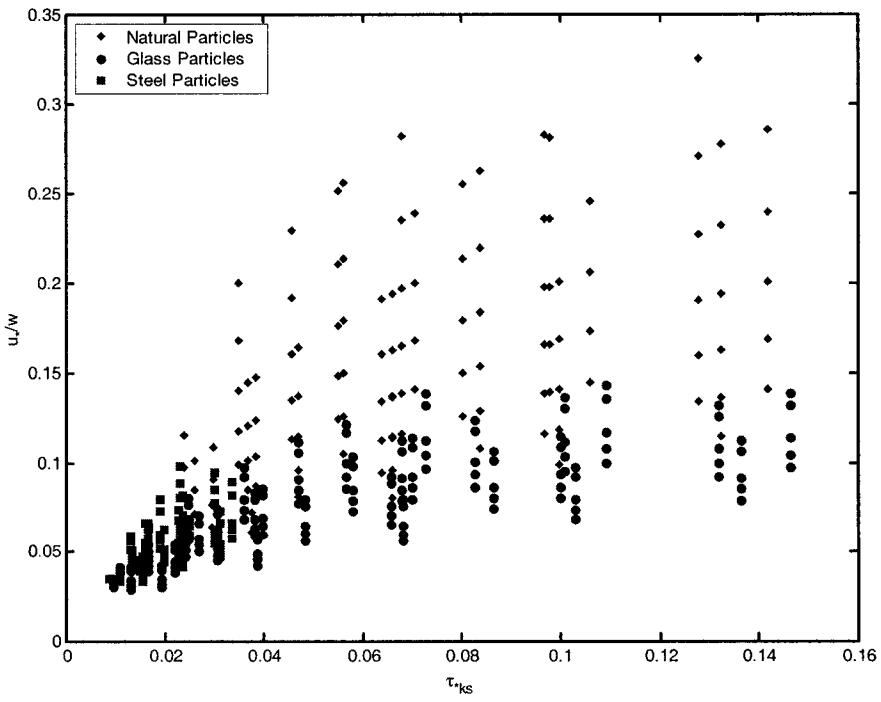

Figure 3.24: u_*/w vs τ_{*ks}

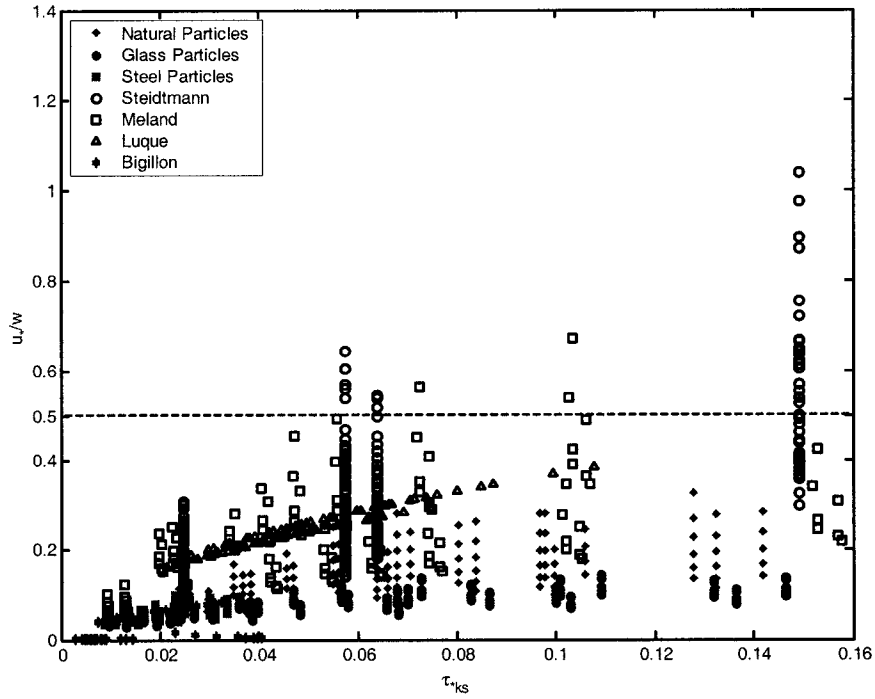

Figure 3.25: u_*/w vs τ_{*ks}, for different database

3.8. SUMMARY

Analysis of the data showed that: (i) for a smooth bed ($k_s = 0$) larger particles move faster than smaller ones. In other words, rolling bedload particle velocity increases with particle sizes; (ii) for a rough bed ($k_s > 0$) lighter particles move faster than heavier ones; (iii) bedload particles move at values of the Shields parameter $\tau_{*ds} < 0.047$ when $d_s > k_s$; (iv) the ratio of particle velocity V_p to mean flow velocity u_f lies in the range of 0.2 to 0.9, while Kalinske (1942) suggested 0.9 to 1.0; (v) the ratio of particle velocity V_p to shear velocity u_* lies in the range of 2.5 to 12.5, while Kalinske (1947) suggested 11.0, Bagnold (1956, 1973) suggested 8.5, Francis (1973) suggested 8.3 to 11.8, Fernandez Luque and van Beek (1976) suggested 11.5, Engelund and Fredsoe (1976, 1982)

suggested 6.0 to 10.0, Fleming and Hunt (1976) suggested 9.0, Abbott and Francis (1977) suggested 13.5 to 14.3, Mantz (1980) suggested 9.2, and Naden (1981) suggested 11.8; (vi) $0.01 < \tau_{*ks} < 0.15$; (vii) $Re_* > 100$; (viii) $V_p < 2w$; (ix) the threshold value for τ_{*ks} appears to be 0.01; (x) $u_*/w < 0.5$.

CHAPTER 4

DIMENSIONAL AND REGRESSION ANALYSIS

The subject of transport velocity of a single particle over rough open channel flow is complicated since it involves several unknown parameters, such as the drag coefficient and the friction coefficient. To date, theoretical solutions of particle velocities are uncertain at best. The approach of this Chapter is to combine the methods of dimensional and regression analysis. Roughness and rolling particle interactions have been proven to be highly dependent on geometrical constraints such as: particle sizes (both roughness and rolling), relative roughness, and bed slope.

The challenge becomes one of deriving an equation that encompasses the correct variables without being too awkward to use. Ideally, the derived equation should predict the desired output relatively well, without the inclusion of empirical coefficients. This Chapter first examines the CSU data and particularly the Shields parameter in term of

rolling particle diameter d_s and boundary roughness k_s. The dimensional and regression analyses are then presented. An empirical equation is finally tested with data from CSU, other laboratories and field measurements.

4.1. EXAMINATION OF SHIELDS APPROACH

The simplest empirical form of estimated bedload particle velocity based on analysis of CSU data is shown in Fig. 4.1, and is a variation of $V_p/[(G-1)gd_s]^{1/2} \sim u_*^2/(G-1)gk_s$.

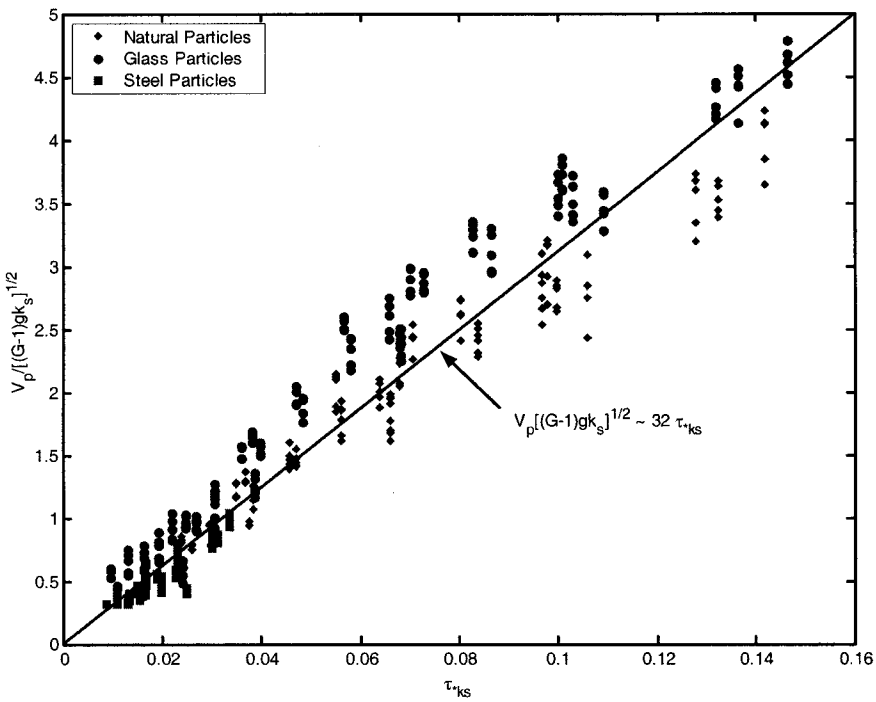

Figure 4.1: $V_p/[(G-1)gk_s]^{1/2}$ vs τ_{*ks}

From Fig. 4.1, we have

$$\frac{V_p}{\sqrt{(G-1)gd_s}} \sim 32\frac{u_*^{\,2}}{(G-1)gk_s} \tag{4.1}$$

or

$$\frac{V_p}{u_*} \sim 32\frac{u_*}{\sqrt{(G-1)gk_s}} \tag{4.2}$$

or

$$\frac{V_p}{u_*} \sim 32\tau_{*ks}^{\,1/2} \tag{4.3}$$

The bedload particle velocity can be estimated by

$$V_p \cong 32u_*\tau_{*ks}^{\,1/2} \tag{4.4}$$

Since the Shields parameter is usually written in term of d_s, a three-parameter empirical model is introduced. The variation of $V_p/[(G\text{-}1)gd_s]^{1/2}$ with Shields parameter $\tau_{*ds} = u_*^2/[(G\text{-}1)gd_s]$, and (k_s/d_s), then transforms (4.4) into power form equation as shown below

$$\frac{V_p}{\sqrt{(G-1)gd_s}} = a\left[\frac{u_*^{\,2}}{(G-1)gd_s}\right]^b\left(\frac{d_s}{k_s}\right)^c \tag{4.5}$$

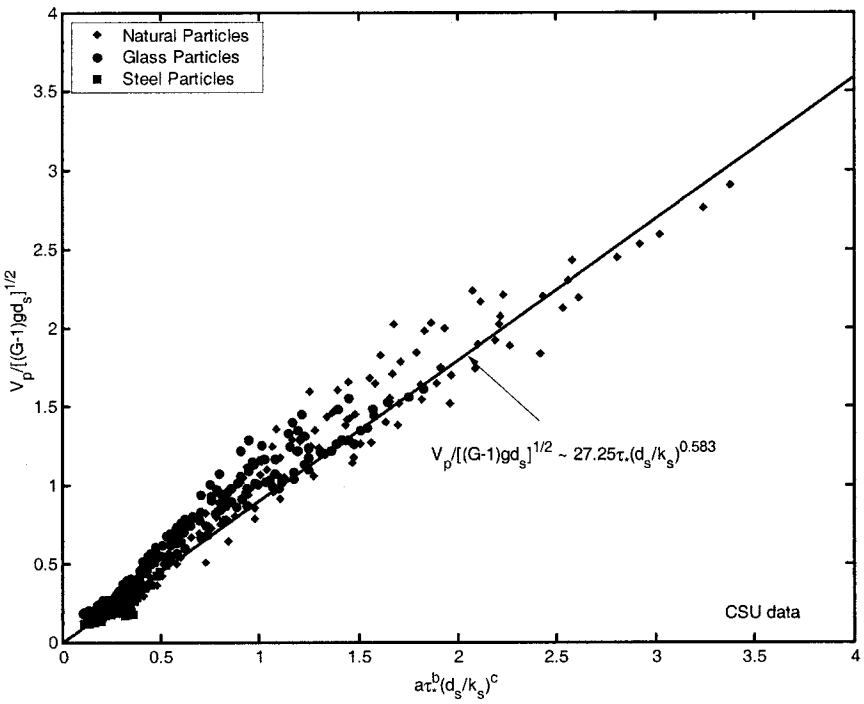

Figure 4.2: $V_p/[(G-1)gd_s]^{1/2} \sim 30.5\tau_{*ds}^{1.0}(d_s/k_s)^{0.583}$

Using EXCEL multiple regression analysis toolbox, the coefficients *a*, *b*, and *c* can be determined using:

$$\log\frac{V_p}{\sqrt{(G-1)gd_s}} = \log a + b\log\tau_{*ds} + c\log\left(\frac{d_s}{k_s}\right) \tag{4.6}$$

Applied to CSU's (1995) database, one obtains

$$V_p = 30.5\left[\frac{u_*^{\,2}}{(G-1)gd_s}\right]^1\left(\frac{d_s}{k_s}\right)^{0.583}\sqrt{(G-1)gd_s} \tag{4.7}$$

Similarly, when applied to the entire database, one obtains

$$V_p = 6.59\left[\frac{u_*^{\,2}}{(G-1)gd_s}\right]^{0.94}\left(\frac{d_s}{k_s}\right)^{1.1}\sqrt{(G-1)gd_s} \tag{4.8}$$

The rolling bedload particle velocity can be estimated by Eqs. (4.7) and (4.8), where: shear velocity $u_* = [gR_hS_f]^{1/2}$ (m/s), d_s = particle size (mm), k_s = bed roughness (mm), G = particle specific gravity, and g = gravitational acceleration (m/s^2). The comparison between calculated and observed rolling bedload particle velocity V_p is shown in Figs. 4.3 and 4.5; Figs 4.4 and 4.6 show a discrepancy ratio distribution using Eqs. (4.7), and (4.8). Since the empirical regression coefficients b and c are quite close to unity, the basic form of Eq. (4.1) is found to be representative of laboratory conditions. It is concluded that the Shields roughness parameter $\tau_{*ks} = u_*^2/[(G-1)gk_s]$ can be useful to determine bedload particle velocity.

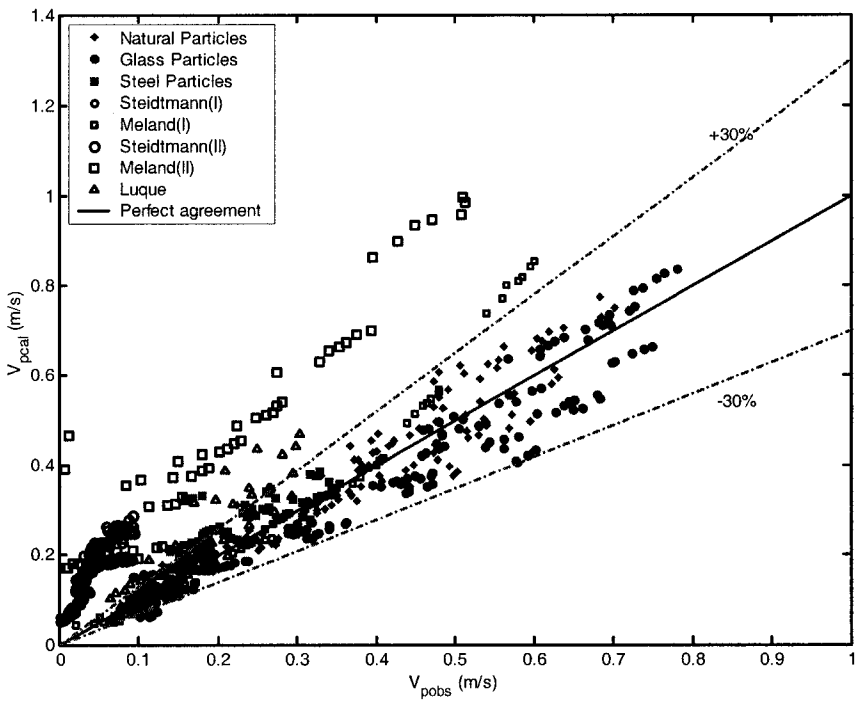

Figure 4.3: Comparison between Calculated and Observed V_p using Eq. (4.7)

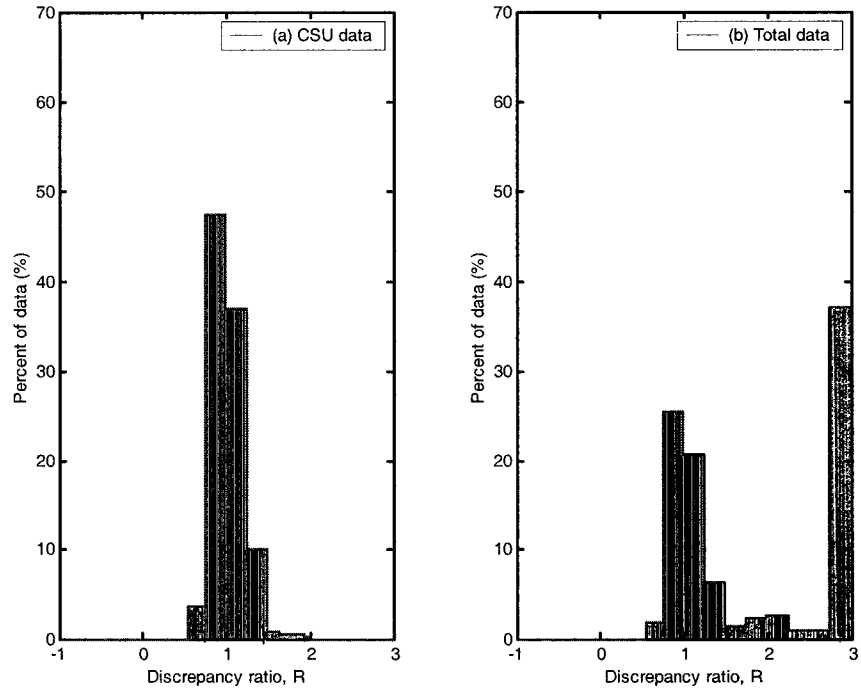

Figure 4.4: Discrepancy Ratio Distribution of V_p using Eq. (4.7)

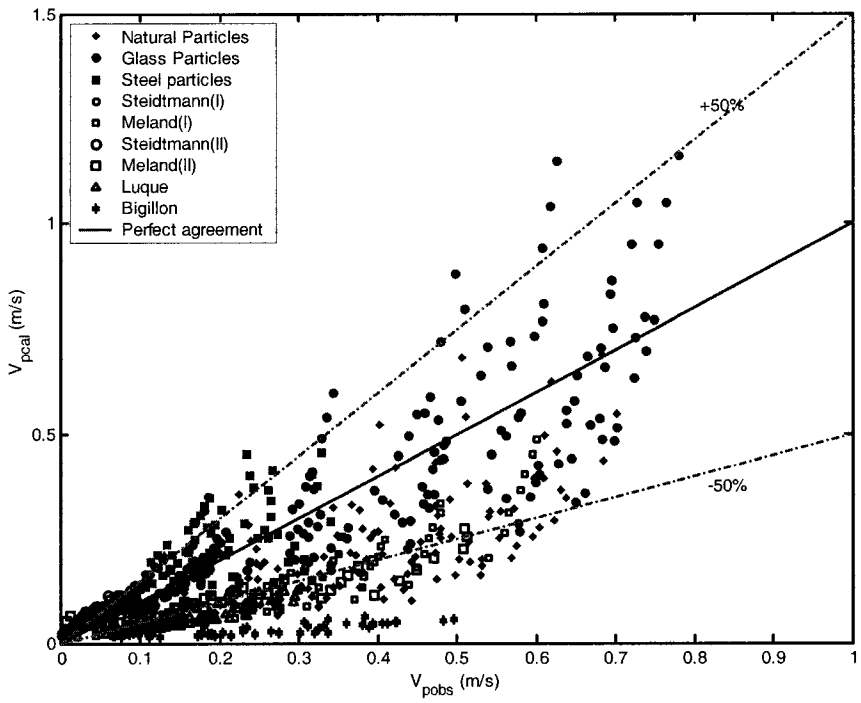

Figure 4.5: Comparison between Calculated and Observed V_p using Eq. (4.8)

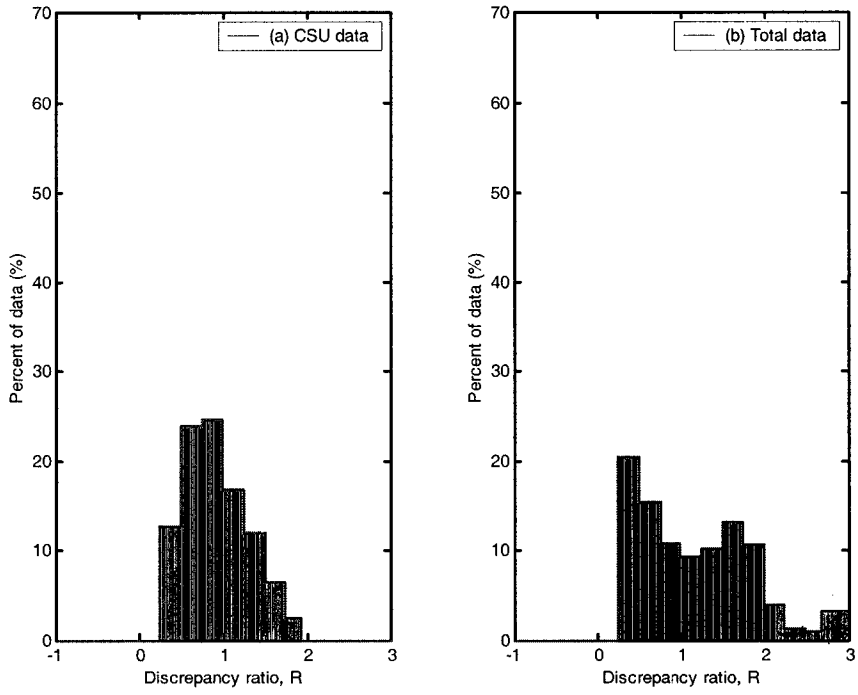

Figure 4.6: Discrepancy Ratio Distribution of V_p using Eq. (4.8)

4.2. DIMENSIONAL ANALYSIS

Dimensional analysis is adopted to find a functional relationship between the parameters affecting bedload particle velocity. The dependent variable is a function of six independent variables, with a total n = 7 variables:

$$V_p = f(u_*, (G-1), \nu, d_s, k_s, g) = 0 \tag{4.9}$$

in which f represents an unspecified function of the shear velocity u_*, particle specific gravity (G-1), kinematic viscosity of the fluid ν, bedload particle diameter d_s, bed roughness k_s, and gravitational acceleration g. After d_s, and g are selected as repeating variables, the two fundamental dimensions (j = 2) are rewritten in terms of repeating variables:

$$\left.\begin{aligned} d_s &= L \\ g &= \frac{L}{T^2} \end{aligned}\right\} \text{thus} \left\{\begin{aligned} L &= d_s \\ T &= \sqrt{\frac{d_s}{g(G-1)}} \end{aligned}\right.$$

After the relationships for L, T are substituted into the non-repeating variables, five π terms (n-j = 7-2 = 5) are obtained, respectively, from V_p, u_*, ν, (G-1), and k_s

π_1:

$$\frac{V_p T}{L} = \frac{V_p}{d_s}\sqrt{\frac{d_s}{g(G-1)}} = \frac{V_p}{\sqrt{(G-1)g d_s}} \tag{4.10}$$

π_2:

$$\frac{u_* T}{L} = \frac{u_*}{d_s}\sqrt{\frac{d_s}{g(G-1)}} = \frac{u_*}{\sqrt{(G-1)g d_s}} \tag{4.11}$$

π_3:

$$\frac{\nu T}{L^2} = \frac{\nu}{d_s^{\,2}}\sqrt{\frac{d_s}{g(G-1)}} = \frac{\nu}{d_s^{\,3/2}[g(G-1)]^{1/2}} \tag{4.12}$$

$$\pi_3^{\,2} = \frac{\nu^2}{d_s^{\,3}(G-1)g} = \frac{1}{d_*^{\,3}} \tag{4.13}$$

π_4:

$$\frac{k_s}{L} = \frac{k_s}{d_s} \tag{4.14}$$

$$\pi_5 = (G-1)$$

From π_1 to π_5, the five dimensionless parameters can thus be written

$$\frac{V_p}{\sqrt{(G-1)gd_s}} = F\left\{\frac{u_*}{\sqrt{(G-1)gd_s}}, \frac{1}{d_*^{\,3}}, \frac{k_s}{d_s}, (G-1)\right\} \tag{4.15}$$

The results from this dimensional analysis indicate that the dimensionless bedload particle velocity parameter is a function of the Shields parameter τ_{*ds}, boundary relative roughness k_s/d_s, dimensionless particle diameter d_*, and excess particle specific gravity (G-1). Further progress can be achieved only through physical understanding or an analysis of laboratory or field experiments. The bedload particle velocity is assumed to be proportional to the product of the powers of the dimensionless parameters

$$\frac{V_p}{\sqrt{(G-1)gd_s}} = a\left[\frac{u_*}{\sqrt{(G-1)gd_s}}\right]^b d_*^{\,c}\left(\frac{d_s}{k_s}\right)^d (G-1)^e \tag{4.16}$$

in which *a*, *b*, *c*, *d*, and *e* are coefficients to be determined from the multiple regression analysis.

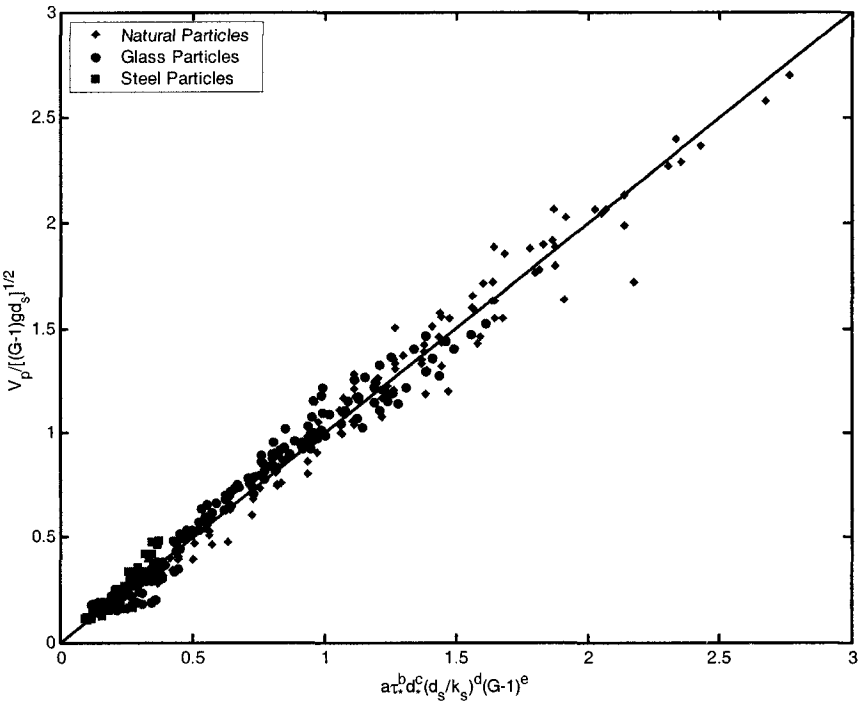

Figure 4.7: $V_p/[(G-1)gd_s]^{1/2}$ vs $11.5\tau_{*ds}^{0.95}d_*^{0.21}(d_s/k_s)^{0.36}(G-1)^{-0.28}$

Using EXCEL multiple regression analysis toolbox, the coefficients *a*, *b*, *c*, *d*, and *e* can be determined as follow

$$\log\frac{V_p}{\sqrt{(G-1)gd_s}} = \log a + b\log\left[\frac{u_*}{\sqrt{(G-1)gd_s}}\right] + c\log d_* + d\log\left(\frac{d_s}{k_s}\right) + e\log(G-1) \quad (4.17)$$

Applied to CSU's (1995) database we have

$$V_p = 11.5\left[\frac{u_*}{\sqrt{(G-1)gd_s}}\right]^{1.9} d_*^{0.21}\left(\frac{d_s}{k_s}\right)^{0.36}(G-1)^{-0.28}\left[(G-1)gd_s\right]^{0.5} \quad (4.18)$$

Similarly, applied to the total database, one obtains

$$V_p = 2.2\left[\frac{u_*}{\sqrt{(G-1)gd_s}}\right]^2 d_*^{0.5}\left(\frac{d_s}{k_s}\right)^{0.57}(G-1)^{-0.4}\left[(G-1)gd_s\right]^{0.5} \tag{4.19}$$

or

$$V_p = 2.2\tau_{*ds} d_*^{0.5}\left(\frac{d_s}{k_s}\right)^{0.57}(G-1)^{-0.4}\left[(G-1)gd_s\right]^{0.5} \tag{4.20}$$

The comparison between calculated and observed bedload particle velocity using Eqs. (4.18) and (4.20) is shown in Figs. 4.8 and 4.10; Figs. 4.9 and 4.11 show a discrepancy ratio distribution using Eqs. (4.18) and (4.20).

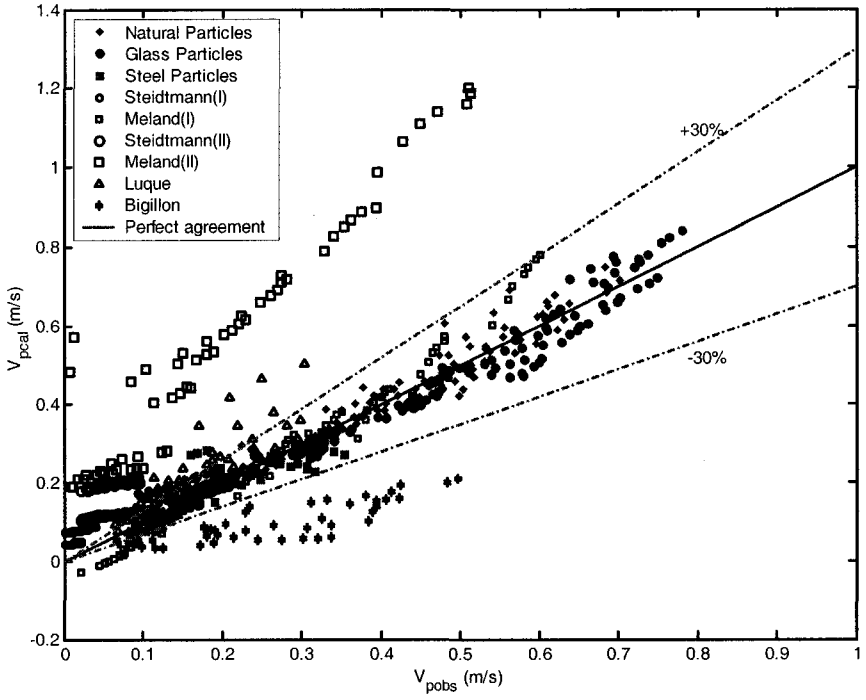

Figure 4.8: Comparison between Calculated and Observed V_p using Eq. (4.18)

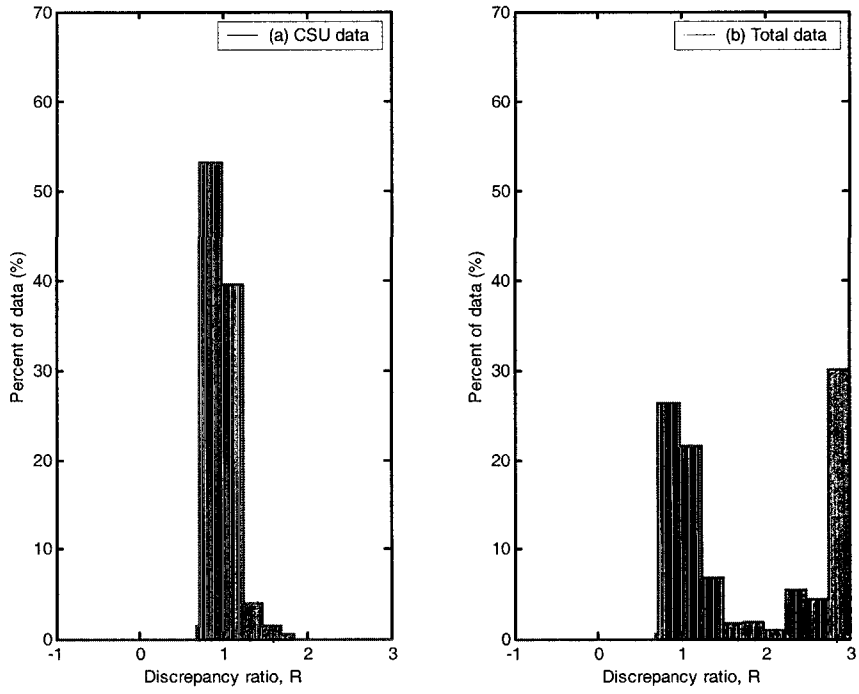

Figure 4.9: Discrepancy Ratio Distribution of V_p using Eq. (4.18)

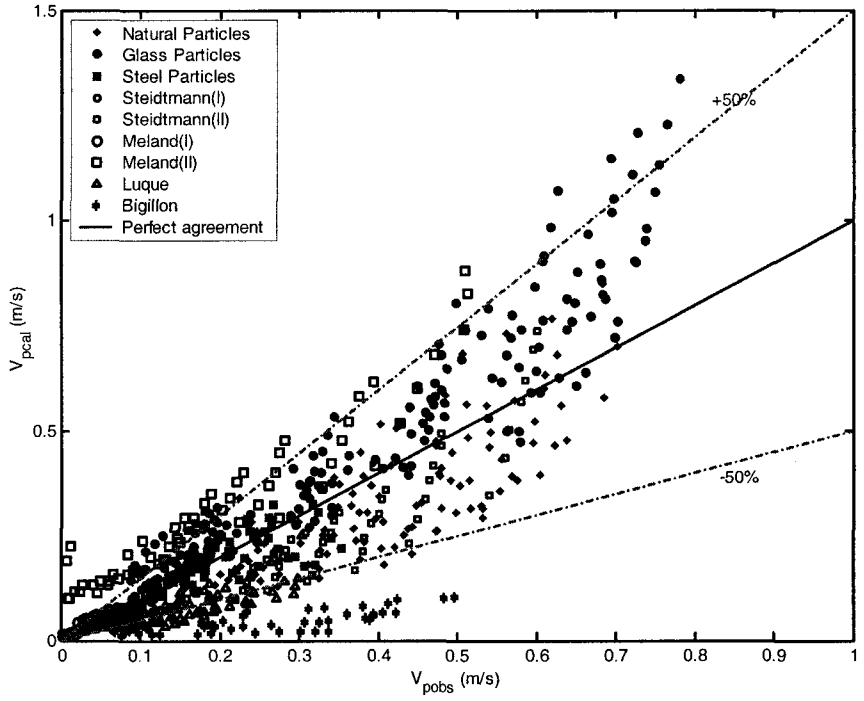

Figure 4.10: Comparison between Calculated and Observed V_p using Eq. (4.20)

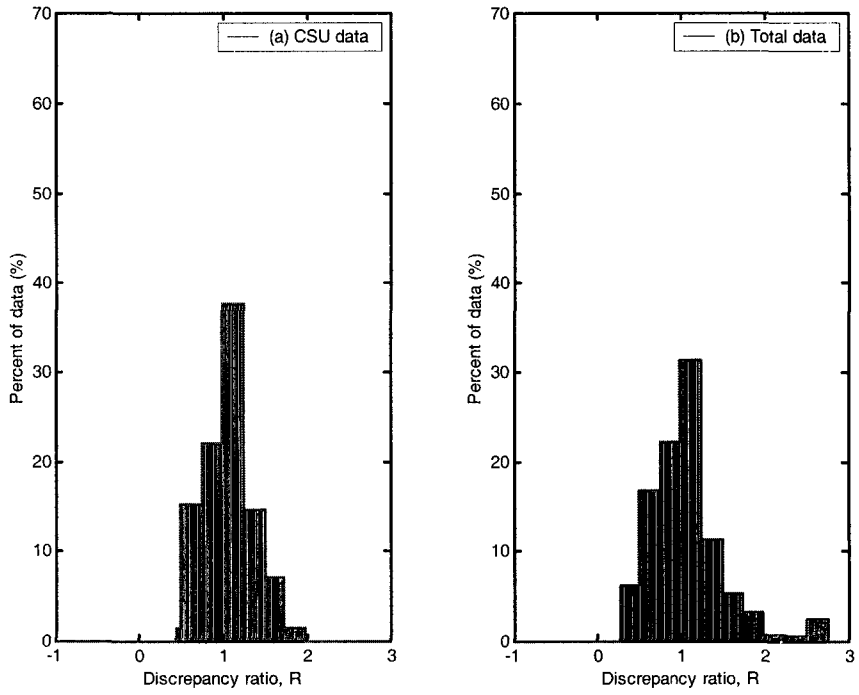

Figure 4.11: Discrepancy Ratio Distribution of V_p using Eq. (4.20)

The comparison between calculated and observed particle velocity using the proposed formula and the values is summarized in Table 4.1. A discrepancy ratio method is used to indicate the goodness of fit between calculated and observed results. It can be seen that for Eqs. (4.7) and (4.8) the percentages of data falling within the range of discrepancy ratios between 0.75 to 1.25 were in the range of 42.5 to 84.5% using the CSU database and 22.5 to 47.5% using the Total database; and for Eqs. (4.18) and (4.20) the percentages of data falling within the range of discrepancy ratios between 0.75 to 1.25 were in the range of 60 to 93% using the CSU database and 49 to 56% using the Total database.

Table 4.1: Comparison between Calculated and Observed V_p using Proposed Formulas

Equation	Data Sources	Data in Range of Discrepancy Ratio, R_i (%)				No. of Data Points	R^2
		0.75-1.25	0.5-1.5	0.25-1.75	0-2.0		
(1)	(2)	(3)	(4)	(5)	(6)	(7)	(8)
Eq. (4.7)	CSU	84.5	98.5	100	100	356	0.9
	Total	47.5	58	63.5	100	1018	0.7
Eq. (4.8)	CSU	42.5	79	98	100	356	0.54
	Total	22.5	49.5	84.5	100	1018	0.69
Eq. (4.18)	CSU	93	96.75	100	100	356	0.96
	Total	49	56.5	59	100	1018	0.7
Eq. (4.20)	CSU	60	92	98.5	100	356	0.77
	Total	56	85	97.5	100	1018	0.84

Eqs. (4.7), (4.8), (4.18), and (4.20) can be reduced to a simple form shown in Eq. (4.21); From Eq. (4.8), the exponents *b* and *c* are close to unity, one can approximate with

$$\frac{V_p}{\sqrt{(G-1)gd_s}} = a\left(\frac{u_*^2}{(G-1)gk_s}\right)$$

or

$$\frac{V_p}{u_*} = f\left[\left(\frac{u_*^2}{(G-1)gd_s}\right)^x\left(\frac{d_s}{k_s}\right)^y\right] \tag{4.21}$$

Notice that $V_p \rightarrow \infty$ when $k_s \rightarrow 0$; and there is no threshold for $V_p \rightarrow 0$ other than $k_s \rightarrow \infty$. Also, when $k_s = d_s$ at τ_{*ds} =0.047, Eq (4.21) does not reduce to $V_p = 0$.

4.3. SUMMARY

This proposed bedload particle velocity function, Eq. (4.20) is derived through the combination of dimensional analysis and regression analysis with a proposed formula in power form. Eq. (4.20) accounts for various flow and particle parameters, such as bed slope S, flow depth *y* (mm), viscosity of the fluid ν (m^2/s), particle size d_s (mm), bed roughness k_s (mm), specific gravity of the particles G, and gravitational acceleration *g* (m/s^2). Results showed that calculated and observed rolling bedload particle velocity fit very well when applied to both CSU and the total database.

The proposed rolling bedload particle velocity Eq. (4.20) predicts very well when $k_s \neq 0$, but when $k_s \rightarrow 0$ (smooth bed), then bedload particle velocity $V_p \rightarrow \infty$ (unbounded); when $d_s = k_s$, there is no value of τ_{*ds} (no threshold) as $V_p \rightarrow 0$. The following Chapter provides further analysis to define the maximum bedload particle velocity on smooth bed, and also the threshold condition for beginning of motion when $k_s \neq d_s$.

CHAPTER 5

BEDLOAD PARTICLE VELOCITY

The results of the dimensional and regression analysis in Chapter 4 indicate that: (i) when $k_s \rightarrow 0$ (smooth bed), then the bedload particle velocity $V_p \rightarrow \infty$; and (ii) there is no threshold value ($V_p \rightarrow 0$) when $k_s = d_s$. This Chapter examines the maximum bedload particle velocity over smooth beds. A theoretical analysis of particle velocity on smooth and rough surfaces are presented. The theoretical equation is then tested with laboratory and field databases. Sections 5.1 and 5.2 were modified from Guo (1997).

5.1. VELOCITY PROFILE NEAR SMOOTH BED

Since the particle moves near the smooth bed, the determination of the particle velocity profile is important. A turbulent flow over a smooth bed is composed of two regions: an inner and an outer region. The inner region is influenced by viscous shear, while the outer region is influenced by turbulent shear. The inner region is further divided

into three layers: the viscous sub-layer, the buffer layer and the log layer. Since the bedload movement always occurs near the bed, it relates to the velocity profile in the inner region. In the viscous sub-layer, the velocity distribution is

$$u^+ = y^+ \tag{5.1}$$

in which $u^+ = u_f / u_*$, $y^+ = u_* y / \nu$, u_f is the velocity at distance y from the bed, u_* is the shear velocity, and ν is the water kinematic viscosity. In the log layer, the velocity distribution is

$$u^+ = \frac{1}{\kappa} \ln y^+ + 5.5 \tag{5.2}$$

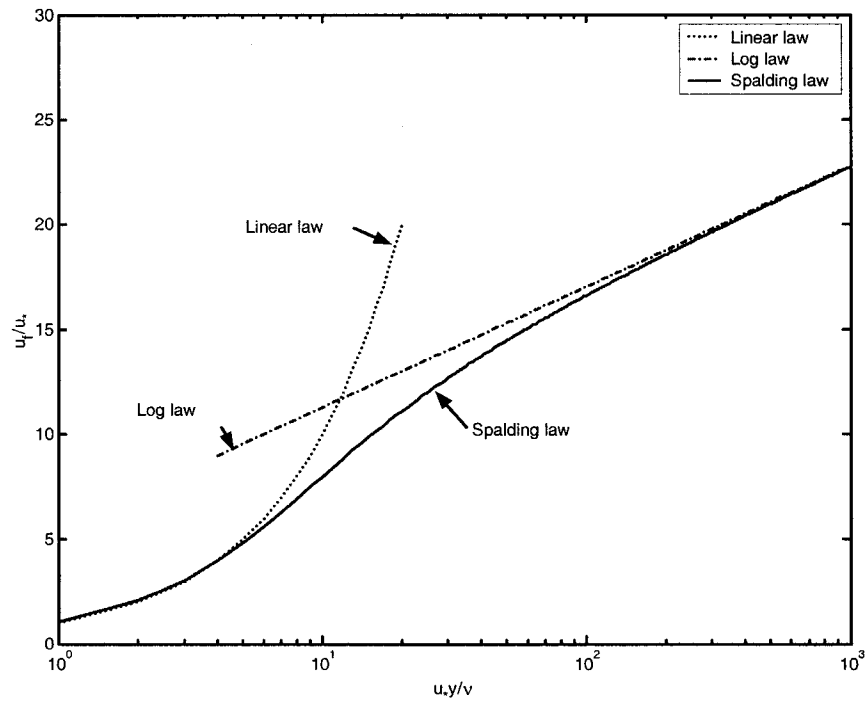

Figure 5.1: Velocity Profile In The Inner Region

In the buffer layer, Spalding's equation can be used (White, 1991, p.415), which is

$$y^+ = u^+ + \exp(-\kappa B)\left[\exp(\kappa u^+) - 1 - \kappa u^+ - \frac{(\kappa u^+)^2}{2} - \frac{(\kappa u^+)^3}{6}\right] \tag{5.3}$$

in which $\kappa = 0.4$ and B = 5.5. From equations (5.1) and (5.2), one has

$$\frac{du^+}{dy^+} = 1, \text{ for } y^+ \to 0 \tag{5.4a}$$

$$\frac{du^+}{dy^+} = \frac{1}{\kappa y^+}, \text{ for } y^+ \to \infty \tag{5.4b}$$

From the above expression, a general velocity gradient may be approximated by

$$\frac{du^+}{dy^+} = \frac{\kappa a^2 + y^+}{\kappa a^2 + \kappa y^{+2}} \tag{5.5}$$

The above equation satisfies the two asymptotic expressions. The integration of the Eq. (5.5) with the boundary condition $u^+ = 0$ at $y^+ = 0$ gives

$$u^+ = a\tan^{-1}\left(\frac{y^+}{a}\right) + \frac{1}{2\kappa}\ln\left[1 + \left(\frac{y^+}{a}\right)^2\right] \tag{5.6}$$

When $y^+ \to \infty$, the above equation reduces to

$$u^+ = \frac{1}{\kappa}\ln y^+ + \frac{\pi}{2}a - \frac{1}{\kappa}\ln a \tag{5.7a}$$

Comparing (5.7) with (5.2) gives

$$\frac{\pi}{2}a - \frac{1}{\kappa}\ln a = 5.5 \tag{5.7b}$$

Solving for a gives

$$a = 6.47 \tag{5.7c}$$

A plot of Eqs. (5.1) and (5.5) with $a = 6.47$ is shown in Figure 5.1.

5.2. MAXIMUM VELOCITY OF A PARTICLE ON SMOOTH BED

Consider that, for a sphere of diameter d_s, the slope angle of the plane is θ. The forces acting on the sphere include drag force, F_D, lift force, F_L, submerged weight of the sphere W_s, and resistance to the movement of the sphere F_f.

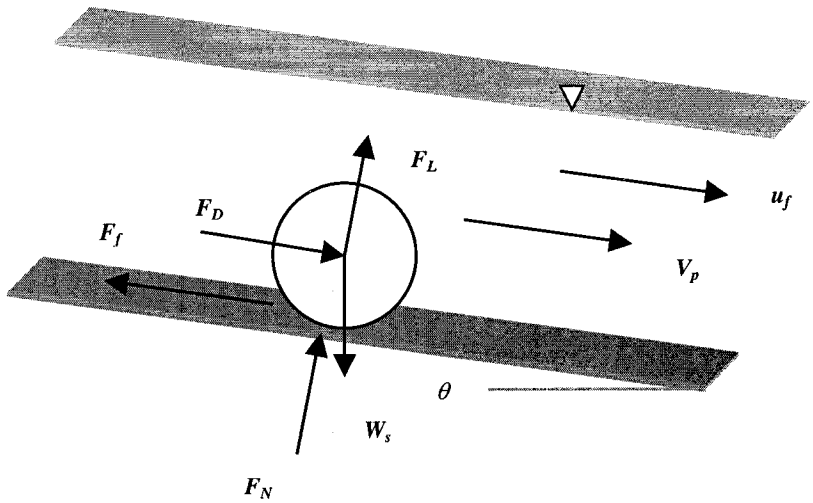

Figure 5.2: Forces Acting on a Sphere Rolling down an Inclined Smooth Bed

Considering the steady state, one can write the following equilibrium equations

$$W_s \sin\theta = F_D - F_f \tag{5.8}$$

$$W_s \cos\theta = F_N + F_L \tag{5.9}$$

The submerged weight is

$$W_s = \frac{1}{6}\pi\rho(G-1)gd_s^{\,3} \tag{5.10}$$

Assumed that the fluid moves faster than the particle, the drag force in the flowing fluid can be used

$$F_D \approx \frac{1}{2}C_D\rho(u_f - V_p)^2\frac{\pi d_s^{\,2}}{4} \tag{5.11}$$

in which α is an experimental coefficient. The lift force points upward and can be calculated

$$F_L = \frac{2}{3}\pi\rho d_s^{\,2}(u_f - V_p)V_p \tag{5.12}$$

The frictional force is

$$F_f \le \mu F_N \tag{5.13}$$

considering the equilibrium in the z-direction, one has

$$F_N = W_s\cos\theta - F_L = \frac{1}{6}\pi\rho(G-1)gd_s^{\,3}\cos\theta - \frac{2}{3}\pi\rho d_s^{\,2}(u_f - V_p)V_p \tag{5.14}$$

similarly, considering the equilibrium in the x-direction, one obtains

$$\frac{1}{6}\pi\rho(G-1)gd_s^{\,3}\sin\theta + \frac{1}{2}C_D\rho(u_f - V_p)^2\frac{\pi d_s^{\,2}}{4} \le \mu\left[\frac{1}{6}\pi\rho(G-1)gd_s^{\,3}\cos\theta - \frac{2}{3}\pi\rho d_s^{\,2}(u_f - V_p)V_p\right] \tag{5.15}$$

which shows that the particle accelerates all the time and a steady state is achieved when the equal sign is used in (5.15). The above equation can be rearranged in terms of $(u_f - V_p)$, i.e.

$$\left(1-\frac{16}{3}\frac{\mu}{C_D}\right)(u_f-V_p)^2+\frac{16}{3}\frac{\mu}{C_D}u_f(u_f-V_p)+\frac{4}{3C_D}(G-1)gd_s(\sin\theta-\mu\cos\theta)=0 \quad (5.16)$$

solving for $(u_f - V_p)$ gives

$$u_f - V_p = \frac{-b \pm \sqrt{b^2-4ac}}{2a} \quad (5.17)$$

in which

$$a = 1-\frac{16}{3}\frac{\mu}{C_D} \quad (5.18)$$

$$b = \frac{16}{3}\frac{\mu u_f}{C_D} \rangle 0 \quad (5.19)$$

$$c = \frac{4}{3C_D}(G-1)gd_s(\sin\theta-\mu\cos\theta) \quad (5.20)$$

since the fluid goes faster than the particle, the positive value of $(u_f - V_p)$ is the required solution, since b>0, the particle velocity is

$$V_p = u_f - \frac{\sqrt{b^2-4ac}-b}{2a} \quad (5.21)$$

For an experimental study, assume μ constant, C_D function of a Reynolds number $\mathrm{Re}_* = u_* d_s / \nu$, then the second term on the right hand side of (5.21) has the following function form

$$\frac{\sqrt{b^2-4ac}-b}{2a} = u_* f\left(\mathrm{Re}_*, \frac{u_f}{u_*}, (G-1)\frac{gd_s}{u_*^2}, \theta, \mu\right) \quad (5.22)$$

Considering u_f / u_* at $y = d_s$ is also a function of Re_* from the velocity profile equation in a smooth bed, and θ has been merged into the shear velocity u_*, the above relation should become primarily dependent on Re* and to a lesser degree depend on θ, μ, and d*

$$\frac{V_p}{u_*} = f(\mathrm{Re}_*, d_*, \mu, \theta) \tag{5.23}$$

As approximation, one can plot V_p/u_* vs Re* as shown in Fig. 5.3. Applying Eq. (5.6) with a correction factor β, one obtains

$$\frac{V_p}{u_*} = a\tan^{-1}\left(\frac{\mathrm{Re}_*}{\beta a}\right) + \frac{1}{2\kappa}\ln\left[1+\left(\frac{\mathrm{Re}_*}{\beta a}\right)^2\right] \tag{5.27}$$

in which $\kappa = 0.4$ and $a = 6.47$, as for Eq. (5.6), Guo (1997) used the Matlab Nonlinear Optimization Toolbox to determine that $\beta = 4$. The rolling bedload particle velocity for smooth bed can be estimated by

$$V_p = \left\{6.47\tan^{-1}\left(\frac{\mathrm{Re}_*}{25.88}\right) + \frac{1}{2\kappa}\ln\left[1+\left(\frac{\mathrm{Re}_*}{25.88}\right)^2\right]\right\} \times u_* \tag{5.28}$$

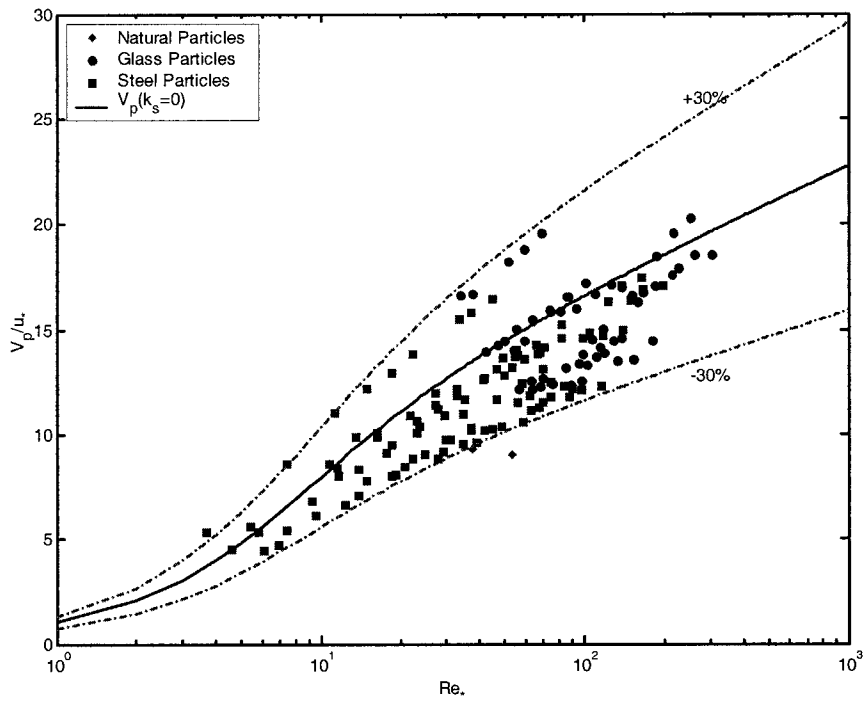

Figure 5.3: V_p/u_* vs Re_* using Eq. (5.28)

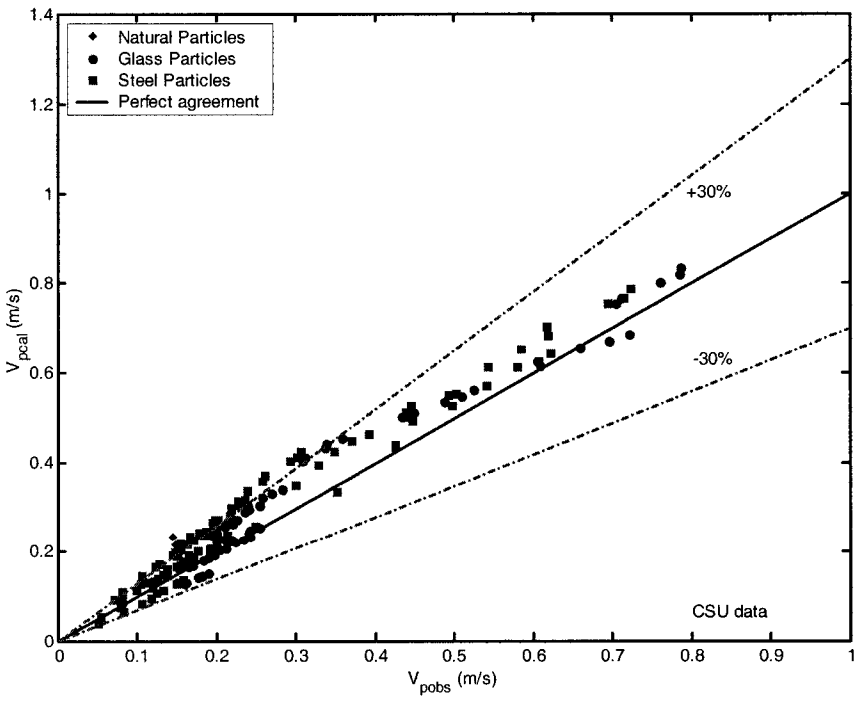

Figure 5.4: Comparison between Calculated and Observed V_p using Eq. (5.28)

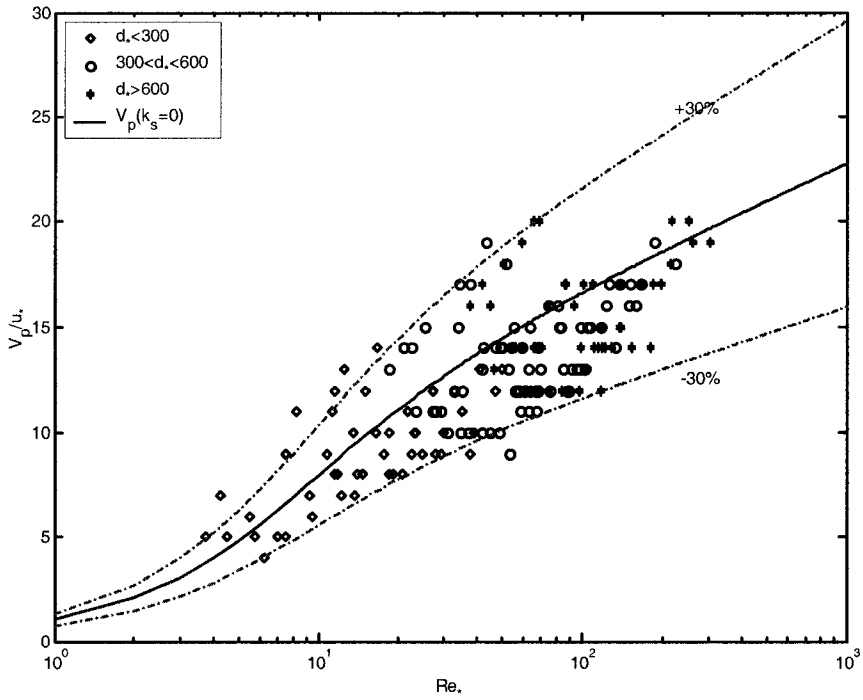

Figure 5.5: V_p/u_* vs Re_* using Eq. (5.28) for different values of d_*

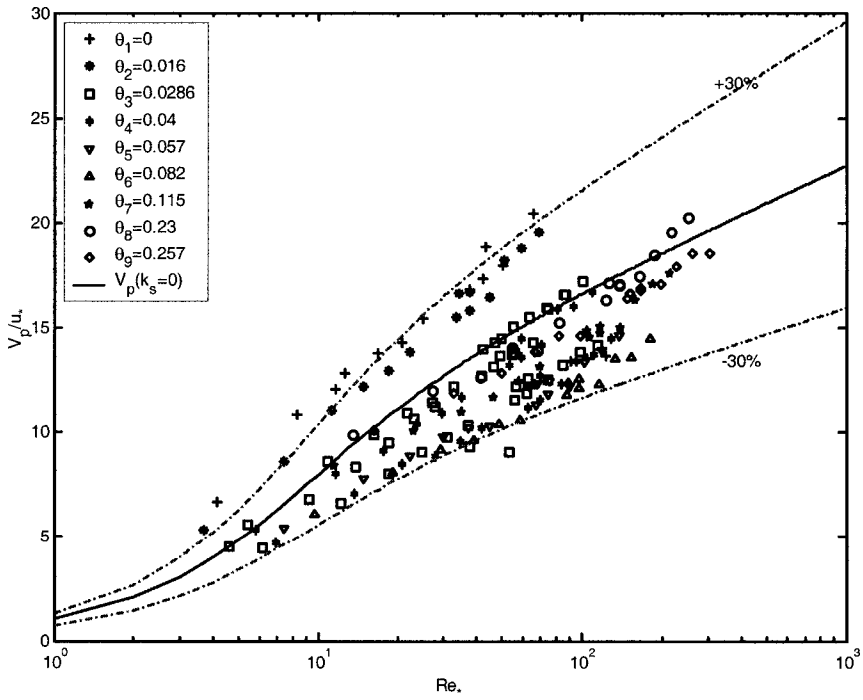

Figure 5.6: V_p/u_* vs Re_* using Eq. (5.28) for different values of θ

5.3. SINGLE PARTICLE ROLLING DOWN AN INCLINED ROUGH BED

Consider a sphere of diameter d_s rolling in a flowing fluid over an inclined bed of roughness. The slope angle of the plane is θ. The forces acting on the sphere include drag force, F_D, lift force, F_L, submerged weight of the sphere W_s, and resistance to the movement of the sphere from boundary F_f.

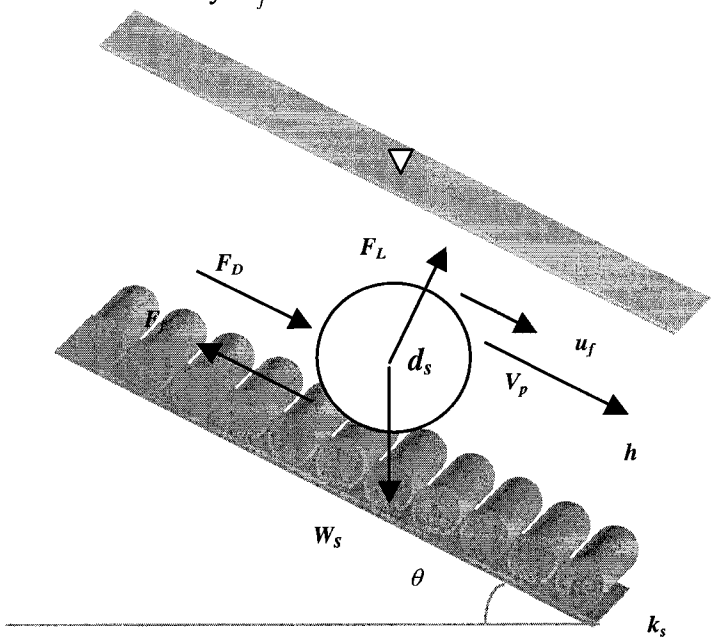

Figure 5.7: Forces Acting on a Sphere Rolling down an Inclined Bed of Roughness

$$\frac{V_p}{u_*} = \frac{V_{psmooth}}{u_*} - \Delta B \tag{5.29}$$

where the boundary roughness function $\Delta B = f(k_s, \tau_{*ds}, d_*)$. A plot of V_p / u_* as a function of Re_* and ΔB for both smooth and rough beds is shown in Fig. 5.9. After substituting Eq. (5.29) to particle velocity on smooth bed, Eq. (5.29) reduces to

$$\frac{V_p}{u_*} = 6.47 \tan^{-1}\left(\frac{\mathrm{Re}_*}{25.88}\right) + \frac{1}{2\kappa} \ln\left[1 + \left(\frac{\mathrm{Re}_*}{25.88}\right)^2\right] - \Delta B \tag{5.30}$$

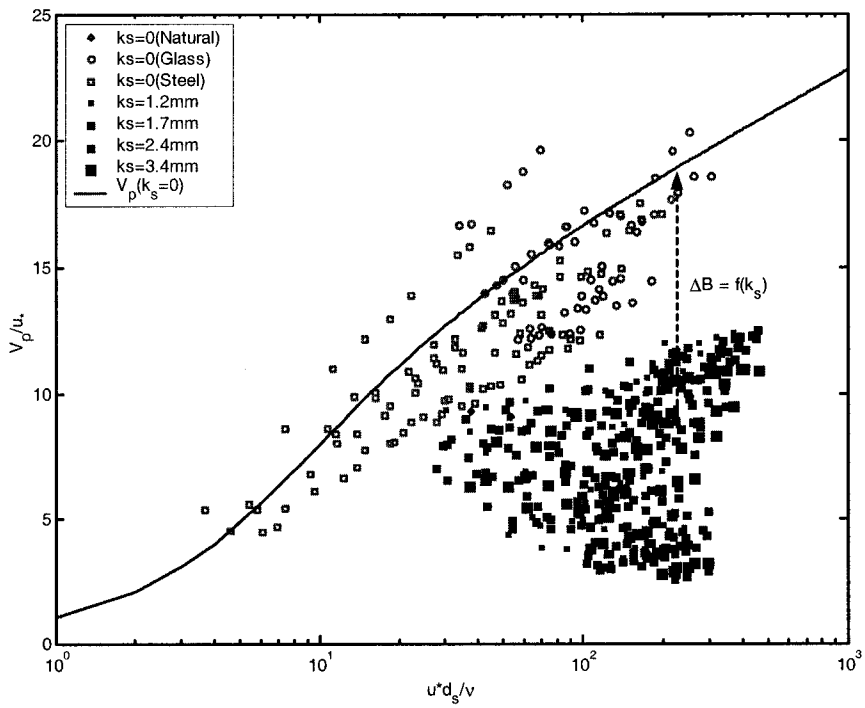

Figure 5.8: V_p/u_* vs Re_* for Smooth ($k_s = 0$) and Rough Bed ($k_s > 0$)

or

$$\Delta B = 6.47 \tan^{-1}\left(\frac{\mathrm{Re}_*}{25.88}\right) + \frac{1}{2\kappa}\ln\left[1+\left(\frac{\mathrm{Re}_*}{25.88}\right)^2\right] - \frac{V_p}{u_*} \tag{5.31}$$

Due to the effect of bed roughness k_s, particle size d_s, shear velocity u_*, and fluid kinematic viscosity ν, on bedload particle velocity V_p, we can assume that the calculated value ΔB_c can be obtained as a function of Shields parameter τ_{*ds}, dimensionless particle diameter d_*, and relative roughness (k_s/d_s) as

$$\Delta B_c = a\tau_{*ds}{}^b d_*{}^c \left(\frac{k_s}{d_s}\right)^d \tag{5.32}$$

or

$$\log \Delta B_c = \log a + b \log \tau_{*ds} + c \log d_* + d \log\left(\frac{k_s}{d_s}\right) \tag{5.33a}$$

the calibration parameters a, b, c, and d are obtained using the EXCEL multiple regression analysis toolbox. The analysis is applied to the CSU database

$$\Delta B_c = 0.884 \tau_{*ds}^{-0.229} d_*^{0.32} \left(\frac{k_s}{d_s}\right)^{0.333} \tag{5.33b}$$

Substituting (5.33b) into (5.30), and solving for V_p, one obtains

$$V_p = \left\{6.47 \tan^{-1}\left(\frac{\mathrm{Re}_*}{25.88}\right) + \frac{1}{2\kappa} \ln\left[1 + \left(\frac{\mathrm{Re}_*}{25.88}\right)^2\right] - 0.884 \tau_{*ds}^{-0.229} d_*^{0.32} \left(\frac{k_s}{d_s}\right)^{0.333}\right\} \times u_* \tag{5.34}$$

The agreement between ΔB and ΔB_c is shown in Fig. 5.9. There is a reasonable good fit ($R^2 = 0.9$) between calculated and observed ΔB.

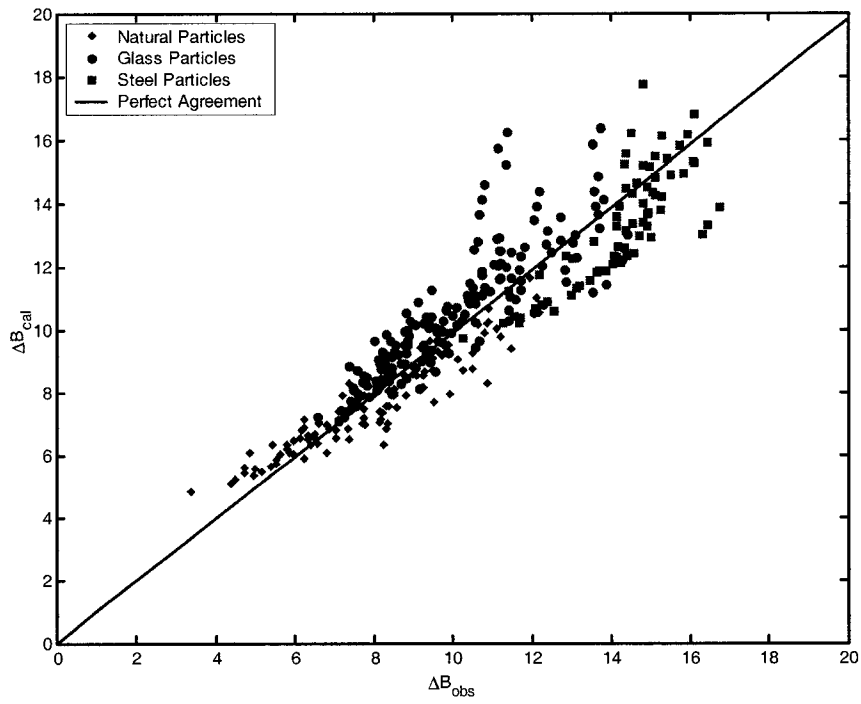

Figure 5.9: ΔB_{cal} vs ΔB_{obs} using Eq. (5.33b) for CSU data

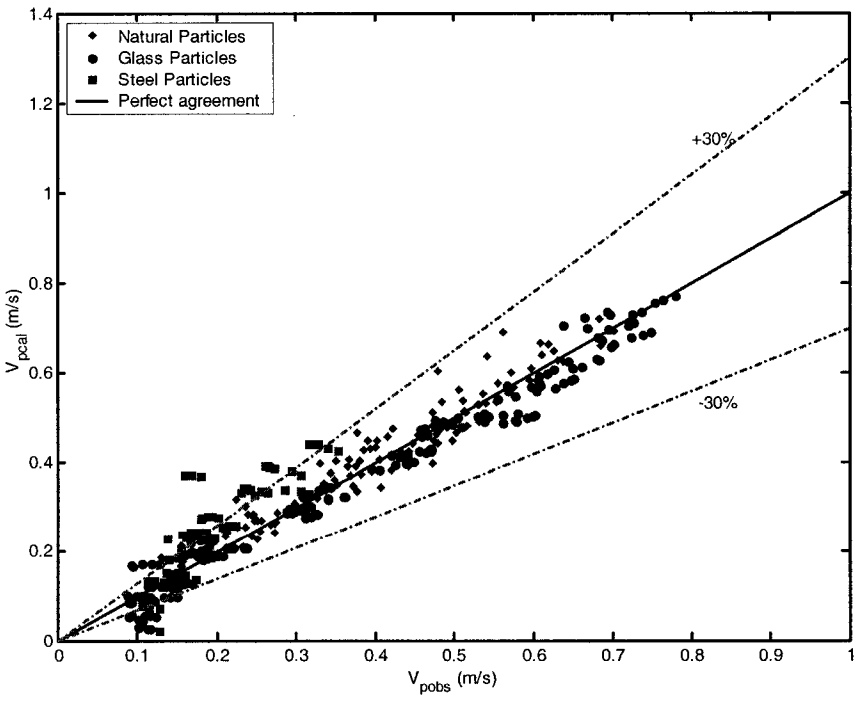

Figure 5.10: Comparison between Calculated and Observed V_p using Eq. (5.34)

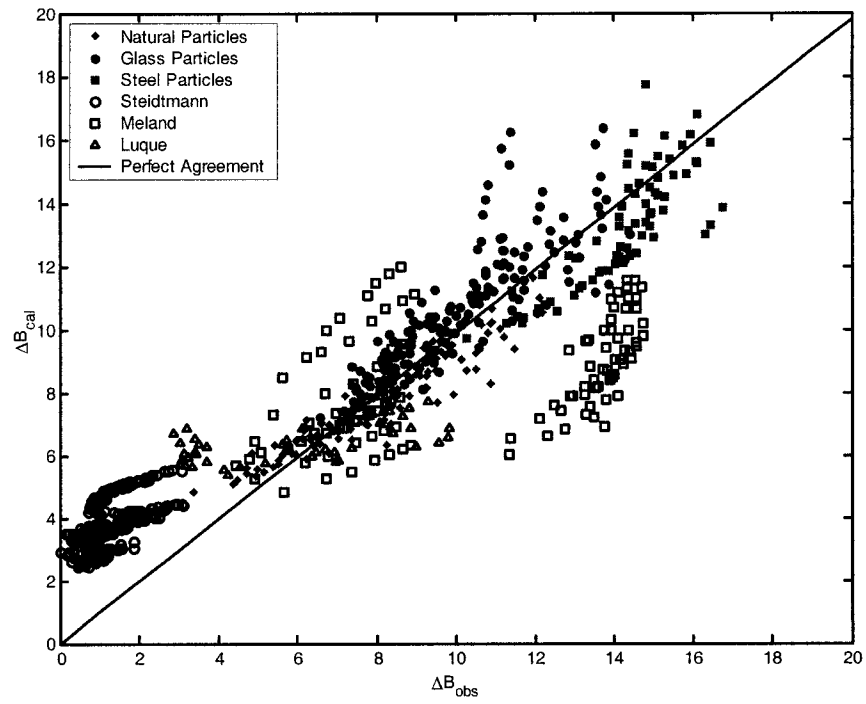

Figure 5.11: ΔB_{cal} vs ΔB_{obs} using Eq. (5.33b) for total data

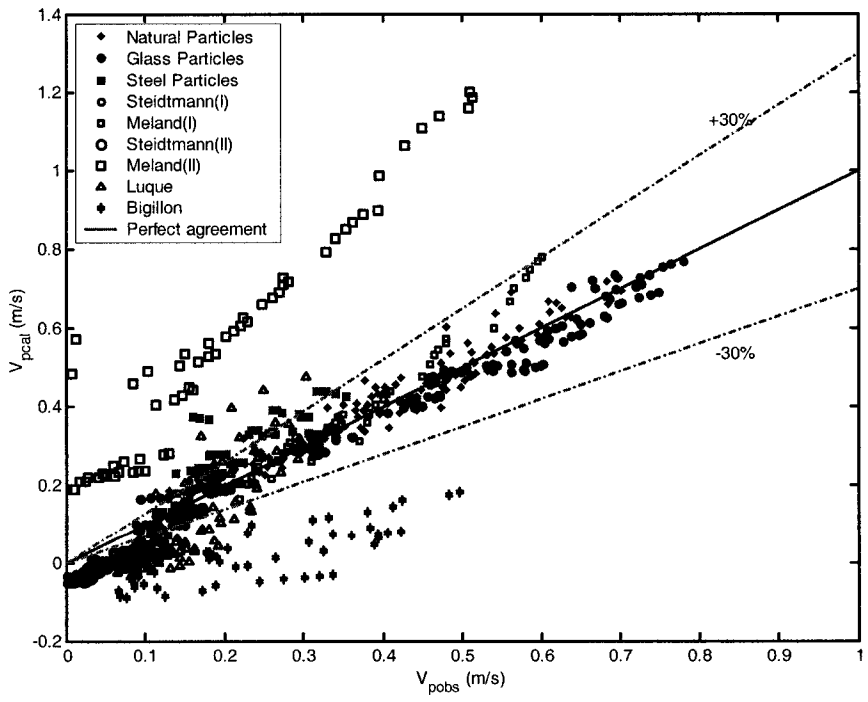

Figure 5.12: Comparison between Calculated and Observed V_p using Eq. (5.34)

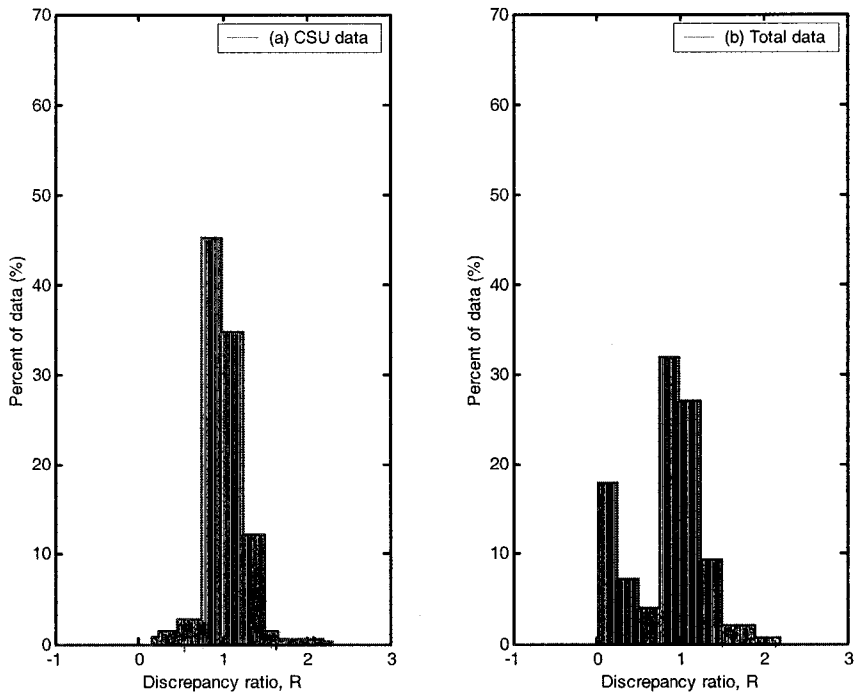

Figure 5.13: Discrepancy Ratio Distribution of V_p using Eq. (5.34)

The analysis is applied to the Total database

$$\Delta B_c = 0.096\tau_{*ds}^{-0.048} d_*^{0.93}\left(\frac{k_s}{d_s}\right)^{0.61} \tag{5.33c}$$

Substituting (5.33c) into (5.30), and solving for V_p, one obtains

$$V_p = \left\{6.47\tan^{-1}\left(\frac{\mathrm{Re}_*}{25.88}\right)+\frac{1}{2\kappa}\ln\left[1+\left(\frac{\mathrm{Re}_*}{25.88}\right)^2\right]-0.096\tau_{*ds}^{-0.048} d_*^{0.93}\left(\frac{k_s}{d_s}\right)^{0.61}\right\}\times u_* \tag{5.35}$$

where: $\mathrm{Re}_* = u_* d_s/\nu$, shear velocity $u_* = [gR_hS]^{1/2}$ (m/s), d_s = particle size (mm), k_s = bed roughness (mm), ν = fluid kinematic viscosity (m^2/s), G = particle specific gravity, g = gravitational acceleration (m/s^2), and Shields parameter $\tau_{*ds} = u_*^2/(G-1)gd_s$, and κ = von Karman constant (0.4);

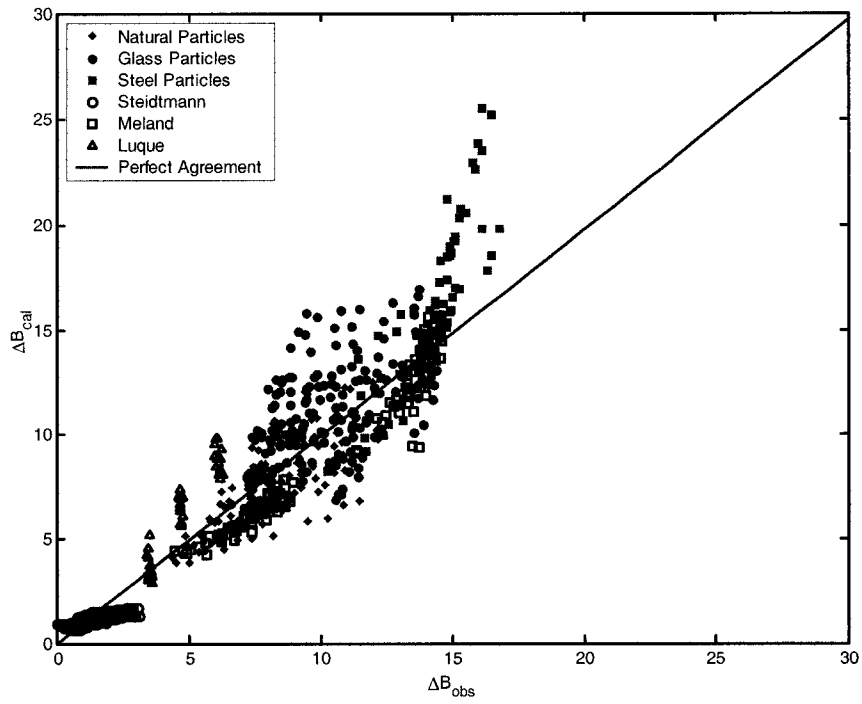

Figure 5.14: ΔB_{cal} vs ΔB_{obs} using (5.33c) for total data

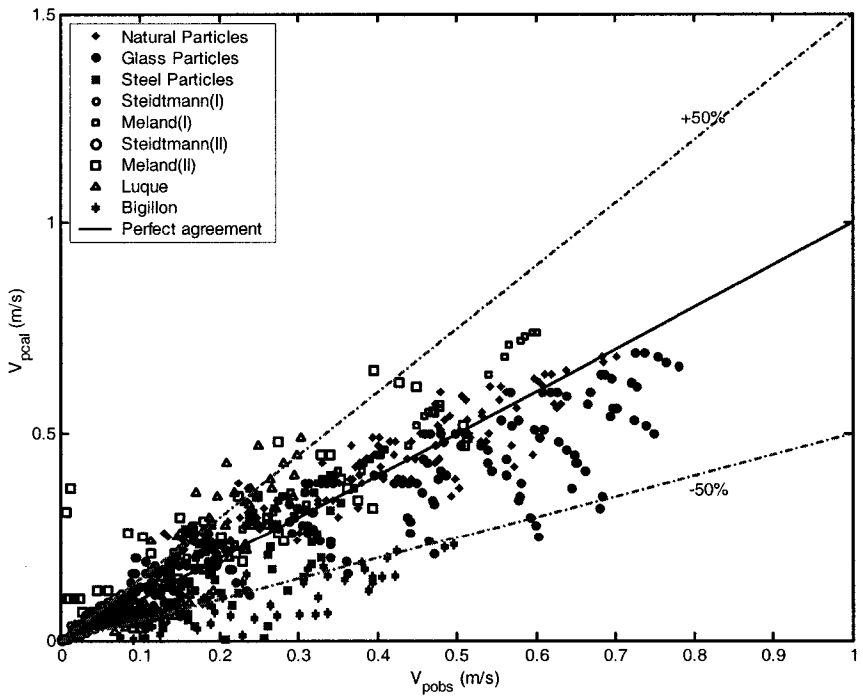

Figure 5.15: Comparison between Calculated and Observed V_p using Eq. (5.35)

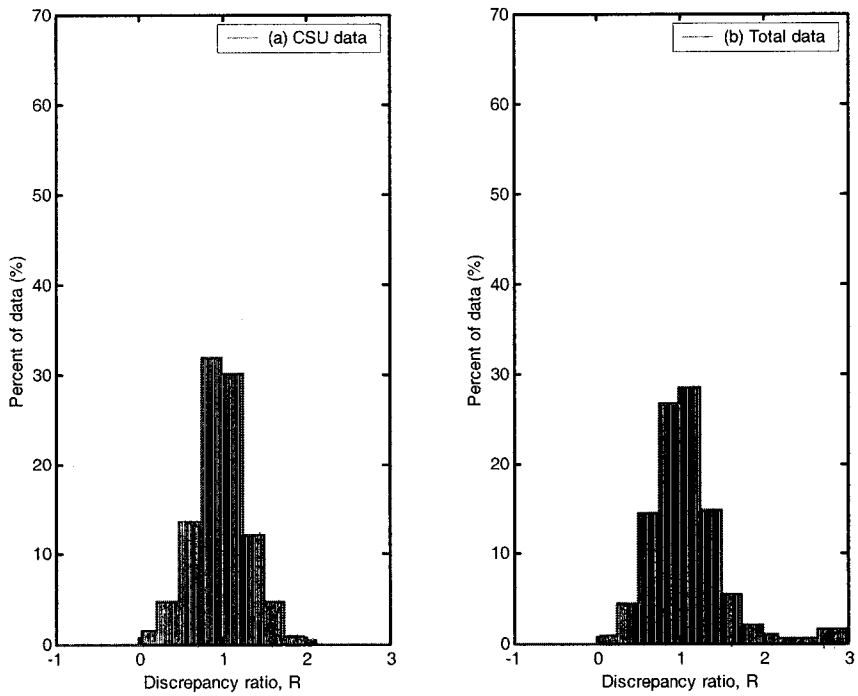

Figure 5.16: Discrepancy Ratio Distribution of V_p using Eq. (5.35)

The bedload particle velocity can be calculated by Eq. (5.34), Fig. 5.12, shows the comparison between calculated and observed rolling bedload particle velocity V_p using Eq. (5.34); and Fig. 5.13, shows the discrepancy ratio distribution for V_p using Eq. (5.34). The comparison between calculated and observed particle velocity using the proposed formula is summarized in Table 5.1. A discrepancy ratio method is used to indicate the goodness of fit between calculated and observed values. It can be seen that the percentages of data falling within the range of discrepancy ratios between 0.75 to 1.25 were at least 60% using the total database.

Table 5.1: Summary of Comparison between Calculated and Observed V_p

Equation	Data Sources	Data in Range of Discrepancy Ratio, R_i (%)				No. of Data Points	R^2
		0.75-1.25	0.5-1.5	0.25-1.75	0-2.0		
(1)	(2)	(3)	(4)	(5)	(6)	(7)	(8)
Eq. (5.34)	CSU	80	95	100	100	356	0.93
	Total[(1)]	60	75	82	100	1018	0.83
Eq. (5.35)	CSU	59.5	84	93.5	100	356	0.68
	Total	54	83	92.5	100	1018	0.82

(1) = Meland (1966) + Luque (1976) + Steidtmann (1982) + Bridge (1984) + CSU (1995) + Bigillon (2001)

5.4. ANALYSIS OF THE THRESHOLD CONDITION

The goal of this section is to find the threshold condition in term of bed roughness size required the particle to stop rolling. The first approach is with reference to the CSU data, Fig. 5.17 shows $\tau_{*ds}/0.047$ against relative roughness d_s/k_s for different values of V_p/u_*.

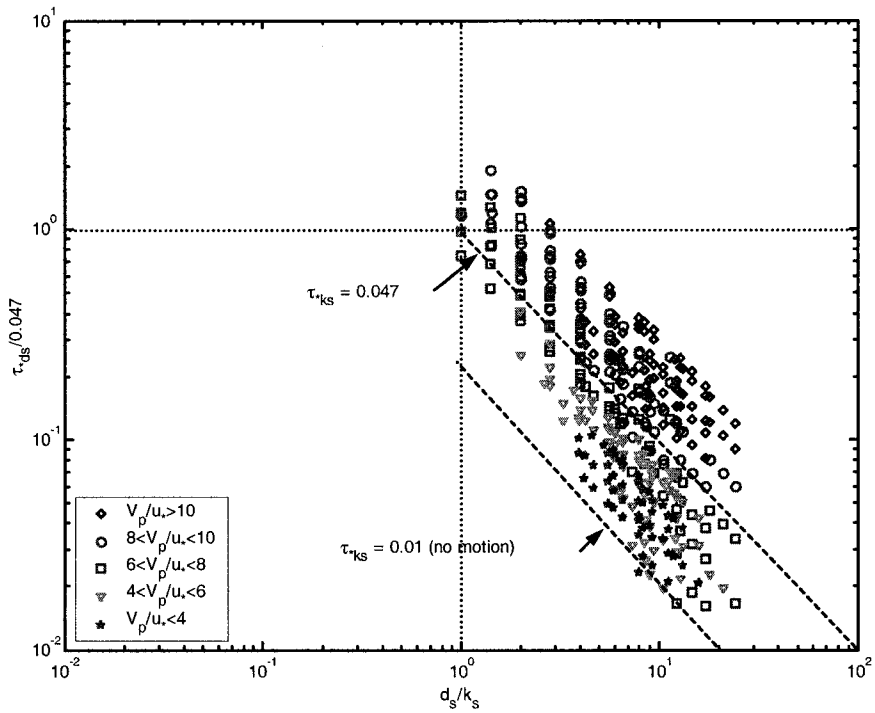

Figure 5.17: $\tau_{*ds}/0.047$ vs d_s/k_s, for different values of V_p/u_*

Very few particles are shown to move at values of shear stress below

$$\frac{\tau_{*ds}}{0.047} = 0.213\frac{k_s}{d_s} \tag{5.36}$$

this defines beginning of motion as

$$(\tau_{*ks})_c = \frac{u_*^{\,2}}{(G-1)gd_s}\left(\frac{d_s}{k_s}\right) = \left[\frac{u_*^{\,2}}{(G-1)gk_s}\right]_c = 0.213\times 0.047 = 0.01 \qquad (5.37)$$

The result describes above $(\tau_{*ks})_c \approx 0.01$. Fig. 5.17 shows there are a few data points have the values of $\tau_{*ks} < 0.01$.

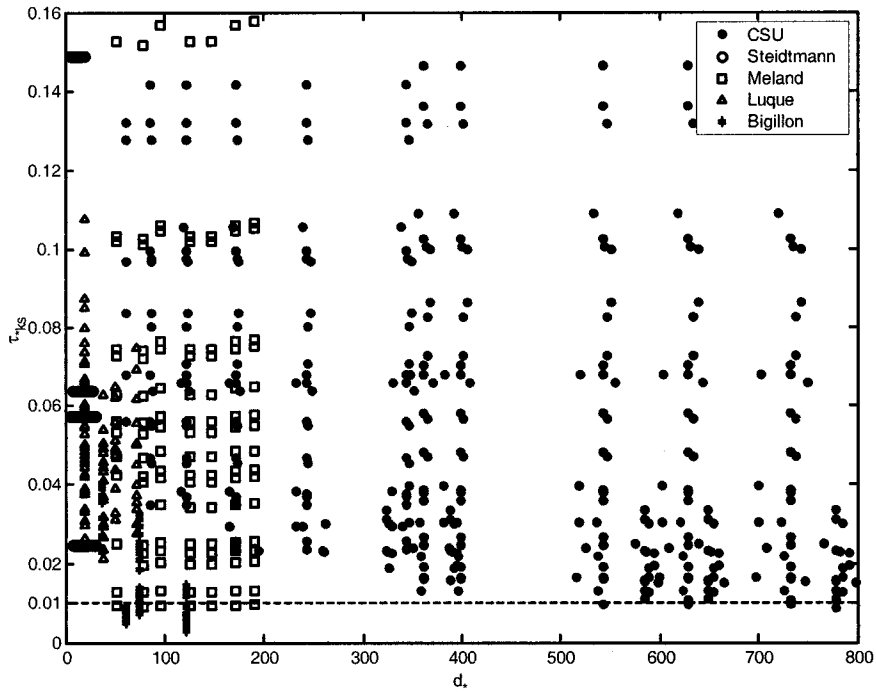

Figure 5.18: τ_{*ks} vs d_* for different databases

The second approach is to find the bed roughness size k_s that correspond to $V_p = 0$ in (5.31). Accordingly, threshold condition occurs from Eq. (5.34) when

$$k_{sc} = d_s\left\{\frac{6.47\tan^{-1}\left(\frac{\mathrm{Re}_*}{25.88}\right)+\frac{1}{2\kappa}\ln\left[1+\left(\frac{\mathrm{Re}_*}{25.88}\right)^2\right]}{0.884\tau_*^{-0.229}d_*^{0.32}}\right\}^{\frac{1}{0.333}} \qquad (5.38)$$

Threshold condition, or $V_p = 0$ (no motion), is obtained when $k_s = k_{sc}$. Particles move when $k_s < k_{sc}$, and stop when $k_s \geq k_{sc}$.

5.5. SUMMARY

Two functions of the transport velocity of a single particle on a smooth bed Eq. (5.28) and on a rough bed Eq. (5.34) are defined through theoretical and empirical analysis. The results show that the bedload particle velocity on smooth beds is approximately equal to the flow at the center of the particles. The roughness function ΔB describes the effect of bed roughness on reducing transport velocity of rolling bedload particles. This function ΔB varies with bed slope S, flow depth y (mm), viscosity of the fluid ν (m^2/s), particle size d_s (mm), bed roughness k_s (mm), specific gravity of the particles G, and gravitational acceleration g (m/s^2). The proposed bedload particle velocity formula, Eq. (5.34) reduces to Eq. (5.28) when $k_s \rightarrow 0$. When $k_s = d_s$, $V_p \sim (5 - 11)u_*$, and τ_{*ds} decreases when $V_p \rightarrow 0$. Particles reach incipient motion when $\tau_{*ks} \approx 0.01$, or when $k_s = k_{sc}$ defined in Eq. (5.38).

CHAPTER 6

LABORATORY AND FIELD APPLICATIONS

In this chapter, a general procedure for the calculation of bedload particle velocity is presented. This procedure is illustrated through a detailed example problem, followed with field applications.

6.1. PROPOSED METHOD

1. Input data

    - Particle diameter d_s (mm)
    - Flow depth y (mm)
    - Bed slope S_f

- Bed roughness k_s (mm)
- Flow viscosity ν (m^2/s)
- Particle specific gravity G

2. Calculation of the basic parameters
   - Shear velocity $u_* = [gR_hS_f]^{1/2}$ (m/s)
   - Shields particle parameter $\tau_{*ds} = u_*^2/(G-1)gd_s$
   - Shields roughness parameter $\tau_{*ks} = u_*^2/(G-1)gk_s$
   - Boundary relative roughness d_s/k_s, and k_s/d_s
   - Particle shear Reynolds number $Re_* = u_*d_s/\nu$
   - Dimensionless particle diameter $d_* = d_s[(G-1)g/\nu^2]^{1/3}$
3. Calculation of bed roughness critical k_{sc} from Eqs. (5.37) and (5.38) to determine the motion of the particle.
4. Calculation of $V_{psmooth}$ use Eq. (5.28); V_p use Eqs. (5.34), (5.35), and may also use Eq. (4.20).

6.2. TESTING EXISTING FORMULAS WITH ENTIRE DATABASE

Figs. 6.1, 6.3 and 6.5 illustrate the comparison between calculated and observed bedload particle velocity V_p, by applying the Meland and Norrman (1966), Fernandez Luque and van Beek (1976), and Bridge and Dominic (1984) equations to all assembled data. Figs. 6.2, 6.4 and 6.6 show a discrepancy ratio distribution for Meland and

Norrman, Fernandez Luque and van Beek, and Bridge and Dominic equations respectively. Results show that Fernandez Luque and van Beek, and Bridge and Dominic predict their own data very well, but none of Meland and Norrman, Fernandez Luque and van Beek, and Bridge and Dominic equations compare well with the entire database.

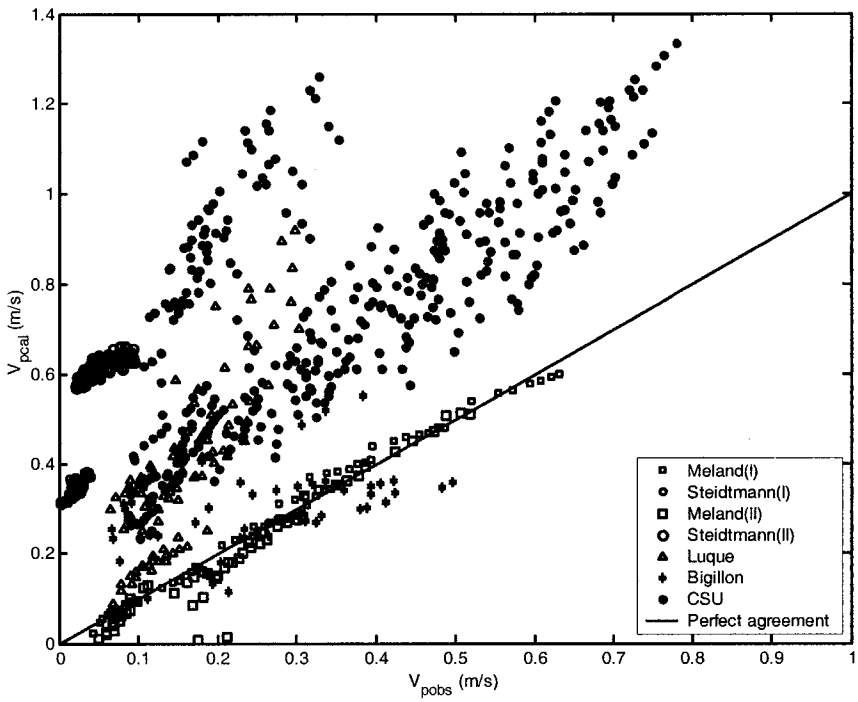

Figure 6.1: Comparison between Calculated and Observed V_p using Eq. (2.9)

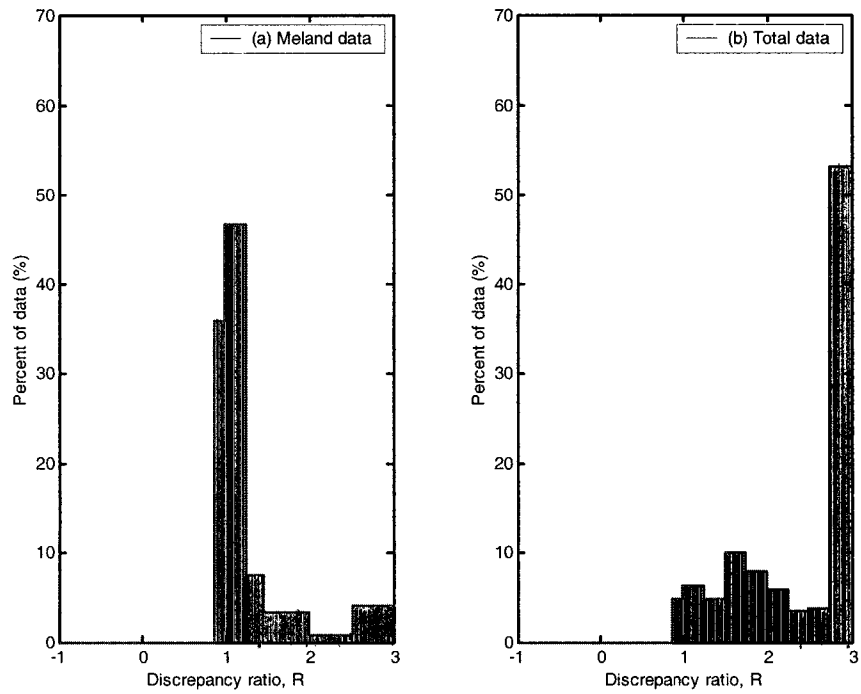

Figure 6.2: Discrepancy Ratio Distribution of V_p using Eq. (2.9)

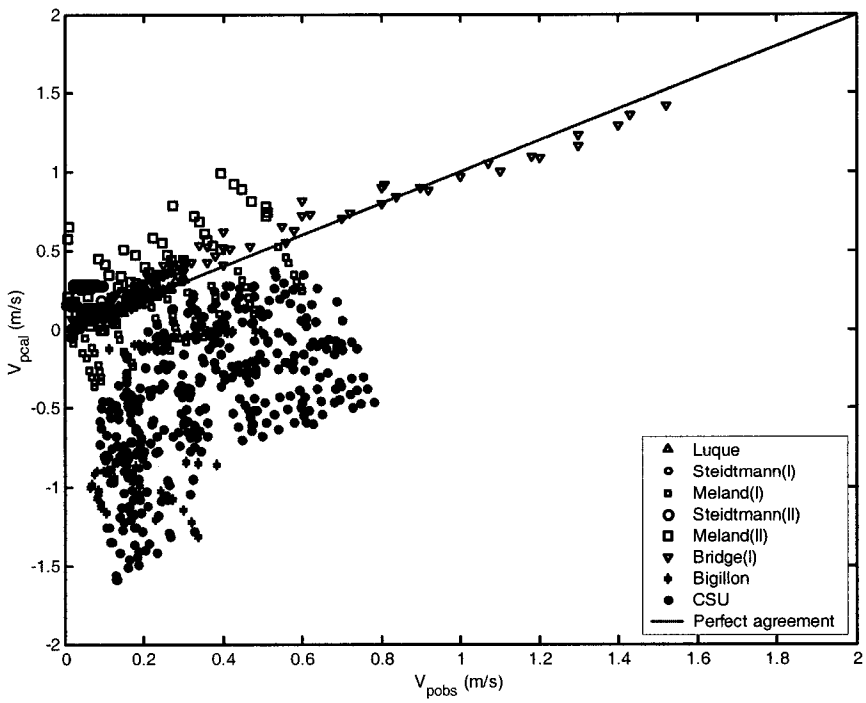

Figure 6.3: Comparison between Calculated and Observed V_p using Eq. (2.15)

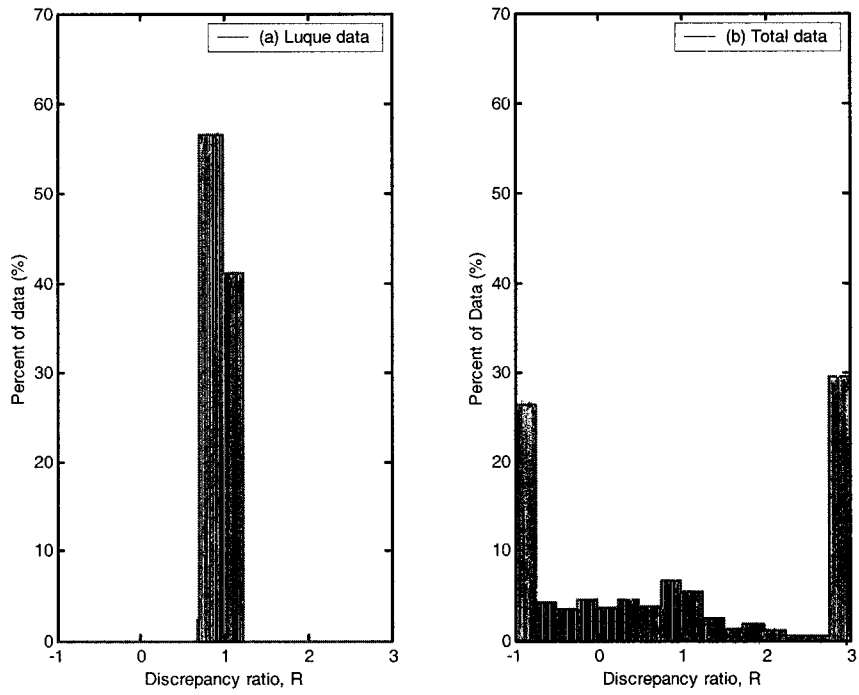

Figure 6.4: Discrepancy Ratio Distribution of V_p using Eq. (2.15)

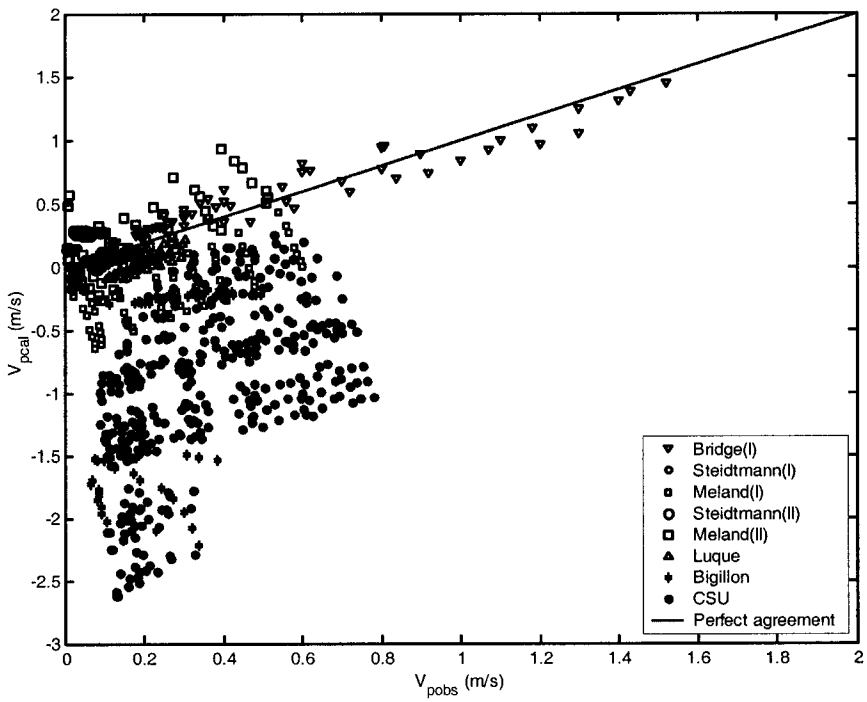

Figure 6.5: Comparison between Calculated and Observed V_p using Eq. (2.22)

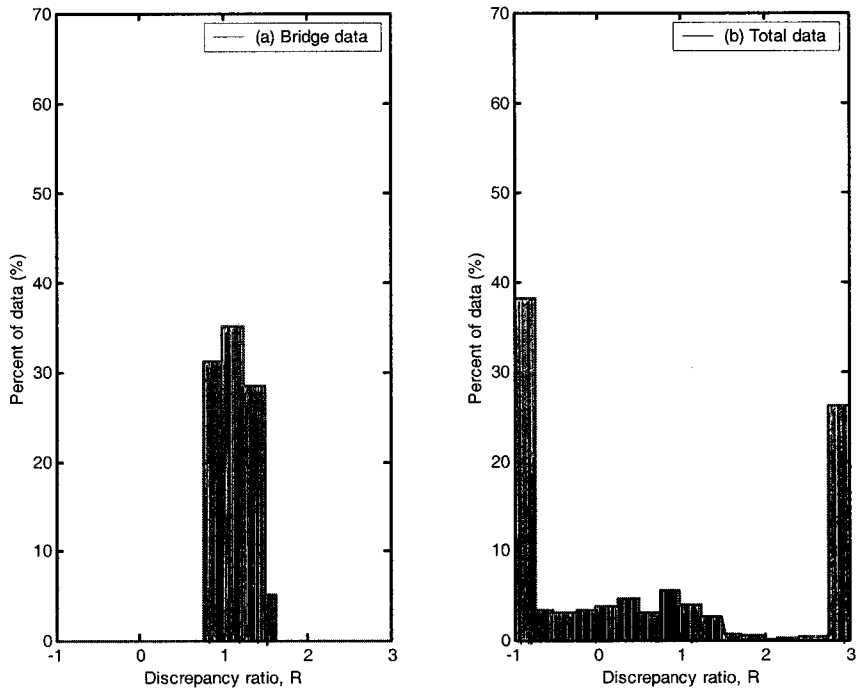

Figure 6.6: Discrepancy Ratio Distribution of V_p using Eq. (2.22)

In Table 6.1, the discrepancy ratio method indicates the goodness of fit between calculated and observed results. The percentages of data falling within the range of discrepancy ratios between 0.75 to 1.25 is 83% using Meland and Norrman's database and reduces to 12% when using the total database. Similarly, for Fernandez Luque and van Beek (1976), the percentages of data falling within the range of discrepancy ratios between 0.75 to 1.25 is 98% using Fernandez Luque and van Beek's database and reduces to 12% when using the total database. For Bridge and Dominic (1984), the percentages of data falling within the range of discrepancy ratios between 0.75 to 1.25 is 68% using Bridge and Dominic's database and reduces to 8.5% when using the total database. There is clear indication that equations of Meland and Norrman, Fernandez Luque and van Beek, and Bridge and Dominic fail to predict bedload particle velocity when applied the database from other sources.

Table 6.1: Summary of Comparison between Calculated and Observed V_p

Equations	Data Sources	Data in Range of Discrepancy Ratio, R_i (%)				No. of Data Points	R^2
		0.75-1.25	0.5-1.5	0.25-1.75	0-2.0		
(1)	(2)	(3)	(4)	(5)	(6)	(7)	(8)
Meland and Norrman (1966)	Meland Total[(1)]	83 12	95 17	100 28	100 100	120 1018	0.95 -0.4
Fernandez Luque and van Beek (1976)	Luque Total[(1)]	98 12	100 20	100 28	100 100	85 1018	0.93 -0.096
Bridge and Dominic (1984)	Bridge Total[(1)]	68 8.5	96.5 16	100 22.5	100 100	77 1018	0.93 -0.27

Where: (1) = Meland (1966) + Luque (1976) + Steidtmann (1982) + Bridge (1984) + CSU (1995) + Bigillon (2001)

6.3. HALFMOON CREEK, COLORADO

Dixon and Ryan (2000) conducted the data collection on 6/9/2000 at the Halfmoon Creek near Leadville, Colorado to observe the bed-load with the underwater video camera. The original movie was obtained from Dr. Bunte at the Engineering Research Center, Colorado State University. At Halfmoon Creek, they observed slurries of sand and pea gravel moving along the bed of the stream. Saltating particles in the coarse sand to fine gravel size class were typically moving too quickly to distinguish them when observing the video frame by frame. These smaller particles, however, were easily seen

while the video was moving at a normal or slow motion speed. Larger particles in the medium to coarse gravel size class were moving slower and were easily view frame by frame. Occasionally sweeps were observed that would briefly entrain small to medium sized gravel.

In some other cases a larger particle would turn over and come to rest. For example, at Halfmoon Creek they observed a relatively large particle (b-axis = 46 mm) move into the frame and come to rest behind a similar sized stationary particle (Fig. 6.7). This particle adjusted its orientation slightly during the next 17 seconds. The particle then rolled over and came to rest downstream against a partially buried large cobble (Fig. 6.8). The particle adjusted its position slightly during next 7 minutes and 19 seconds as smaller particles filled in and subsequently scoured away both on top and beneath. Just before the particle moved out of the view frame, there was a sweep of sediment followed by the particle being struck by another particle (b-axis = 26 mm) that initiated its movement out of the view frame (Fig. 6.9).

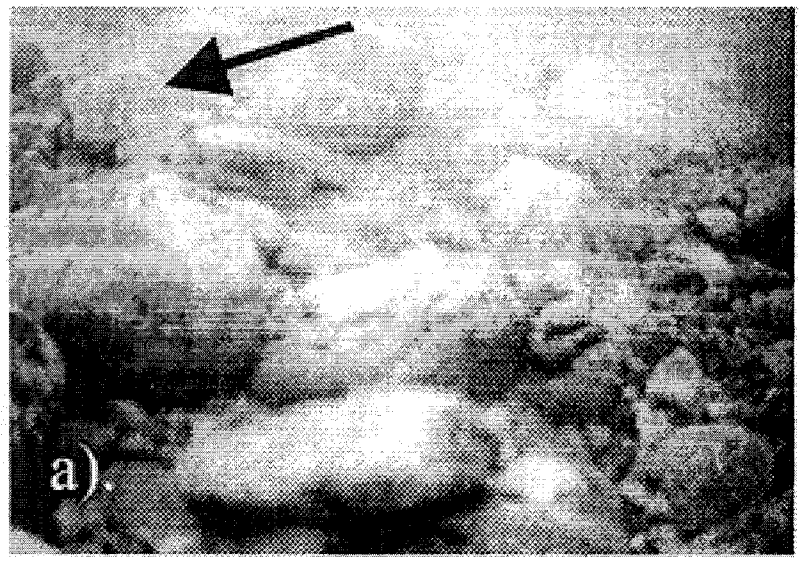

Figure 6.7: Track of a single particle at Halfmoon Creek (Dixon and Ryan, 2000); a) the particle move into view and comes to rest.

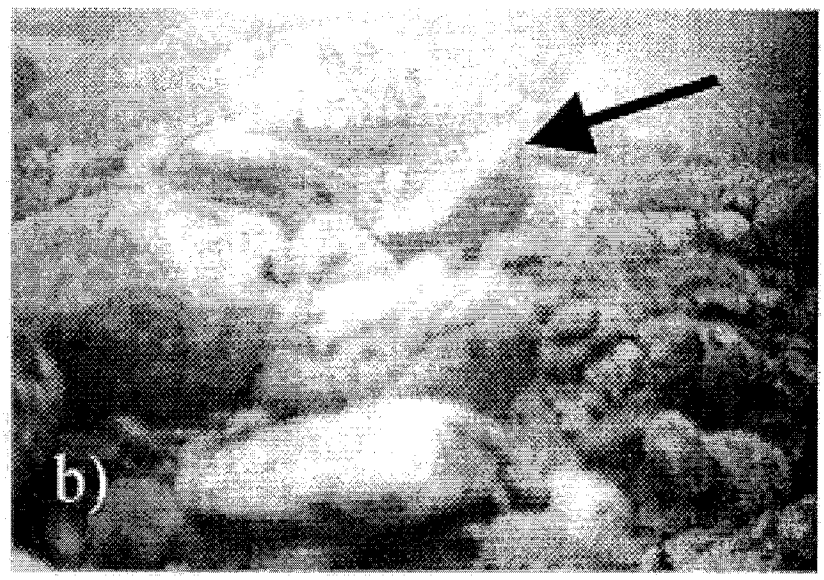

Figure 6.8: Track of a single particle at Halfmoon Creek (Dixon and Ryan, 2000); b) after 17 seconds the particle moves 23 mm and comes to rest again.

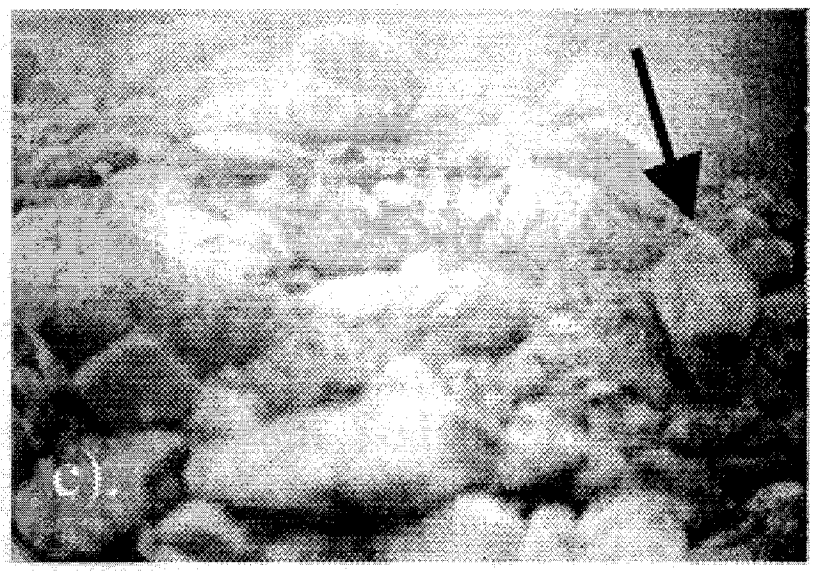

Figure 6.9: Track of a single particle at Halfmoon Creek (Dixon and Ryan, 2000); c) after being stationary for over 7 minutes, the particle moves out of the view.

Due to the lack of measured data, assumptions have been made to estimate bedload particle velocity conducted by Dixon and Ryan (2000). The estimated flow and sediment properties include:

1. Input data: Particle size d_s = 40 mm, bed slope S_f = 0.005, flow rate Q = 5.2 m^3/s, mean flow velocity u_f = 1.27 m/s, bed roughness k_s = 50 mm, mean flow depth y = 480 mm;

2. Calculation of basic parameters

   - Shear velocity $u_* = [gR_hS_f]^{1/2} = [9.81\times0.48\times0.005]^{1/2} = 0.153$ m/s
   - Shields particle parameter $\tau_{*ds} = u_*^2/(G-1)gd_s = (0.153)^2/(2.65-1)\times9.81\times0.04 = 0.036$
   - Shields roughness parameter $\tau_{*ks} = u_*^2/(G-1)gk_s = (0.153)^2/(2.65-1)\times9.81\times0.05 = 0.029$

- Boundary relative roughness $d_s/k_s = 40/50 = 0.8$, and $k_s/d_s = 1.25$
- Particle shear Reynolds number $Re_* = u_* d_s/\nu = 0.153 \times 0.04/1.004 \times 10^{-6} = 6096$
- Dimensionless particle diameter $d_* = d_s[(G-1)g/\nu^2]^{1/3} = 1009$

3. Calculation of bed roughness critical k_{sc} from Eqs. (5.37) and (5.38) to determine the motion of the particle; From Eq. (5.37), one obtains $k_{sc1} = (0.153)^2/(2.65-1) \times 9.81 \times 0.01 = 140$ mm which is comparable to $k_{sc2} = 110$ mm, obtained from Eq. (5.38).

4. Calculation of $V_{psmooth} = 3.64$ m/s by using Eq. (5.28); $V_p = 1.4$ m/s, and 0.79 m/s by using Eqs. (4.20), and (5.34) respectively. Similarly, applied the above procedures for different d_s, k_s, and the results is shown in Fig. 6.10.

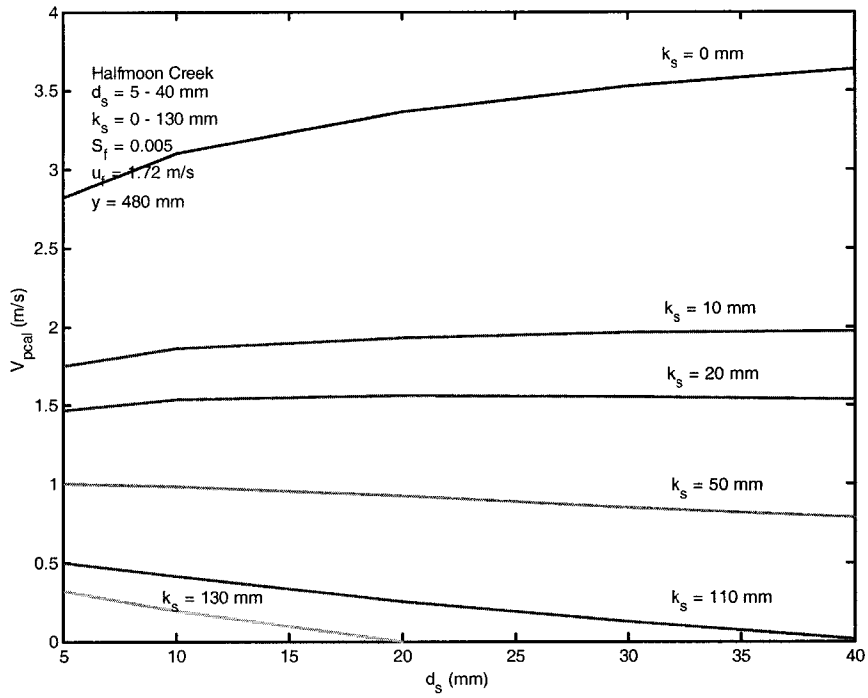

Figure 6.10: Predicted V_p using Eq. (5.34) for different values of d_s and k_s

6.4. AVILA MOUNTAIN, VENEZUELA

Mountain Avila, located on the north of Venezuela, witnessed on December 16th, 1999, a severe debris flows occurring over an area of about 500 km^2. As a faulted-block mountain, the Avila region has abundant neotectonic uplift. Altitude steeply ascends from sea level to 2000 m within only 6-9 km from the ridge to the beach. Average sediment deposition in the river canyon was about 2-3 m and essentially buried most of the standing houses to the rafters. Water level marks as high as 7 m were observed in some of the buildings. The debris surges destroyed approximately 60% of the structures in the town of Tanaguarena and resulted in approximately 100 casualties. The mining operation (Cantera Cerro Grande) reports damages in excess of 3 million dollars in lost structures

and equipment. Structures in the canyon sustained impact damage from debris and boulders in surges. Some structures were completely destroyed by impact, scour and exposure to high velocity flows. Foundations were undermined by scour and collapsed. High velocity surges with boulders and debris were experienced across the entire canyon bottom as the channel conveyance velocity was lost. The structures that remain standing were buried in a coarse-grained mixture of boulders, cobbles, sand and debris (Bello et al., 2000). Fig. 6.11 shows an aerial view of Caraballeda looking Southwest with newly opened channels in the foreground and center right of photograph; Figs. 6.12, and 6.14 shows road damaged in Los Corales; Fig. 6.13 shows an aerial view of Caraballeda looking North with a massive deposition of coarse sediment delivered by debris flows and flash floods in Los Corales section; Fig. 6.15 shows a view of Los Corales with deposited boulder on the road; Fig. 6.16 shows Big boulders transported by debris flow on a fairly smooth bed; Fig. 6.17 Big boulder transported by debris flow in December 1999 in Caraballeda; Fig. 6.18 shows an aerial view of Los Corales sector of Caraballeda with damage to apartment building; Fig. 6.19 shows a view of Los Corales with damage to an apartment building; Fig. 6.20 shows a control canal for debris and mudflow at the Saint Julian Ravine.

Figure 6.11: Aerial view of Caraballeda looking Southwest (Larsen et al., 2000)

Figure 6.12: View of road damaged in Los Corales, Leon and Rojas, 2000 (personal communication)

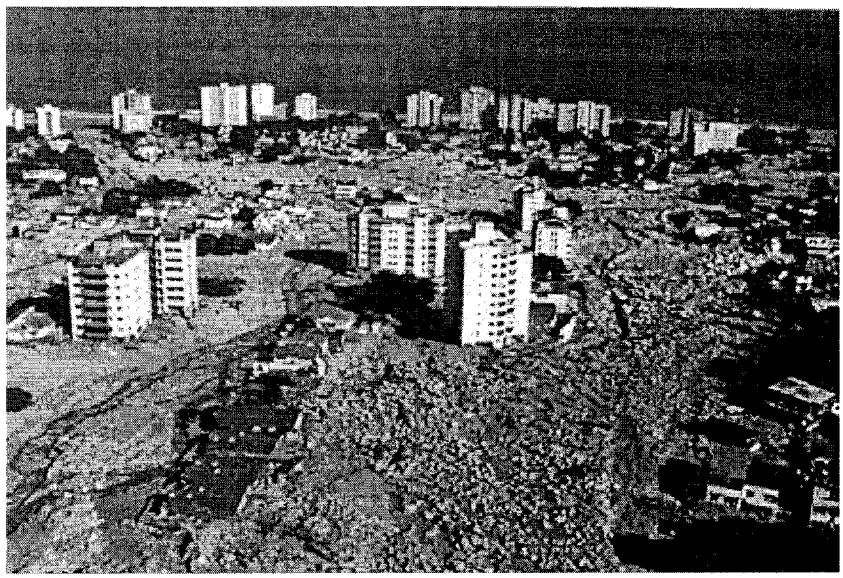

Figure 6.13: Aerial view of Caraballeda looking North (Larsen et al., 2000)

Figure 6.14: View of road damaged in Los Corales, Leon and Rojas, 2000 (personal communication)

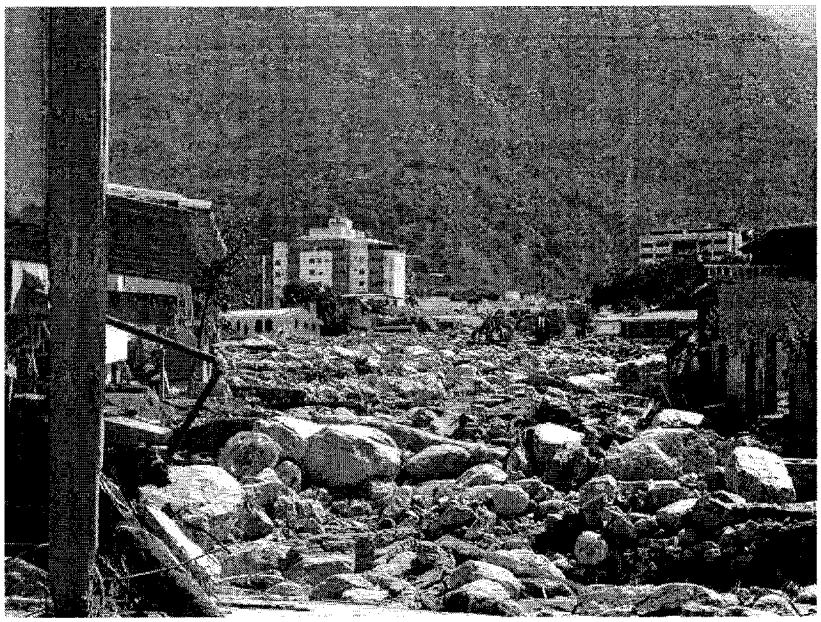

Figure 6.15: View of deposited boulders on the road in Los Corales, Leon and Rojas, 2000 (personal communication)

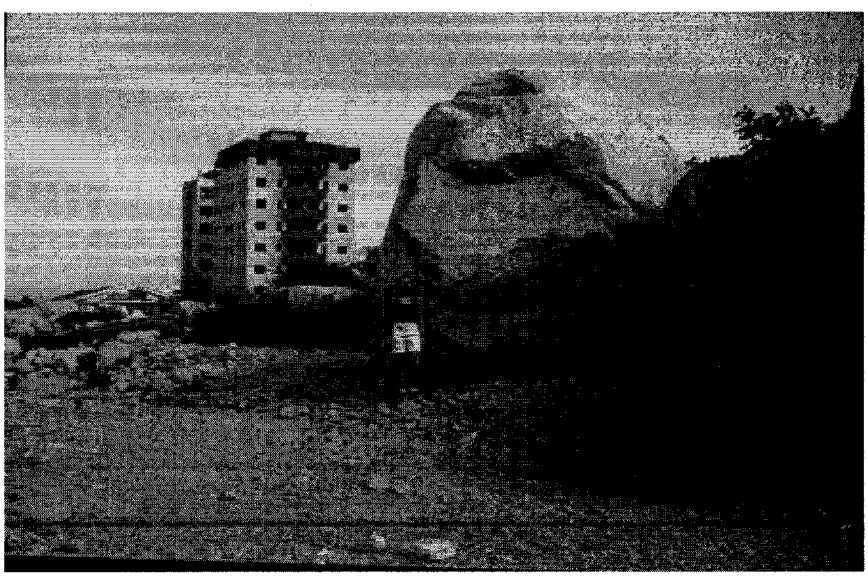

Figure 6.16: Big boulder transported by debris flow, Leon and Rojas, 2000 (personal communication)

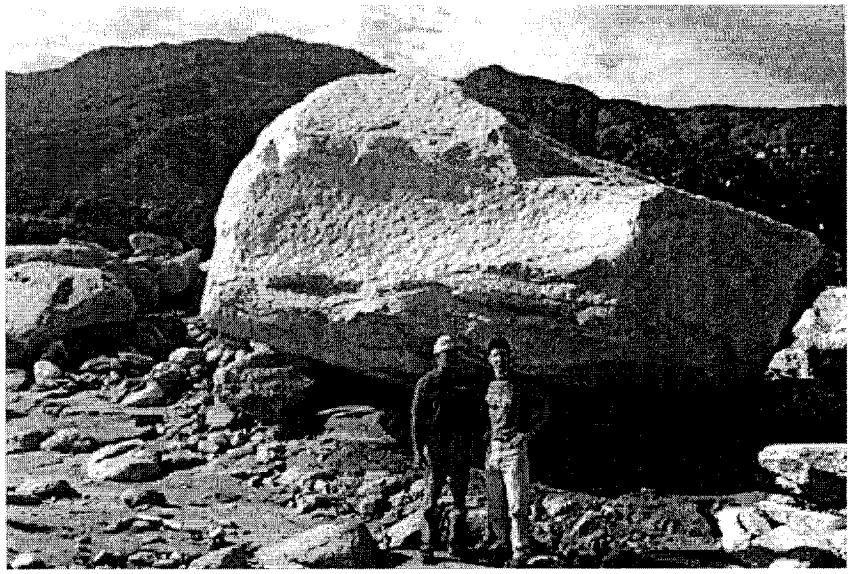

Figure 6.17: Boulder transported by debris flow in December 1999 (Larsen et al., 2000)

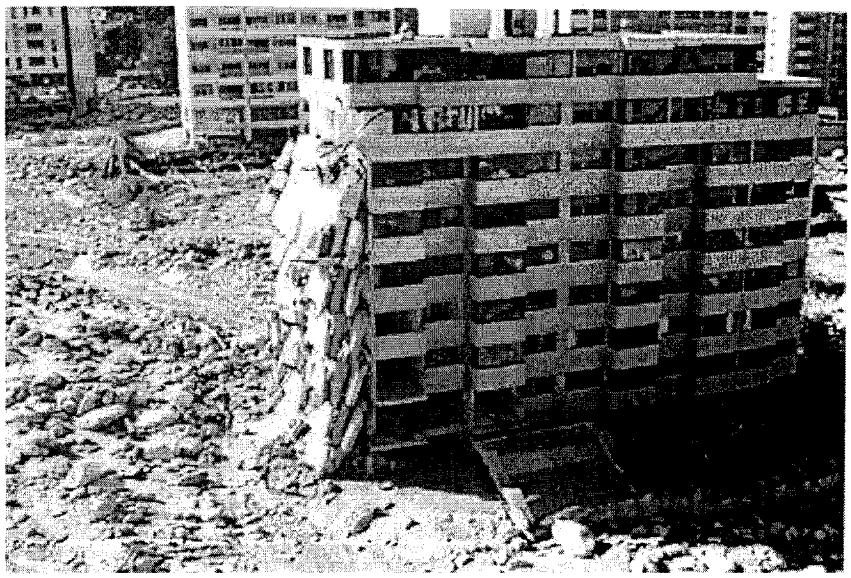

Figure 6.18: Aerial view of Los Corales sector of Caraballeda (Larsen et al., 2000)

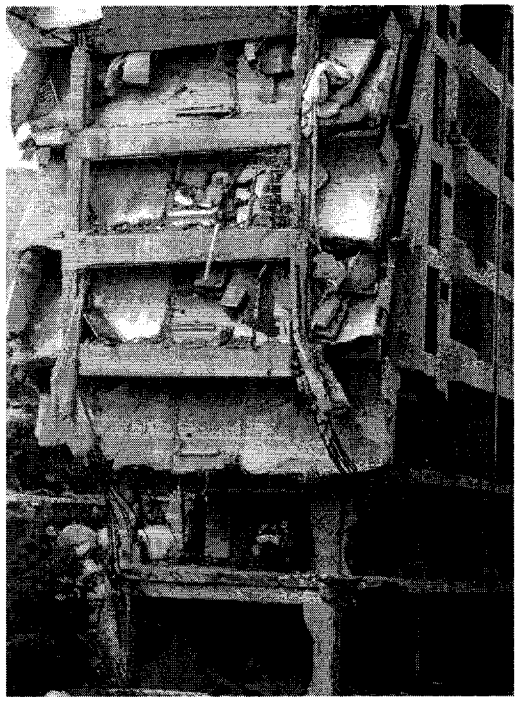

Figure 6.19: View of damaged to apartment building in Los Corales, Leon and Rojas, 2000 (personal communication)

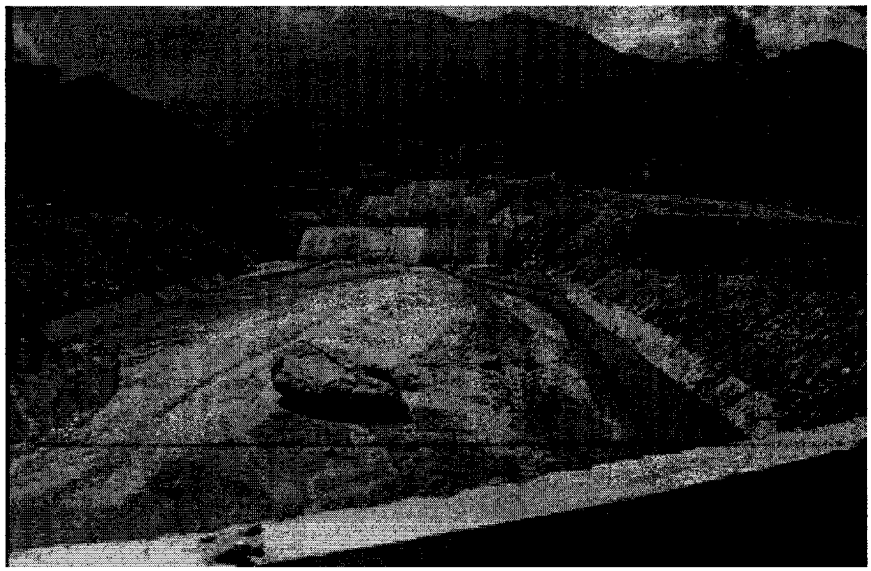

Figure 6.20: Control canal for debris flow at the Saint Julian Ravine, Leon and Rojas, 2000 (personal communication)

This particular example problem is derived from the measurement of field data, due to the insufficient of the nature of the database, some assumptions have been made. Given a uniform flow with T_{water} = 20°C, $\nu_{water} = 1.004\times10^{-6}$ m^2/s, particle diameter d_s = 0.1-3 m, G = 2.65, k_s = 0-250 mm, bed slope S_f = 0.01 (Leon and Rojas, 2000, personal communication), flow depth y = 3 m (Bello et al., 2000), determine the rolling bedload particle velocity, V_{pcal} = ?

Solution:

1) Particle size d_s = 2 m, bed slope S_f = 0.01, bed roughness k_s = 150 mm, mean flow depth y = 3 m;

2) Calculation of basic parameters

- Shear velocity $u_* = [gR_hS_f]^{1/2} = [9.81\times3\times0.01]^{1/2} = 0.54$ m/s
- Shields particle parameter $\tau_{*ds} = u_*^2/(G-1)gd_s = (0.54)^2/(2.65-1)\times9.81\times2 = 0.009$
- Shields roughness parameter $\tau_{*ks} = u_*^2/(G-1)gk_s = (0.54)^2/(2.65-1)\times9.81\times0.15 = 0.12$
- Boundary relative roughness $d_s/k_s = 13.33$, and $k_s/d_s = 0.075$
- Particle shear Reynolds number $Re_* = u_*d_s/\nu = 0.54\times2/1.004\times10^{-6} = 1075697$
- Dimensionless particle diameter $d_* = d_s[(G-1)g/\nu^2]^{1/3} = 50457$

3) Calculation of bed roughness critical k_{sc} from Eqs. (5.37) and (5.38) to determine the motion of the particle; From Eq. (5.37), one obtains $k_{sc1} = (0.54)^2/(2.65-1)\times 9.81\times 0.01 =$ 1.8 m which is about ten times $k_{sc2} = 170$ mm, obtained from Eq. (5.38).

4) Calculation of $V_{psmooth} = 19.85$ m/s by using Eq. (5.28); $V_p = 0.9$ m/s by using Eq. (5.34). Similarly, applied the above procedures for different d_s, and k_s, and the results is shown in Fig. 6.21, where, proposed formula Eq. (5.34) gives realistic estimates of particle velocity values, and therefore it could help define particle velocities during devastating floods.

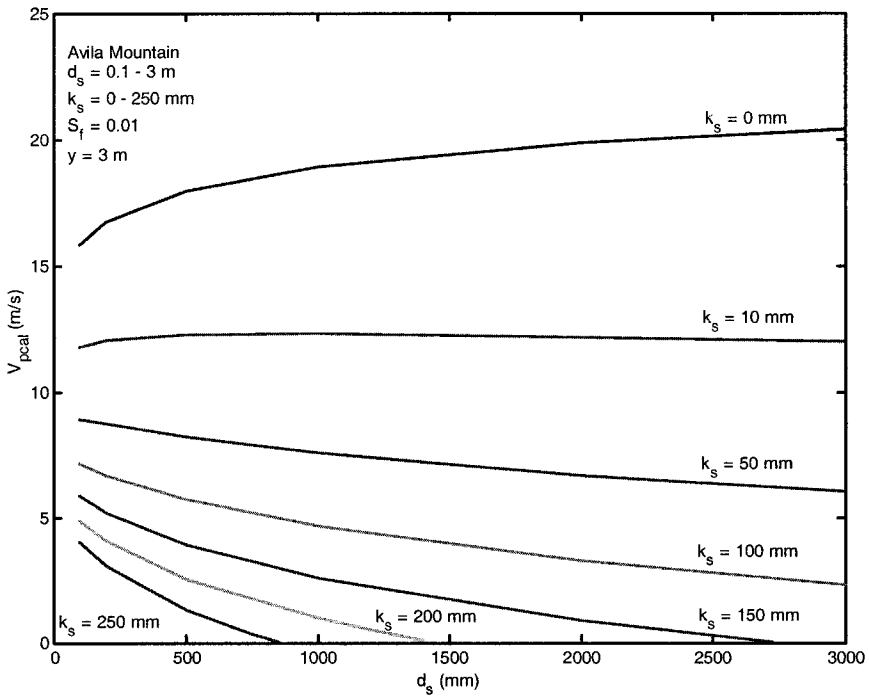

Figure 6.21: Predicted V_p using Eq. (5.34) for different values of d_s and k_s

CHAPTER 7

SUMMMARY AND CONCLUSIONS

This study aims at defining the bedload particle velocity in smooth and rough open channels as a function of the following variables: bed slope S_f, flow depth y, viscosity of the fluid ν, particle size d_s, bed roughness k_s, particle specific gravity G, and gravitational acceleration g.

Sources of data used in this analysis include 6 laboratory data sets for a total of 1018 points collected from different sources. In previous studies documented in the literature, 120 points could be obtained from Meland and Norrman (1966), 85 points from Fernandez Luque and van Beek (1976), 330 points from Steidtmann (1982), and 77 points from Bridge and Dominic (1984). Additionally, 356 points were collected at CSU on plates with bed roughness set at 1.2 mm, 1.7 mm, 2.4 mm, and 3.4mm, and 50 points from Bigillon (2001), with bed roughness set at 1.5 mm and 3 mm. Each set of data contains a complete record for flow and bedload particles information. These data are limited to the particle sizes with median diameters in the range of 0.21 to 29.3 mm, bed

roughness in the range of 0.19 to 7.76 mm, average flow velocity in the range of 0.22 to 1.00 m/s, shear velocity in the range of 0.0097 to 0.1108 m/s, flow depth in the range of 2.13 to 180 mm, and slope in the range of 0.00073 to 0.05.

The existing formulas such as Meland and Norrman (1966), Fernandez Luque and van Beek (1976), and Bridge and Dominic (1984) are verified with the laboratory measurements. Results show that all of the existing formulas fail to predict V_p when applied to the data sources other than their own database.

The analysis of the data leads to the following conclusions:

(1) For a smooth bed ($k_s = 0$), the rolling bedload particle velocity V_p increases with particle sizes d_s;

(2) For a rough bed ($k_s > 0$), particle velocity decreases with particle density G, thus lighter particles move faster than heavier ones; and on a very rough boundary V_p decreases with particle sizes;

(3) Bedload particles move at values of the Shields parameter τ_{*ds} below the critical value of $\tau_{*dsc} = 0.047$;

(4) Very few of the observed particles moved at values of Shields roughness parameter τ_{*ks} less than 0.01;

(5) Particles are observed to move at values of the Shields roughness parameter $0.01 < \tau_{*ks} < 0.15$;

(6) The ratio of particle velocity V_p to mean flow velocity u_f lies in the range of 0.2 to 0.9, while Kalinske (1942) suggested 0.9 to 1.0;

(7) The ratio of particle velocity V_p to shear velocity u_* lies in the range of 2.5 to 12.5, compared to the values cited in the literature $6.0 < V_p/u_* < 14.3$;

New methods for predicting transport velocities of bedload particles in rough and smooth open channels are examined. Two approaches for transport velocities of bedload particles were considered. The first approach combines dimensional analysis and regression analysis to define bedload particle velocity as a power function of the Shields parameter τ_*, boundary relative roughness k_s/d_s, dimensionless particle diameter d_*, and excess specific gravity (G-1). The second approach considers the transport velocity of a single particle on a smooth bed. The reduction in particle velocity due to bed roughness is then examined through a theoretical and empirical analysis. Results show that the bedload particle velocity on smooth beds is approximately equal to the flow velocity at the center of the particle. Bed roughness decreases the transport velocity of rolling bedload particles.

Comparatively, The first approach gives satisfactory results, except when k_s equals 0, then V_p goes to ∞, and when k_s is large, V_p does not stop (unbounded); for the second approach V_{pmax} when k_s equals 0, and when V_p equals 0, then values of k_s follow the criteria a and b described in Chapter 5 (section 5.4) and there is an insufficient evidence to suggest that one criteria is better than other.

The analysis shows that the proposed formula, Eq. (5.34) provides much better predictions than the existing formulas. Plots showing the comparison between calculated and observed bedload particle velocity and the discrepancy ratio distribution are shown in Figs. 5.12, and 5.13 respectively; the discrepancy ratio for the predictions of bedload particle velocity using the newly proposed formula, Eq. (5.34) are normally distributed

and have higher density (close to perfect agreement) than all other formulas. Predictions with extreme discrepancy ratios ($R_i < -1.0$ and $R_i > 3.0$) are very limited in utility; and less than 2.5 % of data with discrepancy ratio $R_i < 0.75$ and $R_i > 1.25$. The statistical results of calculated V_p are shown in Table 5.1, which indicate that the newly proposed formula Eq. (5.34) gives the best prediction amongst all formulas. In addition, the proposed formula, Eq. (5.34) is also verified with the most current laboratory data from Bigillon (2001). Field application to Halfmoon Creek (Dixon and Ryan, 2000), and the devastating flood of the Avila Mountain in Venezuela in December 1999 (Leon and Rojas, 2000, personal communication), the results give realistic estimates of particle velocities.

REFERENCES

Abbott, J. E. and Francis, J. R. D. 1977. "Saltation and suspansion trajectories of solid grains in a water stream." Philos. Trans. Roy. Soc. London, 284 (1321): 225-254p.

Aguirre, M. A., Calvo, A., Henrique, C., Ippolito, I., and Bideau, D. 1997. "Stopping distance: A way to understand energy dissipation in a granular flow experimentally modeled." Powders and Grains 97, Behringer & Jenkins (eds), ISBN 90 5410 884 3, 471-473p.

Aksoy, S. 1973. "Fluid forces acting on a sphere near a boundary." Proc. 15th Congress, IAHR, 121-224p.

Alonso, C. V. 1980. "Selecting a formula to Estimate Sediment Transport in Non-Vegetated Channels." CREAMS: A Field Scale Model for Chemicals, Runoff, Erosiion from Agricultural Management Systems, Conservation Research Report No. 26, United States Department of Agriculture, 1980

Alonso, C. V. and C. Mendoza, 1992. "Near-Bed Sediment Concentration in Gravel Bedded Streams." Water Resources Research WRERAQ; Vol. 28, No. 9, (September 1992): 2459-2468.

Ancey, C., Evesque, P. and Coussot, P. 1996. "Motion of a single bead on a bead row theoretical investigations." J. Phys. I, France, 6:725-751p.

Ancey, C., Evesque, P. and Coussot, P. 1997. "Analogy between granular flows down an inclined channel and the motion of a bead down a bumpy line." Powders and Grains 97, Proceedings of the 3rd Int'l. Conf. On Powders and Grains, 475-478p.

Andrews, E. D. 1984. "Bed-Material Entrainment and Hydraulic Geometry of Gravel-Bed Rivers in Colorado." Geological Society of America Bulletin; V. 95, No. 3, (March 1984): 371-378.

Andrews, E. D. 1983. "Entrainment of Gravel from Naturally Sorted Riverbed Material." U.S. Geological Survey, Geological Society of America Bulletin. V. 94 (October 1983): 1225-1231.

Andrews, E. D. and G. Parker, 1987. "Formation of a Coarse Surface Layer as the Response to Gravel Mobility." Sediment Transfer in Gravel-Bed Rivers. John Wiley & Sons; New York., p 269-300.

Andrews, E. D. and J. D. Smith, 1992. "A Theoretical Model for Calculating Marginal Bedload Transport Rates of Gravel. In Dynamics of Gravel-Bed Rivers." ed., by P. Billi, R. D. Hey, C. R. Thorne & P. Tacconi, John Wiley & Sons Ltd.

Ashworth, P. J. and R. I. Ferguson, 1989. "Size-Selective Entrainment of Bed Load in Gravel Bed Streams. Water Resources Research WRERAO; Vol. 25, No.4, (April 1989): 627-634.

Ashworth, P. J. and R. I. Ferguson, 1989. "Size-Selective Entrainment of Bed Load in Gravel Bed Streams. Water Resources Research WRERAO; Vol. 25, No.4, (April 1989): 627-634.

Bagnold, R. A. 1956. "The flow of cohesionless grains in fluids." Philos. Trans. R. Soc. London Ser. A, 249, 235-297.

Bagnold, R. A. 1973. "The nature of saltation and of bed-load transport in water." Proc. R. Soc. London Ser. A, 332, 473-504.

Bagnold, R. A., 1977. "Bed Load Transport by Natural Rivers." Water Resources Research, Vol. 13, No. 2 (April 1977).

Bello, M. E., O'Brien, J. S., Lopez, J. L., and Garcia-Martinez, R., 2000. "Simulation of flooding and debris flows in the Cerro Grande River." Hydrologic and Geomorphologic Evaluation of the debris flows.

Best, J., Bennet, S., Bridge, J. and Leeder, M. 1997. "Turbulence modulation and particle velocities over flat sand beds at low transport rates." J. Hydraulic Engineering, Vol. 123, No. 12, 1118-1129p.

Bigillon, F. 2001. "Etude du movement bidimensionnel d'une particule dans un courant d'eau sur forte pente." Ph.D.'s dissertation, Universite Grenoble 1- Joseph Fourier, U.F.R de Mechanique.

Bouvard, M. and Petkovic, S. 1985. "Vertical dispersion of spherical, heavy particles in turbulent open channel flow." J. Hydraulic Research, Vol. 23, No. 1, 5-19p.

Bray, D. I. 1972. "Generalized Regime-Type Analysis of Alberta Rivers." Thesis presented to the University of Alberta, at Edmonton, Alberta, Canada, in 1972, in partial fulfillment of the requirements for the degree of Doctor of Philosophy.

Brayshaw, A. C. 1985. "Bed Microtography and Entrainment Thresholds in Gravel-Bed Rivers." Geological Society of America Bulletin; Vol. 96, No. 2, (February 1985): 218-223.

Brayshaw, A. C., Lynne E. Frostick, and Ian Reid, 1983. "The Hydrodynamics of Particle Clusters and Sediment Entrainment in Coarse Alluvial Channels." Sedimentology, Editors: M. E. Tucker, Durham, P. H. Bridges, Derby and J. S. Bridge, Binghamton. Volume 30, No. 1.

Bridge, J. S. 1981a. "A discussion of Bagnold's (1956) bedload transport theory in relation to recent developments in bedload modeling." Earth Surf. Proc., 6, 187-190.

Bridge, J. S. 1981b. "Bed shear stress over sub aqueous dunes, and the transition to upper-stage plane beds." Sedimentology, 28, 33-36.

Bridge, J. S. 1982a. "Bed shear stress over sub aqueous dunes, and the transition to upper-stage plane beds: Reply." Sedimentology, 29, 744-747.

Bridge, J. S. 1982b. "Hydraulic interpretation of grain-size distributions using a physical model for bedload transport: Reply." J. Sediment. Petrol., 52 1336-1338.

Bridge, J. S., and Javis, J. 1982. The dynamics of river bend: A study in flow and sedimentary processes, sedimentology, 29, 499-541, 1982.

Bridge, J. S. and Dominic, D. F. 1984. "Bed load grain velocities and sediment transport rates." J. Water Resources Research, 20(4): 476-490p.

Bridge, J. S. and Bennett, S. J. 1992. "A model for the entrainment and transport of sediment grains of mixed sizes, shapes and densities." J. Water Resources Research, Vol. 28, No. 2, 337-363p.

Brownlie, W. R. 1981. "Prediction of flow depth and sediment discharge in open channels." California Institute of Technology, W. M. Keck Laboratory of Hydraulics and Water Resources, Report No. KH-R-43A.

Burkham, D. E. and Dawdy D. R. 1976. " Resistance Equation for Alluvial Channel Flow." Journal of the Hydraulics Division, Proceedings ASCE, Vol. 102, No. HY10.

Burrows, R. L. and Harrold, P. E. 1983. "Sediment Transport in the Tanana River near Fairbanks, Alaska, 1980-81." United States Geological Survey. Water Resources Investigation Report 83-4064.

Burrows, R. L. and Emmett, W. W. and Parks, B. 1981. "Sediment Transport in the Tanana River near Fairbanks, Alaska, 1977-1979." United States Geological Survey. Water Resources Investigation Report 81-20.

Carling, P. A. 1983. "Threshold of Coarse Sediment Transport in Broad and Narrow Natural Streams." Earth Surface Processes and Landforms Vol. 8: 1-18.

Carson, M. A. and G. A. Griffiths, 1985. "Tractive Stress and the Onset of Bed Particle Movement in Gravel Stream Channels: Different Equations for Different Purposes." J. Hydrology JHYDA7; Vol. 79, No. ¾.

Carty, J. 1957. "Resistance coefficients for sphere on plane boundary." B. S. Thesis, MIT.

Chang, Howard H. 1988. "Fluvial Processes in River Engineering." New York: John Wiley & Sons.

Cheng, D. H. and Clyde, C. G. 1972. "Instantaneous hydrodynamic lift and drag forces on large roughness elements in turbulent open channel flow." Int'l Sedimentation, Symp. to Honor H. A. Einstein, pp3-1:20.

Cheng, N-S. 1997. "Simplified settling velocity formula for sediment particle." J. Hydraulic Engineering, Vol. 123, No. 2, 149-152p.

Cheng, N-S. 1997. "Effect of concentration on settling velocity of sediment particles." J. Hydraulic Engineering, Vol. 123, No. 8, 728-731p.

Chien, N. and Wan, Z. H. 1983. "Sediment transport mechanics." Science Press, Beijing, China (in Chinese).

Chiew, Y-M. and Parker, G. 1994. "Incipient sediment motion on non-horizontal slopes." J. Hydraulic Engineering, Vol. 32, No. 5, 649-660p.

Childers, Dallas, Stephen E. Hammond, and William P. Johnson, 1988. "Hydrologic Data for Computation of Sediment Discharge, Toutle and North Fork Toutle Rivers near Mount St. Helens, Washington, Water Years 1980-84." U.S. Geological Survey Open-File Report 87-548. Vancouver, Washington.

Church, M., J. F. Wolcott, and W. K. Fletcher, 1991. "Test of Equal Mobility in Fluvial Sediment Transport: Behavior of the sand Fraction." Water Resources Research WRERAQ; Vol. 27, No. 11, (November 1991): 2941-2951.

Clauser, F. H. 1954. "Turbulent boundary layers in adverse pressure gradients." J. Aeronotical Science, Vol. 21, pp. 91-108p.

Colby, B. R. 1964. "Discharge of sands and mean velocity relationship in sand bed streams." Sediment Transport in Alluvial Channels, Geological Survey Professional Paper 462-A.

Coleman, N. L. 1967. "A theoretical and experimental study of drag and lift forces acting on a sphere resisting on hypothetical stream bed." Proc. 12th Cong. Intern. Assoc. Hydr. Res., 3.

Coleman, N. L. 1981. "Velocity profiles with suspended sediment." J. Hydraulic Research, Vol. 19, No. 3, 211-229p.

Copeland, R. R., and Thomas, W. A. 1989. "Corte Madera Creek Sedimentation Study." Technical Report HL-89-6, Final Report, Waterways Experiment Station, Corps of Engineers, Vicksburg, MS 39181, p46 +appendix. April 1989.

Davis, A. C., Ellett, B. G. S. and Jacob, R. P. 1998. "Flow measurement in sloping channels with rectangular free overfall." J. Hydraulic Engineering, Vol. 124, No. 7, 760-763p.

Dixon, M. and Ryan S. 2000 "Using an underwater video camera for observing bedload transport in mountain stream." Proc. of the 7th Interagency Sedimentation Conference, March 25 to 29, 2000, Reno, Nevada.

Dominic, D. F. 1983. "Evaluation of bedload sediment transport models." Master's thesis, State Univ. of N. Y. at Binghamton.

Einstein, H. A. 1950. "The bed load function for sediment transport in open channel flows." Technical Report No. 1026, USDA Soil Conservation Service, Washington D.C.

Einstein, H. A. and El-Sami, E. A. 1949. "Hydrodynamic forces on a rough wall." Rev. Modern Physics, 21(3), 520-524p.

Einstein, H. A. 1942. "Formulas for the Transport of Bed-Load." Transactions of the American Society Civil Engineers, Vol. 107.

Emmett, W. W. and Seitz. 1974. "Suspended and Bed load sediment transport in the Snake and Clearwater Rivers in the vicinity of Lewiston, Idaho." U.S. Geological Survey Basic-Data Report.

Engelund, F. and J. Fredsoe, 1976. "A sediment transport model for straight alluvial channels." Nordic Hydrol., 7, 293-306.

Engelund, F., and J. Fredsoe, 1982a. "Sediment ripples and dunes." Ann. Rev. Fluid Mech., 14, 13-37.

Fenton and Abbot, 1977. "Initial Movement of Grain on a StreamBed: The effects of Relative Intrusion." Proceedings of the Royal Society of London, A, Vol. 352.

Fernandez Luque, R. and van Beek, R. 1976. "Erosion and transport of bed load sediment." J. Hydraulic Research, 14(2): 127-144p.

Fleming, C. A., and J. N. Hunt, 1976. "A mathematical sediment transport model for unidirectional flows." Proc. Inst. Civ. Eng., 61, 297-310.

Francis, J. R. D. 1973. "Experiments on the motion of solitary grains along the bed of a water stream." Proc. Roy. Soc. London A 332:443-471p.

Garde, R. and Sethuraman, S. 1969. "Variation of drag coefficient of a sphere rolling along a boundary." La Houille Blanche, No 7. (or this paper can also be found in Selected Works of R. J. Garde, Hydraulic Engineering Section, Civil Engineering Department, University of Roorkee, India, 76-81p.

Gessler, J. 1976. "Stochastic Aspects of Incipient Grain Motion on Riverbeds." Stochastic Approaches to Water Resources, Volume II; Chapter 25, Colorado State University, Fort Collins, (1976): 25-1 – 25-6.

Gessler, J. 1971. "Beginning and ceasing of sediment motion." River Mechanics, Fort Collins, Colorado, H. W. Shen, ed., 1, 7-1 – 7-22.

Gilbert, G. B. 1914. "Transport of Debris by Running Water." U.S. Geological Survey Professional Paper., 86, 1914.

Gilbert, G. K. 1914. "The transportation of debris by running water." USGS Prof. Paper No. 86, 259.

Gomez, B. and M. Church, 1989. " Assessment of Bed Load Sediment Transport Formulae for Gravel Bed Rivers." Water Resources Research WRERAO; Vol. 25, No. 6, (June 1989): 1161-1186.

Graf, W. H. 1984. "Hydraulics of sediment transport." Water Resources Publications, LLC.

Guy, H. P. and Norman, V. W. 1970. "Field methods for measurement of Fluvial Sediment." U.S. Geological Survey Techniques of Water Resources Investigations, Book 3. U.S. Government Printing Office, Washington.

Helley, E. J., and Smith Einchell, 1971. "Development and calibration of a pressure difference bed load sampler." U.S. Geological Survey Open-File Report.

Hubbell, D. W., H. H. Stevens, Jr., J. V. Skinner, and J. P. Beverage, 1987. "Laboratory Data on Coarse-Sediment Transport for Bedload Sampler Calibrations. U.S. Geological Survey Water-Supply Paper 2299, Denver, Colorado.

Ikeda, S. 1971. "Some studies on the mechanics of bed load transport." Proc. Jpn. Soc. Civ. Eng. 185:61-69.

Ikeda, H. and Iseya, F. 1988. "Experimental study of heterogeneous sediment transport." Environmental Research Center, University of Tsukuba, ISSN 0286-5408.

Ippen, A. T. and Verma, R. P. 1955. "Motion of particles on bed of a turbulent stream." Trans. Am. Soc. Civ. Eng. 921-938p.

Jan, C. D. 1992. "Movement of a sphere moving over smooth and rough inclines." Ph. D. dissertation., University of California at Berkeley, California.

Jan, C. D. and Chen, J. C. 1998. "Movements of a sphere rolling down an inclined plane." Journal of Hydraulics Research., ASCE. Vol. 35, No. 5.

Jones, M. L., and Seitz, H. R., 1980. "Sediment transport in the Snake and Clearwater Rivers in the vicinity of Lewiston, Idaho." United States Geological Survey Open-File Report 80-690.

Julien, P. Y., Chen, Y. C. 1989. "Experimental study of horizontal lamination in a tecirculating flume." Report CER88-89-PYJ-YC14, CSU, May 1989,63p.

Julien, P. Y. and Lan, Y. Q. 1989. "Experimental formation of alluvial deposits in a wide rectangular flume." Report CER89-90PYJ-YQL2, CSU, July 1989, 29p.

Julien, P. Y. and Lan, Y. Q. 1990. "Laboratory experiments on sedimentation, lamination and descicattion of sediment mixtures." Report CER89-90PYJ-15, CSU, May 1990, 165p.

Julien, P. Y. 1995. "Erosion and Sedimentation" Cambridge University Press.

Julien, P. Y., Meier, C. I. and Blackard, B. 1995. "Laboratory measurements of bed load particle velocities." Report CER95-96PYJ-MCI-BB., Department of Civil Engineering, Colorado State University, Fort Collins, Colorado.

Julien, P. Y., Lan Y. Q, and Raslan, Y. 1997. "Experimental mechanics of sand stratification." Powders and Grains 97, Proceedings of the 3rd Int'l. Conf. On Powders and Grains, 487-490p.

Julien, P. Y. and Guo, J. 1997. "Transport velocities of individual particles over smooth open channel bed." Report CER97-98PYJ-GJ1., Department of Civil Engineering, Colorado State University, Fort Collins, Colorado.

Julien, P. Y. and Leon, C. 2000. "Mud floods, mudflows and debris flows classification, rheology and structural design."

Julien, P. Y. 2002. "River Mechanics." Cambridge University Press.

Kalinske, A. A. 1942. "Discussion of " Settling velocity and flume behavior of no-spherical particles" by Krumbein, W. C., EOS Trans. AGU 23:632-633p.

Kalinske, A. A. 1947. "Movement of sediment as bedload in rivers." Eos. Trans. AGU, 28, 615-620.

Karim, M. F. and Kennedy, J. F. 1984. "A short list of sediment transport equations." Iowa Institute of Hydraulic Research, The University of Iowa, Iowa City, Iowa 52242, July 1984, p33.

Klimek, K. E. 1997. "Spherical particle velocities on rough dry surfaces." M.S. Thesis, Department of Civil Engineering, Colorado State University, Fort Collins, Colorado.

Kirkgoz, M. S. 1989. "Turbulent velocity profiles for smooth and rough open channel flow." J. Hydraulic Engineering, ASCE, 115(11), 1543-1561p.

Kirkgoz, M. S. and Ardiclioglu, M. 1997. "Velocity profile of developing and developed open channel flow." J. Hydraulic Engineering, ASCE. Vol. 123, No. 12, 1099-1105p.

Knott, James M., and Stephen W. Lipscomb, 1983. "Sediment Discharge Data for Selected Sites in the Susitna River Basin Alaska, 1981-82." U.S. Geological Survey Open-File Report 83-870, Prepared in cooperation with the Alaska Power Authority. U.S. Department of the Interior Geological Survey. Anchorage, Alaska.

Knott, James M., and Stephen W. Lipscomb, 1985. "Sediment Discharge Data for Selected Sites in the Susitna River Basin Alaska, October 1982 to February

1984." U.S. Geological Survey Open-File Report 85-157, prepared in cooperation with the Alaska Power Authority. United States Department of the Interior.

Knott, James M., Stephen W. Lipscomb, and Terry W. Lewis, 1986. "Sediment Transport Characteristics of Selected Streams in the Susitna River Basin, Alaska, October 1983 to September 1984." U.S. Geological Survey Open-File Report 86-424W, Prepared in cooperation with the Alaska Power Authority. U.S. Department of the Interior Geological Survey.

Knott, James M., Stephen W. Lipscomb, and Terry W. Lewis, 1987. "Sediment Transport Characteristics of Selected Streams in the Susitna River Basin, Alaska: Data for Water Year 1985 and Trends in Bedload Discharge, 1981-85." U.S. Geological Survey Open-File Report 87-229. Prepared in cooperation with the Alaska Power Authority. U.S. Department of the Interior Geological Survey.

Komar, P. D. 1987. "Selective Grain Entrainment by a Current from a Bed of Mixed Sizes: A Reanalysis." J. Sedimentary Petrology, Vol. 57, No. 2, (March 1987):203-211.

Krumbein, W. C. 1942. "Settling velocities and flume behavior of non-spherical particles." EOS Trans. AGU 23:621-632p.

Kuhnle, R. A. 1993. "Incipient motion of sand gravel sediment mixtures." J. Hydraulic Engineering, Vol. 119, No. 12, 1400-1415p.

Kundu, P. K. 1990. "Fluid Mechanics." Academic Press, Inc.

Lamberti A. and Paris E. 1992. "Analysis of armouring processes through laboratory experiment." Dynamics of Gravel-Bed Rivers. Edited by Billi, P., Hey R. D., Trorne C. R., Tacconil P., John Wiley & Sons LTD, West Sussex, England.

Larsen, M. C. and Sierra, H. T. 2000. "Preliminary observations: flash-flood and landslide disaster of December, 1999, north coast of Venezuela."

Laursen, E. M. 1958. "The Total Load of Streams." J. Hydraulics Division, Proceedings ASCE, Vol. 84, No. HY1, February 1958. P 1530-1 –1530-36.

Lee, H-Y. and Hsu, I-S. 1996. "Particle spinning motion during saltating process." J. Hydraulic Engineering, Vol. 122, No. 10, 587-590p.

Limerinos, J. T. 1970. "Determination of the Manning Coefficient from Measured Bed Roughness in Natural Channels." Water Supply Paper 1898b, U.S. Geological Survey.

Ling, C-H. 1995. "Criteria for incipient motion of spherical sediment particles." J. Hydraulic Engineering, Vol. 121, No. 6, 472-478p.

Low, H. S. 1989. "Effect of sediment density on bedload transport." J. of Hydraulic Engineering, Vol. 115, No. 1, 124-138p.

Mantz, P. A. 1977. "Incipient transport of fine grains and flakes by fluids: Extended Shields diagram." J. Hydraul. Div. Am. Soc. Civ. Eng., 103, 601-614.

Mantz, P. A. 1980. "Low sediment transport rates over flat bed." J. Hydraul. Div. Am. Soc. Civ. Eng., 106, 1173-1189.

Meland, N. and Norrman, J. O. 1966. "Transport velocities of single particles in bed load motion." Geografiska Annaler 48 A (4):165-182p.

Meier, C. I. 1995. "Transport velocities of single bed load grains in hydraulically smooth open channel flow." Master's thesis, Department of Civil Engineering, Colorado State University, Fort Collins, Colorado.

Meyer-Peter, E. and Muller, R. 1948. "Formulas for bed load transport." Stockholm, Sweden, International Association for Hydraulic Structures Research, 2nd meeting., p. 39-64.

Milhous, R. T., J. B. Bradley, and C. L. Loeffler, 1986. "Sediment Transport Simulation an Armoured Stream." Proceedings of the 4th Federal Interagency Sedimentation Conference; March 24-27, 1986, Las Vegas, Nevada. Volume II, p 270-280.

Milhous, R. T. 1973. "Sediment Transport in Gravel-Bottomed Stream." Thesis, Oregon State University.

Miller, R. L., and R. J. Byrne, 1966. "The angle of repose for a single grain on a fixed rough bed, Sedimentology, 6, 303-314.

Miller, M. C., McCave, I. N. and Komar, P. D. 1977. "Threshold of sediment motion under unidirectional currents." J. Sedimentology, 24, 507-527p.

Muste, M. and Patel, V. C. 1997. "Velocity profiles for particles and liquid in open channel flow with suspended sediment." J. Hydraulic Engineering, Vol. 123, No. 9, 742-751p.

Naden, P. S. 1981. "Gravel in motion." working Pap. 321, School of Geogr., Univ of Leeds, Leeds, U.K.

Nezu, I. and Rodi, W. 1986. "Open channel flow measurements with a lazer doppler anemometer." J. Hydr. Engrg., ASCE, 112(5), 335-355p.

Nino, Y., Garcia, M. and Ayala, L. 1994. "Gravel saltation, 1. Experiments." J. of Water Resources Research, Vol. 30, No. 6, 1907-1914p.

Parsons, D. A. 1972. "The speed of sand grains in laminar flow over a smooth bed." In: Shen, H. W. (Ed). Sedimentation Symposium to honor Einstein, H. A.

Paintal, A. S., 1971. "Concept of critical Shear Stress in Loose Boundary Open Channels." J. Hydraulic Research No. 1 pp 90-113.

Parker, G. 1990. "Surface-Based Bedload Transport Relation for Gravel Rivers." J. Hydraulic Research JHYRAF; Vol. 28, No. 4, (1990):427-437.

Parker, G., S. Dhamotharan, and H. Stefan, 1982. "Model Experiments on Mobile, Paved Gravel Bed Streams." Water Resources Research; Vol. 18, No.5, (October 1982):1395-1408.

Parker, G., and P. C. Klingeman, 1982. "On Why Gravel Bed Streams are Paved." Water Resources Research; Vol. 18, No. 5, (October 1982):1409-1423.

Parker, G., P. C. Klingeman, and D. G. McLean, 1982b. "Bedload and Size Distribution in Paved Gravel-Bed Streams." J. Hydraulic Division, Proceedings of the ASCE; Vol. 108, No. HY4, (April 1982):544-571.

Rakoczi, L. 1991. "Field tracer investigations of grain sorting in gravel bed river." Proc. of International Grain Sorting Seminar, October 21-26, 1991, Ascona, Switzerland., 77-92.

Riguidel F-X., Jullien, R., Ristow, G. H., Hansen, A. and Bideau, D. 1994. "Behaviour of a sphere on a rough inclined plane." J. Physics I, France, 4 (1994), 261-272p.

Ristow, G. H. Riguidel, F-X. and Bideau, D. 1994. "Different characteristics of the motion of a single particle on a bumpy inclined line." J. Phys. I, France, 4 (1994), 1161-1172p.

Romanovskiy, V. V. 1977. "Investigation of the speed of bed load movement." Soviet Hydrol. 16(2):108-112.

Shen, H. W., and Lu, J. Y. 1983. "Development and Prediction of Bed Armouring." J. Hydraulic Engineering, Vol. 109, No. 4.

Shields, A. 1936. "Application of Similarity Principles and Turbulence Research to Bed-Load." English translation by W. P. Ott and J. C. van Uchelon, California Institute of Technology.

Shulits, S. 1935. " The Schoklitsch Bed Load Formula." Engineering, London, England, June 21, 1935, pp 644-646 and June 28, 1935, p687.

Simons, D. B. and Senturk, F. 1992. "Sediment Transport Technology." Water Resources Publication, Fort Collins, Colorado.

Song, T., Chiew, Y-M. and Chin, C. O. 1998. "Effect of bed load movement on flow friction factor." J. Hydraulic Engineering.,ASCE. Vol. 124, No. 2, 165-175p.

Song, T. and Chiew, Y-M. 1997. "Settling characteristics of sediments in moving Bingham fluid." J. Hydraulic Engineering, Vol. 123, No. 9, 812-815p.

Steidtmann J. R. 1982. "Size-density sorting of sand-size spheres during deposition from bedload transport and implications concerning hydraulic equivalence." J. Sedimentology. 29, 877-883p.

Sumer, B. M., and B. Oguz, 1978. "Particle motions near the bottom in turbulent flow in an open channel." J. Fluid Mech., 86, 109-127.

Sumer, B. M., and R. Diegaard, 1981. "Particle motions near the bottom in turbulent flow in an open channel, 2." J. Fluid Mech., 109, 311-337.

Sumer, B. M., Kozakiewicz, A., Fredsoe, J. and Deigaard, R. 1996. "Velocity and concentration profiles in sheet flow layer of movable bed." J. Hydraulic Engineering, Vol. 122, No. 10, 549-558p.

Tait, S. J., Willets, B. B. and Maizels, J. K. 1992. "Laboratory observations of bed armouring and changes in bedload composition." Dynamics of Gravel-Bed Rivers, edited by Billi, P., Hey, R. D., Trorne, C. R., Tacconil, P., John Wiley & Sons LTD, West Sussex, England.

Tominaga, A. and Nezu, I. 1992. "Velocity profiles in steep open channel flows." J. Hydraulic Engineering, Vol. 118, No. 1, 73-90p.

Van Rijn, L. C. 1984. "Sediment transport, Part I: Bedload transport." J. Hydraulic Engineering, Vol. 110, No. 10, 1431-1456p.

Van Rijn, L. C. 1984. "Sediment transport, Part II: Suspended load transport." J. of Hydraulic Engineering, Vol. 111, No. 11, 1613-1641p.

Vanoni, V. A. 1975. "Sedimentation Engineering." Edited by Vito A. Vanoni, 1975. ASCE, Manuals and Reports on Engineering Practice No. 54.

Von Karman, T. 1930. "Mechanische Ahnlichkeit und turbulenz." Gottinger Nachrichten Math. Phys. Klasse, 58-60 (in German).

White, F. M. 1991. Viscous Flows. 2nd Ed., McGraw-Hill, Inc.

Wiberg, P. L. 1987. "Mechanics of bed load sediment transport." Ph.D. dissertation, University of Washington, Seattle, Washington.

Wiberg, P. L. and Smith, J. D. 1989. "Model for calculating bedload transport of sediment." J. Hydraulic Engineering, Vol. 115, No. 1, 101-123p.

Wilcock, P. R. 1988. "Methods for Estimating the Critical Shear Stress of Individual Fractions in Mixed-Size Sediment." Water Resources Research WRERAO; Vol. 24, No. 7, (July 1988):1127-1135.

Wilcock, P. R. and J. B. Southard, 1988. "Experimental Study of Incipient Motion in Mixed-Sized Sediment." Water Resources Research WRERAO; Vol. 24, No. 7, (July 1988):1137-1151.

Williams, G. P. and D. L. Rosgen, 1989. "Measured Total Sediment Loads (Suspended and Bedloads) for 93 United States Streams." U.S. Geological Survey, Open-File Report 89-67, U.S. Department of Interior Geological Survey, Denver, Colorado.

Wilson, K. C. 1966. "Bedload transport at high shear stress." J. Hydraul. Div. Am. Soc. Civ. Eng., 92, 49-59.

Wolman, M. G. 1954. "A Method of Sampling Coarse River bed Material." Trans. American Geophy. Union, 35(6).

Xie, H., Wei, F., and Cui P. 2000. "Causes and characteristics of the Avila debris flows in Venezuela."

Yalin, M. S. 1977. "Mechanics of sediment transport." 2nd ed., Pergamon, New York, Oxford.

Yalin, M. S., and E. Karahan, 1979. "Inception of sediment transport, J. Hydraul. Div. Am. Soc. Civ. Eng., 105, 1433-1443.

Yang, C. T., 1973. "Incipient motion and sediment transport." J. Hydraulics Division, ASCE, Vol. 99, No. HY10, October 1973.

Yang, C. T. 1984. "Unit Stream Power Equation for Gravel." J. Hydraulic Division, ASCE, Vol. 110, No. HY12, 1984.

Yarin, L. P. and Hetsroni, G. 1994. "Turbulence intensity in dilute two phase flows-1: Effect of particle-size distribution on the turbulence of the carrier fluid." Int. J. Multiphase Flow, Vol. 20, No. 1, pp. 1-15.

APPENDIX I

THE CSU DATABASE

Table1: The CSU Experiments Database

Run	Type	d_s (mm)	G	y (mm)	S_f	u_f (m/s)	ν 10^{-6} (m^2/s)	k_s (mm)	n	V_{pobs} (m/s)	σ (m/s)	u_* (m/s)	δ (mm)	k_s/d_s	d_s/k_s	d_*	Re_*	τ_{*ds}	τ_{*ks}
(1)	(2)	(3)	(4)	(5)	(6)	(7)	(8)	(9)	(10)	(11)	(12)	(13)	(14)	(15)	(16)	(17)	(18)	(19)	(20)
1	Steel	1.57	8.02	72.12	0	0.283	1.05	0	11	0.074	0.0023	0.011	1.1	0	-	62	17	0.0012	-
	Steel	3.14	8.02	72.12	0	0.283	1.05	0	10	0.12	0.003	0.011	1.1	0	-	125	33	0.0006	-
	Steel	4.75	8.02	72.12	0	0.283	1.05	0	10	0.142	0.0075	0.011	1.1	0	-	189	50	0.0004	-
	Steel	6.34	8.02	72.12	0	0.283	1.05	0	10	0.153	0.0061	0.011	1.1	0	-	252	67	0.0003	-
	Steel	7.9	8.02	72.12	0	0.283	1.05	0	10	0.159	0.0071	0.011	1.1	0	-	314	84	0.0002	-
	Steel	9.5	8.02	72.12	0	0.283	1.05	0	10	0.171	0.0053	0.011	1.1	0	-	378	101	0.0002	-
	Steel	14.28	8.02	72.12	0	0.283	1.05	0	11	0.187	0.0069	0.011	1.1	0	-	567	151	0.0001	-
	Steel	15.88	8.02	72.12	0	0.283	1.05	0	11	0.193	0.0043	0.011	1.1	0	-	631	168	0.0001	-
	Steel	19.04	8.02	72.12	0	0.283	1.05	0	10	0.2	0.0074	0.011	1.1	0	-	757	202	0.0001	-
	Tin	4.38	7.31	72.12	0	0.283	1.05	0	11	0.134	0.0068	0.011	1.1	0	-	168	46	0.0005	-
	Glass	24.84	2.6	72.12	0	0.283	1.05	0	10	0.227	0.0031	0.011	1.1	0	-	603	263	0.0003	-
	Glass	16.37	2.6	72.12	0	0.283	1.05	0	12	0.209	0.0087	0.011	1.1	0	-	397	173	0.0005	-
2	Glass	14.48	2.6	72.25	0	0.275	1.05	0	15	0.217	0.0058	0.018	0.7	0	-	350	242	0.0014	-
	Glass	15.97	2.6	72.25	0	0.275	1.05	0	15	0.217	0.0051	0.018	0.7	0	-	386	267	0.0013	-
	Glass	21.7	2.6	72.25	0	0.275	1.05	0	15	0.235	0.0082	0.018	0.7	0	-	525	362	0.0009	-
	Glass	25.17	2.6	72.25	0	0.275	1.05	0	15	0.238	0.0098	0.018	0.7	0	-	608	420	0.0008	-
	Glass	29.3	2.6	72.25	0	0.275	1.05	0	15	0.24	0.0083	0.018	0.7	0	-	708	489	0.0007	-
3	Steel	19.04	8.02	60.9	0.0005	0.253	1.02	0	15	0.2	0.0059	0.016	0.74	0	-	769	298	0.0002	-
	Steel	15.88	8.02	60.9	0.0005	0.253	1.02	0	15	0.19	0.0042	0.016	0.74	0	-	641	249	0.0002	-
	Steel	14.28	8.02	60.9	0.0005	0.253	1.02	0	15	0.185	0.0069	0.016	0.74	0	-	577	223	0.0003	-
	Steel	9.5	8.02	60.9	0.0005	0.253	1.02	0	15	0.164	0.0036	0.016	0.74	0	-	384	149	0.0004	-
	Steel	7.9	8.02	60.9	0.0005	0.253	1.02	0	15	0.156	0.0083	0.016	0.74	0	-	319	124	0.0005	-
	Steel	6.34	8.02	60.9	0.0005	0.253	1.02	0	15	0.145	0.0072	0.016	0.74	0	-	256	99	0.0006	-
	Steel	4.75	8.02	60.9	0.0005	0.253	1.02	0	15	0.128	0.0095	0.016	0.74	0	-	192	74	0.0008	-
	Steel	3.14	8.02	60.9	0.0005	0.253	1.02	0	15	0.106	0.0041	0.016	0.74	0	-	127	49	0.0012	-
	Steel	1.57	8.02	60.9	0.0005	0.253	1.02	0	15	0.071	0.002	0.016	0.74	0	-	63	25	0.0024	-
	Glass	29.3	2.6	60.9	0.0005	0.253	1.02	0	15	0.226	0.0062	0.016	0.74	0	-	723	459	0.0006	-
	Glass	25.17	2.6	60.9	0.0005	0.253	1.02	0	15	0.221	0.0059	0.016	0.74	0	-	621	394	0.0007	-
	Glass	21.7	2.6	60.9	0.0005	0.253	1.02	0	15	0.211	0.0098	0.016	0.74	0	-	535	340	0.0008	-
	Glass	15.97	2.6	60.9	0.0005	0.253	1.02	0	15	0.201	0.0068	0.016	0.74	0	-	394	250	0.001	-
	Glass	14.48	2.6	60.9	0.0005	0.253	1.02	0	15	0.194	0.0066	0.016	0.74	0	-	357	227	0.0011	-
	Natural	13.6	2.65	60.9	0.0005	0.253	1.02	0	21	0.145	0.0088	0.016	0.74	0	-	339	213	0.0012	-
	Natural	9.6	2.65	60.9	0.0005	0.253	1.02	0	21	0.148	0.0085	0.016	0.74	0	-	239	150	0.0017	-

Table1: The CSU Experiments Database (Cont'd)

Run	Type	d_s (mm)	G	y (mm)	S_f	u_f (m/s)	ν 10^{-6} (m^2/s)	k_s (mm)	n	V_{pobs} (m/s)	σ (m/s)	u_* (m/s)	δ (mm)	k_s/d_s	d_s/k_s	d_*	Re_*	τ_{*ds}	τ_{*ks}
(1)	(2)	(3)	(4)	(5)	(6)	(7)	(8)	(9)	(10)	(11)	(12)	(13)	(14)	(15)	(16)	(17)	(18)	(19)	(20)
4	Steel	19.04	8.02	41.9	0.0005	0.204	1.02	0	15	0.164	0.0032	0.012	0.99	0	-	772	223	0.0001	-
	Steel	15.88	8.02	41.9	0.0005	0.204	1.02	0	15	0.156	0.0039	0.012	0.99	0	-	644	186	0.0001	-
	Steel	14.28	8.02	41.9	0.0005	0.204	1.02	0	15	0.151	0.0032	0.012	0.99	0	-	579	167	0.0002	-
	Steel	9.5	8.02	41.9	0.0005	0.204	1.02	0	15	0.133	0.0044	0.012	0.99	0	-	385	111	0.0002	-
	Steel	7.9	8.02	41.9	0.0005	0.204	1.02	0	15	0.127	0.0026	0.012	0.99	0	-	320	93	0.0003	-
	Steel	6.34	8.02	41.9	0.0005	0.204	1.02	0	15	0.113	0.0026	0.012	0.99	0	-	257	74	0.0003	-
	Steel	4.75	8.02	41.9	0.0005	0.204	1.02	0	15	0.1	0.0047	0.012	0.99	0	-	193	56	0.0004	-
	Steel	3.14	8.02	41.9	0.0005	0.204	1.02	0	15	0.081	0.0032	0.012	0.99	0	-	127	37	0.0007	-
	Steel	1.57	8.02	41.9	0.0005	0.204	1.02	0	18	0.054	0.0023	0.012	0.99	0	-	64	18	0.0013	-
	Glass	29.3	2.6	41.9	0.0005	0.204	1.02	0	15	0.197	0.0044	0.012	0.99	0	-	726	343	0.0003	-
	Glass	25.17	2.6	41.9	0.0005	0.204	1.02	0	15	0.19	0.0044	0.012	0.99	0	-	623	295	0.0004	-
	Glass	21.7	2.6	41.9	0.0005	0.204	1.02	0	15	0.184	0.0049	0.012	0.99	0	-	538	254	0.0004	-
	Glass	15.97	2.6	41.9	0.0005	0.204	1.02	0	15	0.17	0.0041	0.012	0.99	0	-	396	187	0.0006	-
	Glass	14.48	2.6	41.9	0.0005	0.204	1.02	0	15	0.166	0.0059	0.012	0.99	0	-	359	170	0.0006	-
5	Steel	19.04	8.02	69.32	0.0005	0.278	1.02	0	15	0.201	0.0092	0.014	0.84	0	-	769	263	0.0002	-
	Steel	15.88	8.02	69.32	0.0005	0.278	1.02	0	15	0.194	0.0051	0.014	0.84	0	-	641	219	0.0002	-
	Steel	14.28	8.02	69.32	0.0005	0.278	1.02	0	15	0.192	0.0047	0.014	0.84	0	-	577	197	0.0002	-
	Steel	9.5	8.02	69.32	0.0005	0.278	1.02	0	18	0.172	0.0068	0.014	0.84	0	-	384	131	0.0003	-
	Steel	7.9	8.02	69.32	0.0005	0.278	1.02	0	18	0.161	0.005	0.014	0.84	0	-	319	109	0.0004	-
	Steel	6.34	8.02	69.32	0.0005	0.278	1.02	0	18	0.154	0.0065	0.014	0.84	0	-	256	87	0.0005	-
	Steel	4.75	8.02	69.32	0.0005	0.278	1.02	0	21	0.139	0.008	0.014	0.84	0	-	192	66	0.0006	-
	Steel	3.14	8.02	69.32	0.0005	0.278	1.02	0	18	0.121	0.006	0.014	0.84	0	-	127	43	0.0009	-
	Steel	1.57	8.02	69.32	0.0005	0.278	1.02	0	21	0.079	0.0032	0.014	0.84	0	-	63	22	0.0018	-
	Glass	29.3	2.6	69.32	0.0005	0.278	1.02	0	18	0.243	0.0104	0.014	0.84	0	-	723	404	0.0004	-
	Glass	25.17	2.6	69.32	0.0005	0.278	1.02	0	18	0.234	0.0101	0.014	0.84	0	-	621	347	0.0005	-
	Glass	21.7	2.6	69.32	0.0005	0.278	1.02	0	18	0.224	0.0055	0.014	0.84	0	-	535	299	0.0006	-
	Glass	15.97	2.6	69.32	0.0005	0.278	1.02	0	18	0.212	0.0083	0.014	0.84	0	-	394	220	0.0008	-
	Glass	14.48	2.6	69.32	0.0005	0.278	1.02	0	18	0.204	0.0094	0.014	0.84	0	-	357	200	0.0009	-
6	Steel	19.04	8.02	52.23	0.0007	0.266	1.02	0	15	0.215	0.0058	0.015	0.78	0	-	769	283	0.0002	-
	Steel	15.88	8.02	52.23	0.0007	0.266	1.02	0	15	0.206	0.0078	0.015	0.78	0	-	641	236	0.0002	-
	Steel	14.28	8.02	52.23	0.0007	0.266	1.02	0	15	0.2	0.0052	0.015	0.78	0	-	577	212	0.0002	-
	Steel	9.5	8.02	52.23	0.0007	0.266	1.02	0	15	0.177	0.0036	0.015	0.78	0	-	384	141	0.0004	-
	Steel	7.9	8.02	52.23	0.0007	0.266	1.02	0	15	0.166	0.0063	0.015	0.78	0	-	319	117	0.0004	-

Table1: The CSU Experiments Database (Cont'd)

Run	Type	d_s (mm)	G	y (mm)	S_f	u_f (m/s)	ν 10^{-6} (m^2/s)	k_s (mm)	n	V_{pobs} (m/s)	σ (m/s)	u_* (m/s)	δ (mm)	k_s/d_s	d_s/k_s	d_*	Re_*	τ_{*ds}	τ_{*ks}
(1)	(2)	(3)	(4)	(5)	(6)	(7)	(8)	(9)	(10)	(11)	(12)	(13)	(14)	(15)	(16)	(17)	(18)	(19)	(20)
6	Steel	6.34	8.02	52.23	0.0007	0.266	1.02	0	15	0.158	0.0045	0.015	0.78	0	-	256	94	0.0005	-
	Steel	4.75	8.02	52.23	0.0007	0.266	1.02	0	18	0.138	0.0055	0.015	0.78	0	-	192	71	0.0007	-
	Steel	3.14	8.02	52.23	0.0007	0.266	1.02	0	18	0.122	0.005	0.015	0.78	0	-	127	47	0.0011	-
	Steel	1.57	8.02	52.23	0.0007	0.266	1.02	0	18	0.081	0.0045	0.015	0.78	0	-	63	23	0.0022	-
	Glass	29.3	2.6	52.23	0.0007	0.266	1.02	0	15	0.254	0.0064	0.015	0.78	0	-	723	436	0.0005	-
	Glass	25.17	2.6	52.23	0.0007	0.266	1.02	0	15	0.243	0.0073	0.015	0.78	0	-	621	374	0.0006	-
	Glass	21.7	2.6	52.23	0.0007	0.266	1.02	0	15	0.241	0.007	0.015	0.78	0	-	535	323	0.0007	-
	Glass	15.97	2.6	52.23	0.0007	0.266	1.02	0	15	0.22	0.0078	0.015	0.78	0	-	394	237	0.0009	-
	Glass	14.48	2.6	52.23	0.0007	0.266	1.02	0	15	0.213	0.0058	0.015	0.78	0	-	357	215	0.001	-
7	Steel	19.04	8.02	60.53	0.001	0.305	1.03	0	15	0.236	0.0085	0.019	0.61	0	-	766	359	0.0003	-
	Steel	15.88	8.02	60.53	0.001	0.305	1.03	0	18	0.228	0.0102	0.019	0.61	0	-	639	300	0.0004	-
	Steel	14.28	8.02	60.53	0.001	0.305	1.03	0	15	0.219	0.0078	0.019	0.61	0	-	574	269	0.0004	-
	Steel	9.5	8.02	60.53	0.001	0.305	1.03	0	21	0.199	0.0093	0.019	0.61	0	-	382	179	0.0006	-
	Steel	7.9	8.02	60.53	0.001	0.305	1.03	0	21	0.198	0.01	0.019	0.61	0	-	318	149	0.0007	-
	Steel	6.34	8.02	60.53	0.001	0.305	1.03	0	18	0.188	0.0097	0.019	0.61	0	-	255	120	0.0009	-
	Steel	4.75	8.02	60.53	0.001	0.305	1.03	0	18	0.172	0.0066	0.019	0.61	0	-	191	90	0.0012	-
	Steel	3.14	8.02	60.53	0.001	0.305	1.03	0	15	0.15	0.0058	0.019	0.61	0	-	126	59	0.0018	-
	Steel	1.57	8.02	60.53	0.001	0.305	1.03	0	18	0.105	0.005	0.019	0.61	0	-	63	30	0.0035	-
	Glass	29.3	2.6	60.53	0.001	0.305	1.03	0	15	0.283	0.0071	0.019	0.61	0	-	720	553	0.0008	-
	Glass	25.17	2.6	60.53	0.001	0.305	1.03	0	15	0.269	0.0084	0.019	0.61	0	-	618	475	0.001	-
	Glass	21.7	2.6	60.53	0.001	0.305	1.03	0	15	0.258	0.0069	0.019	0.61	0	-	533	409	0.0011	-
	Glass	15.97	2.6	60.53	0.001	0.305	1.03	0	21	0.24	0.0113	0.019	0.61	0	-	392	301	0.0015	-
	Glass	14.48	2.6	60.53	0.001	0.305	1.03	0	18	0.239	0.0093	0.019	0.61	0	-	356	273	0.0017	-
8	Steel	19.04	8.02	69.15	0.0014	0.411	1.02	0	21	0.307	0.0105	0.025	0.47	0	-	772	467	0.0005	-
	Steel	15.88	8.02	69.15	0.0014	0.411	1.02	0	18	0.302	0.014	0.025	0.47	0	-	644	389	0.0006	-
	Steel	14.28	8.02	69.15	0.0014	0.411	1.02	0	15	0.293	0.0082	0.025	0.47	0	-	579	350	0.0006	-
	Steel	9.5	8.02	69.15	0.0014	0.411	1.02	0	15	0.262	0.0069	0.025	0.47	0	-	385	233	0.001	-
	Steel	7.9	8.02	69.15	0.0014	0.411	1.02	0	18	0.258	0.0081	0.025	0.47	0	-	320	194	0.0012	-
	Steel	6.34	8.02	69.15	0.0014	0.411	1.02	0	18	0.239	0.0084	0.025	0.47	0	-	257	155	0.0014	-
	Steel	4.75	8.02	69.15	0.0014	0.411	1.02	0	18	0.228	0.0092	0.025	0.47	0	-	193	116	0.002	-
	Steel	3.14	8.02	69.15	0.0014	0.411	1.02	0	21	0.201	0.0093	0.025	0.47	0	-	127	77	0.0029	-
	Steel	1.57	8.02	69.15	0.0014	0.411	1.02	0	21	0.152	0.0078	0.025	0.47	0	-	64	38	0.0057	-
	Glass	29.3	2.6	69.15	0.0014	0.411	1.02	0	18	0.359	0.0127	0.025	0.47	0	-	726	718	0.0014	-

Table1: The CSU Experiments Database (Cont'd)

Run	Type	d_s (mm)	G	y (mm)	S_f	u_f (m/s)	ν 10^{-6} (m^2/s)	k_s (mm)	n	V_{pobs} (m/s)	σ (m/s)	u_* (m/s)	δ (mm)	k_s/d_s	d_s/k_s	d_*	Re_*	τ_{*ds}	τ_{*ks}
(1)	(2)	(3)	(4)	(5)	(6)	(7)	(8)	(9)	(10)	(11)	(12)	(13)	(14)	(15)	(16)	(17)	(18)	(19)	(20)
8	Glass	25.17	2.6	69.15	0.0014	0.411	1.02	0	18	0.338	0.0104	0.025	0.47	0	-	623	617	0.0016	-
	Glass	21.7	2.6	69.15	0.0014	0.411	1.02	0	15	0.337	0.0093	0.025	0.47	0	-	538	532	0.0018	-
	Glass	15.97	2.6	69.15	0.0014	0.411	1.02	0	15	0.312	0.0073	0.025	0.47	0	-	396	391	0.0025	-
	Glass	14.48	2.6	69.15	0.0014	0.411	1.02	0	15	0.308	0.0086	0.025	0.47	0	-	359	355	0.0027	-
9	Steel	19.04	8.02	69.92	0.002	0.529	1.02	0	15	0.447	0.0079	0.03	0.39	0	-	772	560	0.0007	-
	Steel	15.88	8.02	69.92	0.002	0.529	1.02	0	15	0.44	0.0072	0.03	0.39	0	-	644	467	0.0008	-
	Steel	14.28	8.02	69.92	0.002	0.529	1.02	0	18	0.444	0.0187	0.03	0.39	0	-	579	420	0.0009	-
	Steel	9.5	8.02	69.92	0.002	0.529	1.02	0	15	0.392	0.0113	0.03	0.39	0	-	385	280	0.0014	-
	Steel	7.9	8.02	69.92	0.002	0.529	1.02	0	18	0.371	0.0108	0.03	0.39	0	-	320	232	0.0017	-
	Steel	6.34	8.02	69.92	0.002	0.529	1.02	0	15	0.348	0.0083	0.03	0.39	0	-	257	187	0.0021	-
	Steel	4.75	8.02	69.92	0.002	0.529	1.02	0	18	0.328	0.0093	0.03	0.39	0	-	193	140	0.0027	-
	Steel	3.14	8.02	69.92	0.002	0.529	1.02	0	18	0.3	0.0116	0.03	0.39	0	-	127	92	0.0041	-
	Steel	1.57	8.02	69.92	0.002	0.529	1.02	0	15	0.25	0.0053	0.03	0.39	0	-	64	46	0.0083	-
	Glass	29.3	2.6	69.92	0.002	0.529	1.02	0	15	0.526	0.0112	0.03	0.39	0	-	726	862	0.002	-
	Glass	25.17	2.6	69.92	0.002	0.529	1.02	0	15	0.51	0.0095	0.03	0.39	0	-	623	741	0.0023	-
	Glass	21.7	2.6	69.92	0.002	0.529	1.02	0	18	0.489	0.0213	0.03	0.39	0	-	538	638	0.0026	-
	Glass	15.97	2.6	69.92	0.002	0.529	1.02	0	15	0.45	0.0179	0.03	0.39	0	-	396	470	0.0036	-
	Glass	14.48	2.6	69.92	0.002	0.529	1.02	0	18	0.434	0.0159	0.03	0.39	0	-	359	426	0.0039	-
10	Steel	19.04	8.02	72.28	0.0007	0.285	1	0	15	0.217	0.0052	0.018	0.66	0	-	778	334	0.0003	-
	Steel	15.88	8.02	72.28	0.0007	0.285	1	0	18	0.203	0.0064	0.018	0.66	0	-	649	278	0.0003	-
	Steel	14.28	8.02	72.28	0.0007	0.285	1	0	15	0.196	0.0034	0.018	0.66	0	-	584	250	0.0003	-
	Steel	9.5	8.02	72.28	0.0007	0.285	1	0	15	0.179	0.0071	0.018	0.66	0	-	388	167	0.0005	-
	Steel	7.9	8.02	72.28	0.0007	0.285	1	0	15	0.168	0.0048	0.018	0.66	0	-	323	138	0.0006	-
	Steel	6.34	8.02	72.28	0.0007	0.285	1	0	18	0.156	0.0071	0.018	0.66	0	-	259	111	0.0007	-
	Steel	4.75	8.02	72.28	0.0007	0.285	1	0	15	0.149	0.004	0.018	0.66	0	-	194	83	0.001	-
	Steel	3.14	8.02	72.28	0.0007	0.285	1	0	21	0.124	0.0039	0.018	0.66	0	-	128	55	0.0014	-
	Steel	1.57	8.02	72.28	0.0007	0.285	1	0	18	0.082	0.0029	0.018	0.66	0	-	64	28	0.0029	-
	Glass	29.3	2.6	72.28	0.0007	0.285	1	0	15	0.254	0.0072	0.018	0.66	0	-	732	514	0.0007	-
	Glass	25.17	2.6	72.28	0.0007	0.285	1	0	18	0.241	0.0095	0.018	0.66	0	-	629	441	0.0008	-
	Glass	21.7	2.6	72.28	0.0007	0.285	1	0	15	0.236	0.007	0.018	0.66	0	-	542	380	0.0009	-
	Glass	15.97	2.6	72.28	0.0007	0.285	1	0	18	0.223	0.0094	0.018	0.66	0	-	399	280	0.0013	-
	Glass	14.48	2.6	72.28	0.0007	0.285	1	0	15	0.215	0.0022	0.018	0.66	0	-	362	254	0.0014	-

Table1: The CSU Experiments Database (Cont'd)

Run	Type	d_s (mm)	G	y (mm)	S_f	u_f (m/s)	ν 10^{-6} (m^2/s)	k_s (mm)	n	V_{pobs} (m/s)	σ (m/s)	u_* (m/s)	δ (mm)	k_s/d_s	d_s/k_s	d_*	Re_*	τ_{*ds}	τ_{*ks}
(1)	(2)	(3)	(4)	(5)	(6)	(7)	(8)	(9)	(10)	(11)	(12)	(13)	(14)	(15)	(16)	(17)	(18)	(19)	(20)
11	Steel	19.04	8.02	43.77	0.004	0.691	1.03	0	15	0.622	0.0153	0.036	0.33	0	-	766	659	0.001	-
	Steel	15.88	8.02	43.77	0.004	0.691	1.03	0	15	0.608	0.0163	0.036	0.33	0	-	639	550	0.0012	-
	Steel	14.28	8.02	43.77	0.004	0.691	1.03	0	18	0.581	0.0338	0.036	0.33	0	-	574	494	0.0013	-
	Steel	9.5	8.02	43.77	0.004	0.691	1.03	0	15	0.542	0.0228	0.036	0.33	0	-	382	329	0.0019	-
	Steel	7.9	8.02	43.77	0.004	0.691	1.03	0	15	0.494	0.0072	0.036	0.33	0	-	318	273	0.0023	-
	Steel	6.34	8.02	43.77	0.004	0.691	1.03	0	18	0.499	0.0178	0.036	0.33	0	-	255	219	0.0029	-
	Steel	4.75	8.02	43.77	0.004	0.691	1.03	0	18	0.448	0.0188	0.036	0.33	0	-	191	164	0.0039	-
	Steel	3.14	8.02	43.77	0.004	0.691	1.03	0	21	0.426	0.0232	0.036	0.33	0	-	126	109	0.0059	-
	Steel	1.57	8.02	43.77	0.004	0.691	1.03	0	21	0.352	0.0202	0.036	0.33	0	-	63	54	0.0117	-
	Glass	29.3	2.6	43.77	0.004	0.691	1.03	0	15	0.722	0.0153	0.036	0.33	0	-	720	1014	0.0028	-
	Glass	25.17	2.6	43.77	0.004	0.691	1.03	0	15	0.696	0.0214	0.036	0.33	0	-	618	871	0.0032	-
	Glass	21.7	2.6	43.77	0.004	0.691	1.03	0	15	0.659	0.0229	0.036	0.33	0	-	533	751	0.0037	-
	Glass	15.97	2.6	43.77	0.004	0.691	1.03	0	15	0.606	0.0203	0.036	0.33	0	-	392	553	0.0051	-
	Glass	14.48	2.6	43.77	0.004	0.691	1.03	0	15	0.61	0.0198	0.036	0.33	0	-	356	501	0.0056	-
12	Steel	19.04	8.02	52.82	0.0003	0.209	1.03	0	18	0.159	0.0052	0.01	1.24	0	-	766	180	0.0001	-
	Steel	15.88	8.02	52.82	0.0003	0.209	1.03	0	15	0.153	0.0043	0.01	1.24	0	-	639	150	0.0001	-
	Steel	14.28	8.02	52.82	0.0003	0.209	1.03	0	15	0.15	0.0039	0.01	1.24	0	-	574	135	0.0001	-
	Steel	9.5	8.02	52.82	0.0003	0.209	1.03	0	15	0.134	0.0031	0.01	1.24	0	-	382	90	0.0002	-
	Steel	7.9	8.02	52.82	0.0003	0.209	1.03	0	18	0.126	0.0051	0.01	1.24	0	-	318	75	0.0002	-
	Steel	6.34	8.02	52.82	0.0003	0.209	1.03	0	18	0.118	0.0042	0.01	1.24	0	-	255	60	0.0002	-
	Steel	4.75	8.02	52.82	0.0003	0.209	1.03	0	18	0.107	00047	0.01	1.24	0	-	191	45	0.0003	-
	Steel	3.14	8.02	52.82	0.0003	0.209	1.03	0	18	0.083	0.0032	0.01	1.24	0	-	126	30	0.0005	-
	Steel	1.57	8.02	52.82	0.0003	0.209	1.03	0	15	0.052	0.0012	0.01	1.24	0	-	63	15	0.0009	-
	Glass	29.3	2.6	52.82	0.0003	0.209	1.03	0	15	0.19	0.003	0.01	1.24	0	-	720	276	0.0002	-
	Glass	25.17	2.6	52.82	0.0003	0.209	1.03	0	15	0.182	0.0048	0.01	1.24	0	-	618	237	0.0003	-
	Glass	21.7	2.6	52.82	0.0003	0.209	1.03	0	18	0.177	0.0057	0.01	1.24	0	-	533	205	0.0003	-
	Glass	15.97	2.6	52.82	0.0003	0.209	1.03	0	15	0.162	0.0023	0.01	1.24	0	-	392	151	0.0004	-
	Glass	14.48	2.6	52.82	0.0003	0.209	1.03	0	15	0.161	0.0024	0.01	1.24	0	-	356	137	0.0004	-
19	Steel	19.04	8.02	54.93	0.0045	0.772	1.02	0	18	0.724	0.0304	0.042	0.28	0	-	772	794	0.0014	-
	Steel	15.88	8.02	54.93	0.0045	0.772	1.02	0	18	0.715	0.0251	0.042	0.28	0	-	644	663	0.0017	-
	Steel	14.28	8.02	54.93	0.0045	0.772	1.02	0	18	0.695	0.0297	0.042	0.28	0	-	579	596	0.0018	-
	Steel	9.5	8.02	54.93	0.0045	0.772	1.02	0	18	0.618	0.0321	0.042	0.28	0	-	385	396	0.0028	-
	Steel	7.9	8.02	54.93	0.0045	0.772	1.02	0	18	0.619	0.0281	0.042	0.28	0	-	320	330	0.0033	-

Table1: The CSU Experiments Database (Cont'd)

Run	Type	d_s (mm)	G	y (mm)	S_f	u_f (m/s)	ν 10^{-6} (m^2/s)	k_s (mm)	n	V_{pobs} (m/s)	σ (m/s)	u_* (m/s)	δ (mm)	k_s/d_s	d_s/k_s	d_*	Re_*	τ_{*ds}	τ_{*ks}
(1)	(2)	(3)	(4)	(5)	(6)	(7)	(8)	(9)	(10)	(11)	(12)	(13)	(14)	(15)	(16)	(17)	(18)	(19)	(20)
19	Steel	6.34	8.02	54.93	0.0045	0.772	1.02	0	18	0.586	0.0288	0.042	0.28	0	-	257	265	0.0041	-
	Steel	4.75	8.02	54.93	0.0045	0.772	1.02	0	18	0.543	0.0197	0.042	0.28	0	-	193	198	0.0055	-
	Steel	3.14	8.02	54.93	0.0045	0.772	1.02	0	18	0.503	0.0206	0.042	0.28	0	-	127	131	0.0083	-
	Steel	1.57	8.02	54.93	0.0045	0.772	1.02	0	18	0.426	0.0214	0.042	0.28	0	-	64	66	0.0166	-
	Glass	29.3	2.6	54.93	0.0045	0.772	1.02	0	18	0.787	0.0344	0.042	0.28	0	-	726	1223	0.0039	-
	Glass	25.17	2.6	54.93	0.0045	0.772	1.02	0	18	0.785	0.0319	0.042	0.28	0	-	623	1050	0.0046	-
	Glass	21.7	2.6	54.93	0.0045	0.772	1.02	0	18	0.76	0.0321	0.042	0.28	0	-	538	905	0.0053	-
	Glass	15.97	2.6	54.93	0.0045	0.772	1.02	0	18	0.711	0.0326	0.042	0.28	0	-	396	666	0.0072	-
	Glass	14.48	2.6	54.93	0.0045	0.772	1.02	0	18	0.705	0.0396	0.042	0.28	0	-	359	604	0.0079	-
45	Glass	29.3	2.6	59.83	0.0009	0.254	1.004	1.2	15	0.122	0.0061	0.019	0.61	0.04	24.42	732	554	0.0008	0.019
	Glass	25.17	2.6	59.83	0.0009	0.254	1.004	1.2	15	0.112	0.0048	0.019	0.61	0.05	20.98	629	476	0.0009	0.019
	Glass	21.7	2.6	59.83	0.0009	0.254	1.004	1.2	15	0.107	0.0045	0.019	0.61	0.06	18.08	542	411	0.0011	0.019
	Glass	15.97	2.6	59.83	0.0009	0.254	1.004	1.2	15	0.094	0.0046	0.019	0.61	0.08	13.31	399	302	0.0015	0.019
	Glass	14.48	2.6	59.83	0.0009	0.254	1.004	1.2	15	0.09	0.0036	0.019	0.61	0.08	12.07	362	274	0.0016	0.019
46	Glass	29.3	2.6	52.65	0.0021	0.352	1.004	1.2	15	0.186	0.0046	0.027	0.43	0.04	24.42	732	788	0.0016	0.039
	Glass	25.17	2.6	52.65	0.0021	0.352	1.004	1.2	15	0.18	0.0079	0.027	0.43	0.05	20.98	629	677	0.0019	0.039
	Glass	21.7	2.6	52.65	0.0021	0.352	1.004	1.2	15	0.169	0.0058	0.027	0.43	0.06	18.08	542	584	0.0022	0.039
	Glass	15.97	2.6	52.65	0.0021	0.352	1.004	1.2	15	0.166	0.0109	0.027	0.43	0.08	13.31	399	429	0.003	0.039
	Glass	14.48	2.6	52.65	0.0021	0.352	1.004	1.2	15	0.161	0.0065	0.027	0.43	0.08	12.07	362	389	0.0032	0.039
	Natural	13.6	2.65	52.65	0.0021	0.352	1.004	1.2	15	0.131	0.0085	0.027	0.43	0.09	11.33	343	366	0.0033	0.038
	Natural	9.6	2.65	52.65	0.0021	0.352	1.004	1.2	15	0.136	0.0159	0.027	0.43	0.13	8	242	258	0.0047	0.038
47	Steel	19.04	8.02	55.57	0.0033	0.468	1.004	1.2	15	0.134	0.0038	0.036	0.33	0.06	15.87	778	679	0.001	0.016
	Steel	15.88	8.02	55.57	0.0033	0.468	1.004	1.2	15	0.121	0.006	0.036	0.33	0.08	13.23	649	566	0.0012	0.016
	Steel	14.28	8.02	55.57	0.0033	0.468	1.004	1.2	15	0.113	0.0039	0.036	0.33	0.08	11.9	584	509	0.0013	0.016
	Glass	29.3	2.6	55.57	0.0033	0.468	1.004	1.2	15	0.344	0.0166	0.036	0.33	0.04	24.42	732	1045	0.0028	0.068
	Glass	25.17	2.6	55.57	0.0033	0.468	1.004	1.2	15	0.336	0.0161	0.036	0.33	0.05	20.98	629	897	0.0033	0.068
	Glass	21.7	2.6	55.57	0.0033	0.468	1.004	1.2	15	0.328	0.0136	0.036	0.33	0.06	18.08	542	774	0.0038	0.068
	Glass	15.97	2.6	55.57	0.0033	0.468	1.004	1.2	15	0.314	0.0095	0.036	0.33	0.08	13.31	399	569	0.0051	0.068
	Glass	14.48	2.6	55.57	0.0033	0.468	1.004	1.2	15	0.309	0.0227	0.036	0.33	0.08	12.07	362	516	0.0057	0.068
	Natural	13.6	2.65	55.57	0.0033	0.468	1.004	1.2	15	0.224	0.0163	0.036	0.33	0.09	11.33	343	485	0.0058	0.066
	Natural	9.6	2.65	55.57	0.0033	0.468	1.004	1.2	15	0.237	0.0257	0.036	0.33	0.13	8	242	342	0.0083	0.066
	Natural	6.8	2.65	55.57	0.0033	0.468	1.004	1.2	15	0.247	0.028	0.036	0.33	0.18	5.67	172	242	0.0116	0.066

Table1: The CSU Experiments Database (Cont'd)

Run	Type	d_s (mm)	G	y (mm)	S_f	u_f (m/s)	ν 10^{-6} (m^2/s)	k_s (mm)	N	V_{pobs} (m/s)	σ (m/s)	u_* (m/s)	δ (mm)	k_s/d_s	d_s/k_s	d_*	Re_*	τ_{*ds}	τ_{*ks}
(1)	(2)	(3)	(4)	(5)	(6)	(7)	(8)	(9)	(10)	(11)	(12)	(13)	(14)	(15)	(16)	(17)	(18)	(19)	(20)
47	Natural	4.8	2.65	55.57	0.0033	0.468	1.004	1.2	15	0.273	0.0218	0.036	0.33	0.25	4	121	171	0.0165	0.066
48	Steel	19.04	8.02	60.65	0.0044	0.682	1.004	1.2	15	0.188	0.0064	0.044	0.26	0.06	15.87	778	834	0.0015	0.024
	Steel	15.88	8.02	60.65	0.0044	0.682	1.004	1.2	15	0.175	0.0061	0.044	0.26	0.08	13.23	649	696	0.0018	0.024
	Steel	14.28	8.02	60.65	0.0044	0.682	1.004	1.2	15	0.167	0.0063	0.044	0.26	0.08	11.9	584	626	0.002	0.024
	Steel	9.5	8.02	60.65	0.0044	0.682	1.004	1.2	15	0.157	0.0095	0.044	0.26	0.13	7.92	388	416	0.003	0.024
	Steel	7.9	8.02	60.65	0.0044	0.682	1.004	1.2	15	0.166	0.0163	0.044	0.26	0.15	6.58	323	346	0.0036	0.024
	Steel	6.34	8.02	60.65	0.0044	0.682	1.004	1.2	15	0.167	0.0207	0.044	0.26	0.19	5.28	259	278	0.0044	0.024
	Steel	4.75	8.02	60.65	0.0044	0.682	1.004	1.2	15	0.19	0.0245	0.044	0.26	0.25	3.96	194	208	0.0059	0.024
	Glass	29.3	2.6	60.65	0.0044	0.682	1.004	1.2	15	0.499	0.0252	0.044	0.26	0.04	24.42	732	1284	0.0042	0.103
	Glass	25.17	2.6	60.65	0.0044	0.682	1.004	1.2	15	0.51	0.0269	0.044	0.26	0.05	20.98	629	1103	0.0049	0.103
	Glass	21.7	2.6	60.65	0.0044	0.682	1.004	1.2	15	0.479	0.0255	0.044	0.26	0.06	18.08	542	951	0.0057	0.103
	Glass	15.97	2.6	60.65	0.0044	0.682	1.004	1.2	15	0.467	0.0326	0.044	0.26	0.08	13.31	399	700	0.0077	0.103
	Glass	14.48	2.6	60.65	0.0044	0.682	1.004	1.2	15	0.46	0.0336	0.044	0.26	0.08	12.07	362	635	0.0085	0.103
	Natural	13.6	2.65	60.65	0.0044	0.682	1.004	1.2	15	0.403	0.0464	0.044	0.26	0.09	11.33	343	596	0.0088	0.1
	Natural	9.6	2.65	60.65	0.0044	0.682	1.004	1.2	15	0.394	0.0277	0.044	0.26	0.13	8	242	421	0.0125	0.1
	Natural	6.8	2.65	60.65	0.0044	0.682	1.004	1.2	15	0.368	0.0418	0.044	0.26	0.18	5.67	172	298	0.0176	0.1
	Natural	4.8	2.65	60.65	0.0044	0.682	1.004	1.2	15	0.396	0.0305	0.044	0.26	0.25	4	121	210	0.0249	0.1
	Natural	3.4	2.65	60.65	0.0044	0.682	1.004	1.2	15	0.372	0.0398	0.044	0.26	0.35	2.83	86	149	0.0352	0.1
49	Steel	19.04	8.02	64.12	0.0056	0.794	1.004	1.2	15	0.234	0.011	0.051	0.23	0.06	15.87	778	961	0.002	0.031
	Steel	15.88	8.02	64.12	0.0056	0.794	1.004	1.2	15	0.237	0.0208	0.051	0.23	0.08	13.23	649	802	0.0024	0.031
	Steel	14.28	8.02	64.12	0.0056	0.794	1.004	1.2	15	0.243	0.0203	0.051	0.23	0.08	11.9	584	721	0.0026	0.031
	Steel	9.5	8.02	64.12	0.0056	0.794	1.004	1.2	15	0.231	0.0176	0.051	0.23	0.13	7.92	388	480	0.0039	0.031
	Steel	7.9	8.02	64.12	0.0056	0.794	1.004	1.2	15	0.249	0.0221	0.051	0.23	0.15	6.58	323	399	0.0047	0.031
	Glass	29.3	2.6	64.12	0.0056	0.794	1.004	1.2	15	0.626	0.0345	0.051	0.23	0.04	24.42	732	1480	0.0056	0.137
	Glass	25.17	2.6	64.12	0.0056	0.794	1.004	1.2	15	0.618	0.037	0.051	0.23	0.05	20.98	629	1271	0.0065	0.137
	Glass	21.7	2.6	64.12	0.0056	0.794	1.004	1.2	15	0.607	0.0147	0.051	0.23	0.06	18.08	542	1096	0.0076	0.137
	Glass	15.97	2.6	64.12	0.0056	0.794	1.004	1.2	15	0.608	0.0539	0.051	0.23	0.08	13.31	399	806	0.0103	0.137
	Glass	14.48	2.6	64.12	0.0056	0.794	1.004	1.2	15	0.567	0.0458	0.051	0.23	0.08	12.07	362	731	0.0113	0.137
	Natural	13.6	2.65	64.12	0.0056	0.794	1.004	1.2	15	0.506	0.0503	0.051	0.23	0.09	11.33	343	687	0.0117	0.132
	Natural	9.6	2.65	64.12	0.0056	0.794	1.004	1.2	15	0.512	0.0423	0.051	0.23	0.13	8	242	485	0.0166	0.132
	Natural	6.8	2.65	64.12	0.0056	0.794	1.004	1.2	15	0.473	0.0484	0.051	0.23	0.18	5.67	172	343	0.0234	0.132
	Natural	4.8	2.65	64.12	0.0056	0.794	1.004	1.2	15	0.492	0.0333	0.051	0.23	0.25	4	121	242	0.0331	0.132
	Natural	3.4	2.65	64.12	0.0056	0.794	1.004	1.2	15	0.48	0.0354	0.051	0.23	0.35	2.83	86	172	0.0467	0.132

Table1: The CSU Experiments Database (Cont'd)

Run	Type	d_s (mm)	G	y (mm)	S_f	u_f (m/s)	ν 10^{-6} (m^2/s)	k_s (mm)	n	V_{pobs} (m/s)	σ (m/s)	u_* (m/s)	δ (mm)	k_s/d_s	d_s/k_s	d_*	Re_*	τ_{*ds}	τ_{*ks}
(1)	(2)	(3)	(4)	(5)	(6)	(7)	(8)	(9)	(10)	(11)	(12)	(13)	(14)	(15)	(16)	(17)	(18)	(19)	(20)
49	Natural	2.4	2.65	64.12	0.0056	0.794	1.004	1.2	15	0.473	0.0351	0.051	0.23	0.5	2	61	121	0.0662	0.132
28	Steel	19.04	8.02	56.42	0.01	0.891	1.004	1.7	21	0.328	0.0319	0.063	0.19	0.09	11.2	778	1185	0.003	0.033
	Steel	15.88	8.02	56.42	0.01	0.891	1.004	1.7	21	0.317	0.0268	0.063	0.19	0.11	9.34	649	989	0.0036	0.033
	Steel	14.28	8.02	56.42	0.01	0.891	1.004	1.7	21	0.324	0.0349	0.063	0.19	0.12	8.4	584	889	0.004	0.033
	Steel	9.5	8.02	56.42	0.01	0.891	1.004	1.7	21	0.34	0.0285	0.063	0.19	0.18	5.59	388	591	0.006	0.033
	Steel	7.9	8.02	56.42	0.01	0.891	1.004	1.7	21	0.354	0.029	0.063	0.19	0.22	4.65	323	492	0.0072	0.033
	Glass	29.3	2.6	56.42	0.01	0.891	1.004	1.7	15	0.78	0.0265	0.063	0.19	0.06	17.24	732	1824	0.0085	0.146
	Glass	25.17	2.6	56.42	0.01	0.891	1.004	1.7	21	0.764	0.047	0.063	0.19	0.07	14.81	629	1567	0.0099	0.146
	Glass	21.7	2.6	56.42	0.01	0.891	1.004	1.7	15	0.753	0.0255	0.063	0.19	0.08	12.76	542	1351	0.0115	0.146
	Glass	15.97	2.6	56.42	0.01	0.891	1.004	1.7	18	0.737	0.0409	0.063	0.19	0.11	9.39	399	994	0.0156	0.146
	Glass	14.48	2.6	56.42	0.01	0.891	1.004	1.7	21	0.725	0.0412	0.063	0.19	0.12	8.52	362	901	0.0172	0.146
	Natural	13.6	2.65	56.42	0.01	0.891	1.004	1.7	21	0.683	0.0562	0.063	0.19	0.13	8	343	847	0.0178	0.142
	Natural	9.6	2.65	56.42	0.01	0.891	1.004	1.7	21	0.702	0.0522	0.063	0.19	0.18	5.65	242	598	0.025	0.142
	Natural	6.8	2.65	56.42	0.01	0.891	1.004	1.7	18	0.686	0.035	0.063	0.19	0.25	4	172	423	0.0355	0.142
	Natural	4.8	2.65	56.42	0.01	0.891	1.004	1.7	21	0.638	0.0682	0.063	0.19	0.35	2.82	121	299	0.0503	0.142
	Natural	3.4	2.65	56.42	0.01	0.891	1.004	1.7	21	0.605	0.0295	0.063	0.19	0.5	2	86	212	0.071	0.142
29	Steel	19.04	8.02	56.8	0.0086	0.847	0.992	1.7	21	0.266	0.0138	0.059	0.19	0.09	11.2	785	1138	0.0027	0.03
	Steel	15.88	8.02	56.8	0.0086	0.847	0.992	1.7	21	0.262	0.0185	0.059	0.19	0.11	9.34	654	949	0.0032	0.03
	Steel	14.28	8.02	56.8	0.0086	0.847	0.992	1.7	21	0.265	0.0207	0.059	0.19	0.12	8.4	588	854	0.0036	0.03
	Steel	9.5	8.02	56.8	0.0086	0.847	0.992	1.7	21	0.273	0.0245	0.059	0.19	0.18	5.59	392	568	0.0054	0.03
	Steel	7.9	8.02	56.8	0.0086	0.847	0.992	1.7	21	0.295	0.039	0.059	0.19	0.22	4.65	326	472	0.0065	0.03
	Steel	6.34	8.02	56.8	0.0086	0.847	0.992	1.7	21	0.307	0.0322	0.059	0.19	0.27	3.73	261	379	0.0081	0.03
	Glass	29.3	2.6	56.8	0.0086	0.847	0.992	1.7	21	0.727	0.033	0.059	0.19	0.06	17.24	738	1752	0.0077	0.132
	Glass	25.17	2.6	56.8	0.0086	0.847	0.992	1.7	21	0.721	0.035	0.059	0.19	0.07	14.81	634	1505	0.0089	0.132
	Glass	21.7	2.6	56.8	0.0086	0.847	0.992	1.7	21	0.695	0.04	0.059	0.19	0.08	12.76	546	1297	0.0103	0.132
	Glass	15.97	2.6	56.8	0.0086	0.847	0.992	1.7	21	0.681	0.0383	0.059	0.19	0.11	9.39	402	955	0.014	0.132
	Glass	14.48	2.6	56.8	0.0086	0.847	0.992	1.7	21	0.687	0.0587	0.059	0.19	0.12	8.52	365	866	0.0155	0.132
	Natural	13.6	2.65	56.8	0.0086	0.847	0.992	1.7	21	0.619	0.0456	0.059	0.19	0.13	8	346	813	0.016	0.128
	Natural	9.6	2.65	56.8	0.0086	0.847	0.992	1.7	21	0.61	0.0399	0.059	0.19	0.18	5.65	244	574	0.0226	0.128
	Natural	6.8	2.65	56.8	0.0086	0.847	0.992	1.7	21	0.597	0.0526	0.059	0.19	0.25	4	173	407	0.032	0.128
	Natural	4.8	2.65	56.8	0.0086	0.847	0.992	1.7	21	0.555	0.056	0.059	0.19	0.35	2.82	122	287	0.0453	0.128
	Natural	3.4	2.65	56.8	0.0086	0.847	0.992	1.7	21	0.554	0.0556	0.059	0.19	0.5	2	86	203	0.0639	0.128
	Natural	2.4	2.65	56.8	0.0086	0.847	0.992	1.7	21	0.531	0.0492	0.059	0.19	0.71	1.41	61	143	0.0905	0.128

Table1: The CSU Experiments Database (Cont'd)

Run	Type	d_s (mm)	G	y (mm)	S_f	u_f (m/s)	ν 10^{-6} (m^2/s)	k_s (mm)	N	V_{pobs} (m/s)	σ (m/s)	u_* (m/s)	δ (mm)	k_s/d_s	d_s/k_s	d_*	Re_*	τ_{*ds}	τ_{*ks}
(1)	(2)	(3)	(4)	(5)	(6)	(7)	(8)	(9)	(10)	(11)	(12)	(13)	(14)	(15)	(16)	(17)	(18)	(19)	(20)
30	Steel	19.04	8.02	53.48	0.007	0.725	0.98	1.7	15	0.202	0.0075	0.052	0.22	0.09	11.2	791	1002	0.002	0.023
	Steel	15.88	8.02	53.48	0.007	0.725	0.98	1.7	21	0.194	0.0089	0.052	0.22	0.11	9.34	660	836	0.0024	0.023
	Steel	14.28	8.02	53.48	0.007	0.725	0.98	1.7	18	0.189	0.0071	0.052	0.22	0.12	8.4	593	752	0.0027	0.023
	Steel	9.5	8.02	53.48	0.007	0.725	0.98	1.7	21	0.182	0.0144	0.052	0.22	0.18	5.59	395	500	0.0041	0.023
	Steel	7.9	8.02	53.48	0.007	0.725	0.98	1.7	21	0.181	0.0172	0.052	0.22	0.22	4.65	328	416	0.0049	0.023
	Glass	29.3	2.6	53.48	0.007	0.725	0.98	1.7	21	0.609	0.0258	0.052	0.22	0.06	17.24	744	1543	0.0058	0.1
	Glass	25.17	2.6	53.48	0.007	0.725	0.98	1.7	21	0.598	0.0251	0.052	0.22	0.07	14.81	639	1325	0.0067	0.1
	Glass	21.7	2.6	53.48	0.007	0.725	0.98	1.7	21	0.569	0.0294	0.052	0.22	0.08	12.76	551	1142	0.0078	0.1
	Glass	15.97	2.6	53.48	0.007	0.725	0.98	1.7	21	0.578	0.0378	0.052	0.22	0.11	9.39	405	841	0.0106	0.1
	Glass	14.48	2.6	53.48	0.007	0.725	0.98	1.7	21	0.555	0.0474	0.052	0.22	0.12	8.52	367	762	0.0117	0.1
	Natural	13.6	2.65	53.48	0.007	0.725	0.98	1.7	21	0.486	0.0306	0.052	0.22	0.13	8	349	716	0.0121	0.097
	Natural	9.6	2.65	53.48	0.007	0.725	0.98	1.7	21	0.514	0.0428	0.052	0.22	0.18	5.65	246	505	0.0171	0.097
	Natural	6.8	2.65	53.48	0.007	0.725	0.98	1.7	21	0.476	0.0432	0.052	0.22	0.25	4	174	358	0.0242	0.097
	Natural	4.8	2.65	53.48	0.007	0.725	0.98	1.7	21	0.455	0.0516	0.052	0.22	0.35	2.82	123	253	0.0343	0.097
	Natural	3.4	2.65	53.48	0.007	0.725	0.98	1.7	21	0.442	0.0367	0.052	0.22	0.5	2	87	179	0.0484	0.097
	Natural	2.4	2.65	53.48	0.007	0.725	0.98	1.7	21	0.42	0.0487	0.052	0.22	0.71	1.41	62	126	0.0685	0.097
31	Steel	19.04	8.02	55.75	0.0057	0.674	0.98	1.7	15	0.184	0.0056	0.048	0.24	0.09	11.2	791	932	0.0018	0.02
	Steel	15.88	8.02	55.75	0.0057	0.674	0.98	1.7	15	0.168	0.0047	0.048	0.24	0.11	9.34	660	778	0.0021	0.02
	Steel	14.28	8.02	55.75	0.0057	0.674	0.98	1.7	15	0.162	0.007	0.048	0.24	0.12	8.4	593	699	0.0023	0.02
	Steel	9.5	8.02	55.75	0.0057	0.674	0.98	1.7	21	0.139	0.0091	0.048	0.24	0.18	5.59	395	465	0.0035	0.02
	Glass	29.3	2.6	55.75	0.0057	0.674	0.98	1.7	18	0.539	0.0226	0.048	0.24	0.06	17.24	744	1435	0.005	0.086
	Glass	25.17	2.6	55.75	0.0057	0.674	0.98	1.7	18	0.531	0.0227	0.048	0.24	0.07	14.81	639	1233	0.0058	0.086
	Glass	21.7	2.6	55.75	0.0057	0.674	0.98	1.7	18	0.505	0.0197	0.048	0.24	0.08	12.76	551	1063	0.0068	0.086
	Glass	15.97	2.6	55.75	0.0057	0.674	0.98	1.7	21	0.484	0.0337	0.048	0.24	0.11	9.39	405	782	0.0092	0.086
	Glass	14.48	2.6	55.75	0.0057	0.674	0.98	1.7	21	0.483	0.0386	0.048	0.24	0.12	8.52	367	709	0.0101	0.086
	Natural	13.6	2.65	55.75	0.0057	0.674	0.98	1.7	21	0.423	0.0257	0.048	0.24	0.13	8	349	666	0.0105	0.084
	Natural	9.6	2.65	55.75	0.0057	0.674	0.98	1.7	21	0.416	0.0398	0.048	0.24	0.18	5.65	246	470	0.0148	0.084
	Natural	6.8	2.65	55.75	0.0057	0.674	0.98	1.7	21	0.4	0.0407	0.048	0.24	0.25	4	174	333	0.0209	0.084
	Natural	4.8	2.65	55.75	0.0057	0.674	0.98	1.7	21	0.407	0.0348	0.048	0.24	0.35	2.82	123	235	0.0297	0.084
	Natural	3.4	2.65	55.75	0.0057	0.674	0.98	1.7	21	0.383	0.0297	0.048	0.24	0.5	2	87	167	0.0419	0.084
	Natural	2.4	2.65	55.75	0.0057	0.674	0.98	1.7	21	0.378	0.0334	0.048	0.24	0.71	1.41	62	118	0.0593	0.084
32	Steel	19.04	8.02	56.08	0.0043	0.629	0.97	1.7	21	0.16	0.0052	0.042	0.27	0.09	11.2	797	824	0.0013	0.015
	Steel	15.88	8.02	56.08	0.0043	0.629	0.97	1.7	21	0.146	0.0037	0.042	0.27	0.11	9.34	665	687	0.0016	0.015

Table1: The CSU Experiments Database (Cont'd)

Run	Type	d_s (mm)	G	y (mm)	S_f	u_f (m/s)	ν 10^{-6} (m^2/s)	k_s (mm)	N	V_{pobs} (m/s)	σ (m/s)	u_* (m/s)	δ (mm)	k_s/d_s	d_s/k_s	d_*	Re_*	τ_{*ds}	τ_{*ks}
(1)	(2)	(3)	(4)	(5)	(6)	(7)	(8)	(9)	(10)	(11)	(12)	(13)	(14)	(15)	(16)	(17)	(18)	(19)	(20)
32	Steel	14.28	8.02	56.08	0.0043	0.629	0.97	1.7	21	0.138	0.0057	0.042	0.27	0.12	8.4	598	618	0.0018	0.015
	Glass	29.3	2.6	56.08	0.0043	0.629	0.97	1.7	21	0.449	0.0239	0.042	0.27	0.06	17.24	749	1268	0.0038	0.066
	Glass	25.17	2.6	56.08	0.0043	0.629	0.97	1.7	21	0.439	0.0241	0.042	0.27	0.07	14.81	644	1089	0.0044	0.066
	Glass	21.7	2.6	56.08	0.0043	0.629	0.97	1.7	21	0.426	0.0226	0.042	0.27	0.08	12.76	555	939	0.0052	0.066
	Glass	15.97	2.6	56.08	0.0043	0.629	0.97	1.7	21	0.396	0.0319	0.042	0.27	0.11	9.39	409	691	0.007	0.066
	Glass	14.48	2.6	56.08	0.0043	0.629	0.97	1.7	21	0.406	0.0265	0.042	0.27	0.12	8.52	370	627	0.0077	0.066
	Natural	13.6	2.65	56.08	0.0043	0.629	0.97	1.7	21	0.344	0.0241	0.042	0.27	0.13	8	351	588	0.008	0.064
	Natural	9.6	2.65	56.08	0.0043	0.629	0.97	1.7	21	0.348	0.0316	0.042	0.27	0.18	5.65	248	415	0.0113	0.064
	Natural	6.8	2.65	56.08	0.0043	0.629	0.97	1.7	21	0.332	0.0351	0.042	0.27	0.25	4	176	294	0.016	0.064
	Natural	4.8	2.65	56.08	0.0043	0.629	0.97	1.7	21	0.327	0.0292	0.042	0.27	0.35	2.82	124	208	0.0226	0.064
	Natural	3.4	2.65	56.08	0.0043	0.629	0.97	1.7	21	0.312	0.0311	0.042	0.27	0.5	2	88	147	0.0319	0.064
33	Steel	19.04	8.02	62.97	0.003	0.523	1.004	1.7	21	0.129	0.0049	0.036	0.32	0.09	11.2	778	681	0.001	0.011
	Steel	15.88	8.02	62.97	0.003	0.523	1.004	1.7	21	0.116	0.0052	0.036	0.32	0.11	9.34	649	568	0.0012	0.011
	Steel	14.28	8.02	62.97	0.003	0.523	1.004	1.7	21	0.106	0.0063	0.036	0.32	0.12	8.4	584	511	0.0013	0.011
	Glass	29.3	2.6	62.97	0.003	0.523	1.004	1.7	21	0.317	0.0144	0.036	0.32	0.06	17.24	732	1048	0.0028	0.048
	Glass	25.17	2.6	62.97	0.003	0.523	1.004	1.7	21	0.318	0.0236	0.036	0.32	0.07	14.81	629	900	0.0033	0.048
	Glass	21.7	2.6	62.97	0.003	0.523	1.004	1.7	21	0.3	0.0201	0.036	0.32	0.08	12.76	542	776	0.0038	0.048
	Glass	15.97	2.6	62.97	0.003	0.523	1.004	1.7	21	0.299	0.0191	0.036	0.32	0.11	9.39	399	571	0.0052	0.048
	Glass	14.48	2.6	62.97	0.003	0.523	1.004	1.7	21	0.29	0.0196	0.036	0.32	0.12	8.52	362	518	0.0057	0.048
	Natural	13.6	2.65	62.97	0.003	0.523	1.004	1.7	21	0.239	0.0273	0.036	0.32	0.13	8	343	486	0.0059	0.047
	Natural	9.6	2.65	62.97	0.003	0.523	1.004	1.7	21	0.257	0.0243	0.036	0.32	0.18	5.65	242	343	0.0083	0.047
	Natural	6.8	2.65	62.97	0.003	0.523	1.004	1.7	21	0.235	0.0231	0.036	0.32	0.25	4	172	243	0.0117	0.047
	Natural	4.8	2.65	62.97	0.003	0.523	1.004	1.7	21	0.245	0.0257	0.036	0.32	0.35	2.82	121	172	0.0166	0.047
	Natural	3.4	2.65	62.97	0.003	0.523	1.004	1.7	21	0.234	0.0223	0.036	0.32	0.5	2	86	122	0.0234	0.047
34	Glass	29.3	2.6	68.52	0.0016	0.353	1.016	1.7	21	0.169	0.0061	0.024	0.49	0.06	17.24	726	698	0.0013	0.022
	Glass	25.17	2.6	68.52	0.0016	0.353	1.016	1.7	21	0.158	0.0042	0.024	0.49	0.07	14.81	623	599	0.0015	0.022
	Glass	21.7	2.6	68.52	0.0016	0.353	1.016	1.7	21	0.148	0.0059	0.024	0.49	0.08	12.76	538	517	0.0017	0.022
	Glass	15.97	2.6	68.52	0.0016	0.353	1.016	1.7	21	0.137	0.0058	0.024	0.49	0.11	9.39	396	380	0.0023	0.022
	Glass	14.48	2.6	68.52	0.0016	0.353	1.016	1.7	21	0.135	0.0082	0.024	0.49	0.12	8.52	359	345	0.0026	0.022
35	Glass	29.3	2.6	60.77	0.0022	0.424	1.022	1.7	21	0.207	0.007	0.029	0.42	0.06	17.24	723	817	0.0018	0.031
	Glass	25.17	2.6	60.77	0.0022	0.424	1.022	1.7	21	0.2	0.0084	0.029	0.42	0.07	14.81	621	702	0.0021	0.031
	Glass	21.7	2.6	60.77	0.0022	0.424	1.022	1.7	21	0.194	0.0113	0.029	0.42	0.08	12.76	535	605	0.0024	0.031

Table1: The CSU Experiments Database (Cont'd)

Run	Type	d_s (mm)	G	y (mm)	S_f	u_f (m/s)	ν 10^{-6} (m^2/s)	k_s (mm)	n	V_{pobs} (m/s)	σ (m/s)	u_* (m/s)	δ (mm)	k_s/d_s	d_s/k_s	d_*	Re_*	τ_{*ds}	τ_{*ks}
(1)	(2)	(3)	(4)	(5)	(6)	(7)	(8)	(9)	(10)	(11)	(12)	(13)	(14)	(15)	(16)	(17)	(18)	(19)	(20)
35	Glass	15.97	2.6	60.77	0.0022	0.424	1.022	1.7	21	0.188	0.0115	0.029	0.42	0.11	9.39	394	445	0.0032	0.031
	Glass	14.48	2.6	60.77	0.0022	0.424	1.022	1.7	21	0.182	0.0116	0.029	0.42	0.12	8.52	357	404	0.0036	0.031
	Natural	13.6	2.65	60.77	0.0022	0.424	1.022	1.7	21	0.158	0.0118	0.029	0.42	0.13	8	339	379	0.0037	0.03
	Natural	9.6	2.65	60.77	0.0022	0.424	1.022	1.7	21	0.156	0.0177	0.029	0.42	0.18	5.65	239	268	0.0052	0.03
36	Glass	29.3	2.6	71.15	0.0007	0.269	1.016	1.7	21	0.123	0.004	0.019	0.63	0.06	17.24	726	536	0.0008	0.013
	Glass	25.17	2.6	71.15	0.0007	0.269	1.016	1.7	21	0.116	0.0038	0.019	0.63	0.07	14.81	623	461	0.0009	0.013
	Glass	21.7	2.6	71.15	0.0007	0.269	1.016	1.7	21	0.11	0.0039	0.019	0.63	0.08	12.76	538	397	0.001	0.013
	Glass	15.97	2.6	71.15	0.0007	0.269	1.016	1.7	21	0.093	0.003	0.019	0.63	0.11	9.39	396	292	0.0014	0.013
	Glass	14.48	2.6	71.15	0.0007	0.269	1.016	1.7	21	0.09	0.0045	0.019	0.63	0.12	8.52	359	265	0.0015	0.013
13	Glass	29.3	2.6	69.08	0.002	0.348	1.054	2.4	18	0.128	0.006	0.03	0.41	0.08	12.21	708	837	0.002	0.024
	Glass	25.17	2.6	69.08	0.002	0.348	1.054	2.4	18	0.119	0.0049	0.03	0.41	0.1	10.49	608	719	0.0023	0.024
	Glass	21.7	2.6	69.08	0.002	0.348	1.054	2.4	18	0.107	0.0048	0.03	0.41	0.11	9.04	525	620	0.0027	0.024
	Glass	15.97	2.6	69.08	0.002	0.348	1.054	2.4	8	0.093	0.0059	0.03	0.41	0.15	6.65	386	456	0.0036	0.024
	Glass	14.48	2.6	69.08	0.002	0.348	1.054	2.4	2	0.095	0.007	0.03	0.41	0.17	6.03	350	414	0.004	0.024
14	Glass	29.3	2.6	60.9	0.004	0.611	1.074	2.4	21	0.291	0.022	0.039	0.32	0.08	12.21	700	1054	0.0032	0.04
	Glass	25.17	2.6	60.9	0.004	0.611	1.074	2.4	21	0.311	0.027	0.039	0.32	0.1	10.49	601	905	0.0038	0.04
	Glass	21.7	2.6	60.9	0.004	0.611	1.074	2.4	21	0.305	0.0316	0.039	0.32	0.11	9.04	518	780	0.0044	0.04
	Glass	15.97	2.6	60.9	0.004	0.611	1.074	2.4	21	0.289	0.0308	0.039	0.32	0.15	6.65	381	574	0.0059	0.04
	Glass	14.48	2.6	60.9	0.004	0.611	1.074	2.4	21	0.295	0.0317	0.039	0.32	0.17	6.03	346	521	0.0066	0.04
	Natural	13.6	2.65	60.9	0.004	0.611	1.074	2.4	21	0.246	0.029	0.039	0.32	0.18	5.67	328	489	0.0068	0.038
	Natural	9.6	2.65	60.9	0.004	0.611	1.074	2.4	21	0.249	0.0247	0.039	0.32	0.25	4	232	345	0.0096	0.038
	Natural	6.8	2.65	60.9	0.004	0.611	1.074	2.4	21	0.226	0.0344	0.039	0.32	0.35	2.83	164	245	0.0135	0.038
	Natural	4.8	2.65	60.9	0.004	0.611	1.074	2.4	21	0.211	0.0203	0.039	0.32	0.5	2	116	173	0.0192	0.038
15	Glass	29.3	2.6	69.12	0.0014	0.3	1.08	2.4	15	0.107	0.0031	0.025	0.5	0.08	12.21	697	678	0.0014	0.017
	Glass	25.17	2.6	69.12	0.0014	0.3	1.08	2.4	21	0.1	0.0058	0.025	0.5	0.1	10.49	599	583	0.0016	0.017
	Glass	21.7	2.6	69.12	0.0014	0.3	1.08	2.4	9	0.088	0.0064	0.025	0.5	0.11	9.04	516	502	0.0018	0.017
16	Glass	29.3	2.6	61.97	0.003	0.499	1.074	2.4	15	0.196	0.0072	0.034	0.37	0.08	12.21	700	925	0.0025	0.031
	Glass	25.17	2.6	61.97	0.003	0.499	1.074	2.4	18	0.193	0.012	0.034	0.37	0.1	10.49	601	795	0.003	0.031
	Glass	21.7	2.6	61.97	0.003	0.499	1.074	2.4	18	0.179	0.0082	0.034	0.37	0.11	9.04	518	685	0.0034	0.031
	Glass	15.97	2.6	61.97	0.003	0.499	1.074	2.4	21	0.168	0.0112	0.034	0.37	0.15	6.65	381	504	0.0046	0.031

Table1: The CSU Experiments Database (Cont'd)

Run	Type	d_s (mm)	G	y (mm)	S_f	u_f (m/s)	ν 10^{-6} (m^2/s)	k_s (mm)	N	V_{pobs} (m/s)	σ (m/s)	u_* (m/s)	δ (mm)	k_s/d_s	d_s/k_s	d_*	Re_*	τ_{*ds}	τ_{*ks}
(1)	(2)	(3)	(4)	(5)	(6)	(7)	(8)	(9)	(10)	(11)	(12)	(13)	(14)	(15)	(16)	(17)	(18)	(19)	(20)
16	Glass	14.48	2.6	61.97	0.003	0.499	1.074	2.4	21	0.167	0.0137	0.034	0.37	0.17	6.03	346	457	0.0051	0.031
	Natural	13.6	2.65	61.97	0.003	0.499	1.074	2.4	21	0.156	0.0145	0.034	0.37	0.18	5.67	328	429	0.0052	0.03
	Natural	9.6	2.65	61.97	0.003	0.499	1.074	2.4	21	0.155	0.0212	0.034	0.37	0.25	4	232	303	0.0074	0.03
	Natural	6.8	2.65	61.97	0.003	0.499	1.074	2.4	9	0.154	0.0265	0.034	0.37	0.35	2.83	164	215	0.0105	0.03
17	Steel	19.04	8.02	60.3	0.006	0.702	1.067	2.4	21	0.14	0.0056	0.051	0.25	0.13	7.93	747	903	0.002	0.016
	Glass	29.3	2.6	60.3	0.006	0.702	1.067	2.4	21	0.477	0.0321	0.051	0.25	0.08	12.21	703	1389	0.0056	0.068
	Glass	25.17	2.6	60.3	0.006	0.702	1.067	2.4	21	0.487	0.0362	0.051	0.25	0.1	10.49	604	1194	0.0065	0.068
	Glass	21.7	2.6	60.3	0.006	0.702	1.067	2.4	21	0.48	0.0301	0.051	0.25	0.11	9.04	520	1029	0.0075	0.068
	Glass	15.97	2.6	60.3	0.006	0.702	1.067	2.4	21	0.463	0.0384	0.051	0.25	0.15	6.65	383	757	0.0102	0.068
	Glass	14.48	2.6	60.3	0.006	0.702	1.067	2.4	21	0.458	0.0329	0.051	0.25	0.17	6.03	347	687	0.0113	0.068
	Natural	13.6	2.65	60.3	0.006	0.702	1.067	2.4	21	0.377	0.0235	0.051	0.25	0.18	5.67	329	645	0.0116	0.066
	Natural	9.6	2.65	60.3	0.006	0.702	1.067	2.4	21	0.39	0.0458	0.051	0.25	0.25	4	233	455	0.0165	0.066
	Natural	6.8	2.65	60.3	0.006	0.702	1.067	2.4	21	0.386	0.0457	0.051	0.25	0.35	2.83	165	322	0.0233	0.066
	Natural	4.8	2.65	60.3	0.006	0.702	1.067	2.4	21	0.33	0.029	0.051	0.25	0.5	2	116	228	0.033	0.066
18	Steel	19.04	8.02	56.37	0.01	0.854	1.029	2.4	21	0.181	0.0093	0.064	0.19	0.13	7.93	766	1187	0.0031	0.025
	Steel	15.88	8.02	56.37	0.01	0.854	1.029	2.4	21	0.169	0.0117	0.064	0.19	0.15	6.62	639	990	0.0038	0.025
	Steel	14.28	8.02	56.37	0.01	0.854	1.029	2.4	21	0.161	0.0125	0.064	0.19	0.17	5.95	574	890	0.0042	0.025
	Glass	29.3	2.6	56.37	0.01	0.854	1.029	2.4	21	0.693	0.0383	0.064	0.19	0.08	12.21	720	1826	0.0089	0.109
	Glass	25.17	2.6	56.37	0.01	0.854	1.029	2.4	21	0.697	0.0353	0.064	0.19	0.1	10.49	618	1569	0.0104	0.109
	Glass	21.7	2.6	56.37	0.01	0.854	1.029	2.4	21	0.664	0.019	0.064	0.19	0.11	9.04	533	1352	0.0121	0.109
	Glass	15.97	2.6	56.37	0.01	0.854	1.029	2.4	21	0.638	0.0363	0.064	0.19	0.15	6.65	392	995	0.0164	0.109
	Glass	14.48	2.6	56.37	0.01	0.854	1.029	2.4	21	0.668	0.045	0.064	0.19	0.17	6.03	356	902	0.0181	0.109
	Natural	13.6	2.65	56.37	0.01	0.854	1.029	2.4	21	0.562	0.0497	0.064	0.19	0.18	5.67	338	848	0.0187	0.106
	Natural	9.6	2.65	56.37	0.01	0.854	1.029	2.4	21	0.609	0.0566	0.064	0.19	0.25	4	238	598	0.0264	0.106
	Natural	6.8	2.65	56.37	0.01	0.854	1.029	2.4	21	0.542	0.0515	0.064	0.19	0.35	2.83	169	424	0.0373	0.106
	Natural	4.8	2.65	56.37	0.01	0.854	1.029	2.4	21	0.479	0.0552	0.064	0.19	0.5	2	119	299	0.0529	0.106
37	Steel	19.04	8.02	53.22	0.01	0.827	0.998	2.4	21	0.264	0.0186	0.062	0.19	0.13	7.93	782	1175	0.0029	0.023
	Steel	15.88	8.02	53.22	0.01	0.827	0.998	2.4	21	0.257	0.0201	0.062	0.19	0.15	6.62	652	980	0.0035	0.023
	Steel	14.28	8.02	53.22	0.01	0.827	0.998	2.4	21	0.261	0.0233	0.062	0.19	0.17	5.95	586	881	0.0039	0.023
	Steel	9.5	8.02	53.22	0.01	0.827	0.998	2.4	21	0.286	0.0259	0.062	0.19	0.25	3.96	390	586	0.0058	0.023
	Steel	7.9	8.02	53.22	0.01	0.827	0.998	2.4	21	0.307	0.0344	0.062	0.19	0.3	3.29	324	488	0.007	0.023
	Steel	6.34	8.02	53.22	0.01	0.827	0.998	2.4	21	0.316	0.033	0.062	0.19	0.38	2.64	260	391	0.0087	0.023

Table1: The CSU Experiments Database (Cont'd)

Run	Type	d_s (mm)	G	y (mm)	S_f	u_f (m/s)	ν 10^{-6} (m^2/s)	k_s (mm)	N	V_{pobs} (m/s)	σ (m/s)	u_* (m/s)	δ (mm)	k_s/d_s	d_s/k_s	d_*	Re_*	τ_{*ds}	τ_{*ks}
(1)	(2)	(3)	(4)	(5)	(6)	(7)	(8)	(9)	(10)	(11)	(12)	(13)	(14)	(15)	(16)	(17)	(18)	(19)	(20)
37	Glass	29.3	2.6	53.22	0.01	0.827	0.998	2.4	21	0.748	0.033	0.062	0.19	0.08	12.21	735	1809	0.0083	0.101
	Glass	25.17	2.6	53.22	0.01	0.827	0.998	2.4	21	0.738	0.0341	0.062	0.19	0.1	10.49	631	1554	0.0096	0.101
	Glass	21.7	2.6	53.22	0.01	0.827	0.998	2.4	21	0.723	0.0414	0.062	0.19	0.11	9.04	544	1339	0.0111	0.101
	Glass	15.97	2.6	53.22	0.01	0.827	0.998	2.4	21	0.701	0.0379	0.062	0.19	0.15	6.65	400	986	0.0151	0.101
	Glass	14.48	2.6	53.22	0.01	0.827	0.998	2.4	21	0.7	0.0506	0.062	0.19	0.17	6.03	363	894	0.0167	0.101
	Natural	13.6	2.65	53.22	0.01	0.827	0.998	2.4	21	0.626	0.0438	0.062	0.19	0.18	5.67	344	839	0.0172	0.098
	Natural	9.6	2.65	53.22	0.01	0.827	0.998	2.4	21	0.632	0.0478	0.062	0.19	0.25	4	243	593	0.0244	0.098
	Natural	6.8	2.65	53.22	0.01	0.827	0.998	2.4	21	0.623	0.0815	0.062	0.19	0.35	2.83	72	420	0.0345	0.098
	Natural	4.8	2.65	53.22	0.01	0.827	0.998	2.4	21	0.576	0.041	0.062	0.19	0.5	2	122	296	0.0488	0.098
	Natural	3.4	2.65	53.22	0.01	0.827	0.998	2.4	21	0.532	0.055	0.062	0.19	0.71	1.42	86	210	0.0689	0.098
38	Steel	19.04	8.02	52.97	0.0084	0.767	0.992	2.4	21	0.213	0.0091	0.056	0.21	0.13	7.93	785	1071	0.0024	0.019
	Steel	15.88	8.02	52.97	0.0084	0.767	0.992	2.4	21	0.211	0.0143	0.056	0.21	0.15	6.62	654	893	0.0029	0.019
	Steel	14.28	8.02	52.97	0.0084	0.767	0.992	2.4	21	0.208	0.0127	0.056	0.21	0.17	5.95	588	803	0.0032	0.019
	Steel	9.5	8.02	52.97	0.0084	0.767	0.992	2.4	21	0.216	0.0216	0.056	0.21	0.25	3.96	392	534	0.0048	0.019
	Steel	7.9	8.02	52.97	0.0084	0.767	0.992	2.4	21	0.225	0.0327	0.056	0.21	0.3	3.29	326	444	0.0057	0.019
	Glass	29.3	2.6	52.97	0.0084	0.767	0.992	2.4	21	0.651	0.0269	0.056	0.21	0.08	12.21	738	1648	0.0068	0.083
	Glass	25.17	2.6	52.97	0.0084	0.767	0.992	2.4	21	0.648	0.0203	0.056	0.21	0.1	10.49	634	1416	0.0079	0.083
	Glass	21.7	2.6	52.97	0.0084	0.767	0.992	2.4	21	0.638	0.021	0.056	0.21	0.11	9.04	546	1221	0.0092	0.083
	Glass	15.97	2.6	52.97	0.0084	0.767	0.992	2.4	21	0.628	0.035	0.056	0.21	0.15	6.65	402	898	0.0124	0.083
	Glass	14.48	2.6	52.97	0.0084	0.767	0.992	2.4	21	0.605	0.0409	0.056	0.21	0.17	6.03	365	815	0.0137	0.083
	Natural	13.6	2.65	52.97	0.0084	0.767	0.992	2.4	21	0.537	0.0386	0.056	0.21	0.18	5.67	346	765	0.0142	0.08
	Natural	9.6	2.65	52.97	0.0084	0.767	0.992	2.4	21	0.541	0.0544	0.056	0.21	0.25	4	244	540	0.02	0.08
	Natural	6.8	2.65	52.97	0.0084	0.767	0.992	2.4	21	0.514	0.0438	0.056	0.21	0.35	2.83	173	383	0.0283	0.08
	Natural	4.8	2.65	52.97	0.0084	0.767	0.992	2.4	21	0.517	0.0529	0.056	0.21	0.5	2	122	270	0.04	0.08
	Natural	3.4	2.65	52.97	0.0084	0.767	0.992	2.4	21	0.475	0.0468	0.056	0.21	0.71	1.42	86	191	0.0566	0.08
39	Steel	19.04	8.02	52.68	0.007	0.7	1.004	2.4	21	0.188	0.0066	0.051	0.23	0.13	7.93	778	975	0.002	0.016
	Steel	15.88	8.02	52.68	0.007	0.7	1.004	2.4	21	0.178	0.0079	0.051	0.23	0.15	6.62	649	813	0.0024	0.016
	Steel	14.28	8.02	52.68	0.007	0.7	1.004	2.4	21	0.174	0.0108	0.051	0.23	0.17	5.95	584	731	0.0027	0.016
	Steel	9.5	8.02	52.68	0.007	0.7	1.004	2.4	21	0.155	0.0135	0.051	0.23	0.25	3.96	388	486	0.0041	0.016
	Glass	29.3	2.6	52.68	0.007	0.7	1.004	2.4	21	0.58	0.0252	0.051	0.23	0.08	12.21	732	1500	0.0058	0.07
	Glass	25.17	2.6	52.68	0.007	0.7	1.004	2.4	21	0.563	0.0298	0.051	0.23	0.1	10.49	629	1289	0.0067	0.07
	Glass	21.7	2.6	52.68	0.007	0.7	1.004	2.4	21	0.543	0.0345	0.051	0.23	0.11	9.04	542	1111	0.0078	0.07
	Glass	15.97	2.6	52.68	0.007	0.7	1.004	2.4	21	0.538	0.0258	0.051	0.23	0.15	6.65	399	818	0.0105	0.07

Table1: The CSU Experiments Database (Cont'd)

Run	Type	d_s (mm)	G	y (mm)	S_f	u_f (m/s)	ν 10^{-6} (m^2/s)	k_s (mm)	N	V_{pobs} (m/s)	σ (m/s)	u_* (m/s)	δ (mm)	k_s/d_s	d_s/k_s	d_*	Re_*	τ_{*ds}	τ_{*ks}
(1)	(2)	(3)	(4)	(5)	(6)	(7)	(8)	(9)	(10)	(11)	(12)	(13)	(14)	(15)	(16)	(17)	(18)	(19)	(20)
39	Glass	14.48	2.6	52.68	0.007	0.7	1.004	2.4	21	0.562	0.0259	0.051	0.23	0.17	6.03	362	741	0.0116	0.07
	Natural	13.6	2.65	52.68	0.007	0.7	1.004	2.4	21	0.472	0.0391	0.051	0.23	0.18	5.67	343	696	0.012	0.068
	Natural	9.6	2.65	52.68	0.007	0.7	1.004	2.4	21	0.478	0.0421	0.051	0.23	0.25	4	242	491	0.017	0.068
	Natural	6.8	2.65	52.68	0.007	0.7	1.004	2.4	21	0.448	0.0495	0.051	0.23	0.35	2.83	172	348	0.024	0.068
	Natural	4.8	2.65	52.68	0.007	0.7	1.004	2.4	21	0.438	0.0542	0.051	0.23	0.5	2	121	246	0.034	0.068
	Natural	3.4	2.65	52.68	0.007	0.7	1.004	2.4	21	0.404	0.0489	0.051	0.23	0.71	1.42	86	174	0.048	0.068
	Natural	2.4	2.65	52.68	0.007	0.7	1.004	2.4	21	0.407	0.0381	0.051	0.23	1	1	61	123	0.068	0.068
40	Steel	19.04	8.02	52.43	0.0056	0.6	1.004	2.4	21	0.164	0.0047	0.047	0.25	0.13	7.93	778	886	0.0017	0.013
	Steel	15.88	8.02	52.43	0.0056	0.6	1.004	2.4	21	0.151	0.007	0.047	0.25	0.15	6.62	649	739	0.002	0.013
	Steel	14.28	8.02	52.43	0.0056	0.6	1.004	2.4	21	0.143	0.007	0.047	0.25	0.17	5.95	584	664	0.0022	0.013
	Glass	29.3	2.6	52.43	0.0056	0.6	1.004	2.4	21	0.471	0.0218	0.047	0.25	0.08	12.21	732	1363	0.0047	0.058
	Glass	25.17	2.6	52.43	0.0056	0.6	1.004	2.4	21	0.47	0.025	0.047	0.25	0.1	10.49	629	1171	0.0055	0.058
	Glass	21.7	2.6	52.43	0.0056	0.6	1.004	2.4	21	0.456	0.0238	0.047	0.25	0.11	9.04	542	1009	0.0064	0.058
	Glass	15.97	2.6	52.43	0.0056	0.6	1.004	2.4	21	0.421	0.0249	0.047	0.25	0.15	6.65	399	743	0.0087	0.058
	Glass	14.48	2.6	52.43	0.0056	0.6	1.004	2.4	21	0.431	0.0295	0.047	0.25	0.17	6.03	362	674	0.0096	0.058
	Natural	13.6	2.65	52.43	0.0056	0.6	1.004	2.4	21	0.38	0.029	0.047	0.25	0.18	5.67	343	633	0.0099	0.056
	Natural	9.6	2.65	52.43	0.0056	0.6	1.004	2.4	21	0.365	0.0279	0.047	0.25	0.25	4	242	447	0.0141	0.056
	Natural	6.8	2.65	52.43	0.0056	0.6	1.004	2.4	21	0.368	0.0368	0.047	0.25	0.35	2.83	172	316	0.0198	0.056
	Natural	4.8	2.65	52.43	0.0056	0.6	1.004	2.4	21	0.352	0.034	0.047	0.25	0.5	2	121	223	0.0281	0.056
	Natural	3.4	2.65	52.43	0.0056	0.6	1.004	2.4	21	0.317	0.0273	0.047	0.25	0.71	1.42	86	158	0.0396	0.056
	Natural	2.4	2.65	52.43	0.0056	0.6	1.004	2.4	21	0.326	0.0302	0.047	0.25	1	1	61	112	0.0561	0.056
41	Steel	19.04	8.02	56.1	0.0037	0.532	1.004	2.4	21	0.129	0.0052	0.038	0.31	0.13	7.93	778	717	0.0011	0.009
	Glass	29.3	2.6	56.1	0.0037	0.532	1.004	2.4	21	0.327	0.0132	0.038	0.31	0.08	12.21	732	1103	0.0031	0.038
	Glass	25.17	2.6	56.1	0.0037	0.532	1.004	2.4	21	0.323	0.0203	0.038	0.31	0.1	10.49	629	948	0.0036	0.038
	Glass	21.7	2.6	56.1	0.0037	0.532	1.004	2.4	21	0.311	0.0188	0.038	0.31	0.11	9.04	542	817	0.0042	0.038
	Glass	15.97	2.6	56.1	0.0037	0.532	1.004	2.4	21	0.318	0.018	0.038	0.31	0.15	6.65	399	601	0.0057	0.038
	Glass	14.48	2.6	56.1	0.0037	0.532	1.004	2.4	21	0.311	0.0256	0.038	0.31	0.17	6.03	362	545	0.0063	0.038
	Natural	13.6	2.65	56.1	0.0037	0.532	1.004	2.4	21	0.252	0.027	0.038	0.31	0.18	5.67	343	512	0.0065	0.037
	Natural	9.6	2.65	56.1	0.0037	0.532	1.004	2.4	21	0.268	0.023	0.038	0.31	0.25	4	242	361	0.0092	0.037
	Natural	6.8	2.65	56.1	0.0037	0.532	1.004	2.4	21	0.255	0.0235	0.038	0.31	0.35	2.83	172	256	0.013	0.037
	Natural	4.8	2.65	56.1	0.0037	0.532	1.004	2.4	9	0.252	0.0203	0.038	0.31	0.5	2	121	181	0.0184	0.037
42	Glass	29.3	2.6	62.25	0.0021	0.407	1.004	2.4	21	0.196	0.0063	0.032	0.37	0.08	12.21	732	925	0.0022	0.027

Table1: The CSU Experiments Database (Cont'd)

Run	Type	d_s (mm)	G	y (mm)	S_f	u_f (m/s)	ν 10^{-6} (m^2/s)	k_s (mm)	N	V_{pobs} (m/s)	σ (m/s)	u_* (m/s)	δ (mm)	k_s/d_s	d_s/k_s	d_*	Re_*	τ_{*ds}	τ_{*ks}
(1)	(2)	(3)	(4)	(5)	(6)	(7)	(8)	(9)	(10)	(11)	(12)	(13)	(14)	(15)	(16)	(17)	(18)	(19)	(20)
42	Glass	25.17	2.6	62.25	0.0021	0.407	1.004	2.4	21	0.191	0.0081	0.032	0.37	0.1	10.49	629	795	0.0026	0.027
	Glass	21.7	2.6	62.25	0.0021	0.407	1.004	2.4	21	0.186	0.0117	0.032	0.37	0.11	9.04	542	685	0.003	0.027
	Glass	15.97	2.6	62.25	0.0021	0.407	1.004	2.4	21	0.176	0.0102	0.032	0.37	0.15	6.65	399	504	0.004	0.027
	Glass	14.48	2.6	62.25	0.0021	0.407	1.004	2.4	21	0.175	0.0115	0.032	0.37	0.17	6.03	362	457	0.0044	0.027
	Natural	13.6	2.65	62.25	0.0021	0.407	1.004	2.4	9	0.148	0.0144	0.032	0.37	0.18	5.67	343	429	0.0046	0.026
	Natural	9.6	2.65	62.25	0.0021	0.407	1.004	2.4	9	0.156	0.0252	0.032	0.37	0.25	4	242	303	0.0065	0.026
	Natural	6.8	2.65	62.25	0.0021	0.407	1.004	2.4	9	0.155	0.0205	0.032	0.37	0.35	2.83	172	215	0.0092	0.026
43	Glass	29.3	2.6	68.35	0.0009	0.262	1.004	2.4	21	0.117	0.0069	0.019	0.61	0.08	12.21	732	554	0.0008	0.01
	Glass	25.17	2.6	68.35	0.0009	0.262	1.004	2.4	21	0.113	0.0043	0.019	0.61	0.1	10.49	629	476	0.0009	0.01
	Glass	21.7	2.6	68.35	0.0009	0.262	1.004	2.4	21	0.102	0.0043	0.019	0.61	0.11	9.04	542	411	0.0011	0.01
44	Glass	29.3	2.6	57.72	0.0015	0.312	1.004	2.4	21	0.151	0.0037	0.025	0.47	0.08	12.21	732	724	0.0013	0.016
	Glass	25.17	2.6	57.72	0.0015	0.312	1.004	2.4	21	0.142	0.0038	0.025	0.47	0.1	10.49	629	622	0.0016	0.016
	Glass	21.7	2.6	57.72	0.0015	0.312	1.004	2.4	21	0.134	0.0039	0.025	0.47	0.11	9.04	542	536	0.0018	0.016
	Glass	15.97	2.6	57.72	0.0015	0.312	1.004	2.4	21	0.117	0.0044	0.025	0.47	0.15	6.65	399	394	0.0025	0.016
	Glass	14.48	2.6	57.72	0.0015	0.312	1.004	2.4	21	0.113	0.0039	0.025	0.47	0.17	6.03	362	358	0.0027	0.016
20	Steel	19.04	8.02	55.32	0.01	0.825	0.992	3.4	18	0.197	0.0049	0.062	0.19	0.18	5.6	785	1196	0.003	0.017
	Steel	15.88	8.02	55.32	0.01	0.825	0.992	3.4	21	0.187	0.014	0.062	0.19	0.21	4.67	654	997	0.0035	0.017
	Steel	14.28	8.02	55.32	0.01	0.825	0.992	3.4	21	0.186	0.0159	0.062	0.19	0.24	4.2	588	897	0.0039	0.017
	Glass	29.3	2.6	55.32	0.01	0.825	0.992	3.4	21	0.679	0.0435	0.062	0.19	0.12	8.62	738	1840	0.0085	0.073
	Glass	25.17	2.6	55.32	0.01	0.825	0.992	3.4	21	0.683	0.0282	0.062	0.19	0.14	7.4	634	1581	0.0098	0.073
	Glass	21.7	2.6	55.32	0.01	0.825	0.992	3.4	21	0.645	0.0299	0.062	0.19	0.16	6.38	546	1363	0.0114	0.073
	Glass	15.97	2.6	55.32	0.01	0.825	0.992	3.4	21	0.662	0.0505	0.062	0.19	0.21	4.7	402	1003	0.0155	0.073
	Glass	14.48	2.6	55.32	0.01	0.825	0.992	3.4	21	0.65	0.0359	0.062	0.19	0.23	4.26	365	909	0.0171	0.073
	Natural	13.6	2.65	55.32	0.01	0.825	0.992	3.4	21	0.573	0.0512	0.062	0.19	0.25	4	346	854	0.0176	0.071
	Natural	9.6	2.65	55.32	0.01	0.825	0.992	3.4	21	0.596	0.047	0.062	0.19	0.35	2.82	244	603	0.025	0.071
	Natural	6.8	2.65	55.32	0.01	0.825	0.992	3.4	21	0.57	0.0552	0.062	0.19	0.5	2	173	427	0.0353	0.071
	Natural	4.8	2.65	55.32	0.01	0.825	0.992	3.4	21	0.53	0.0649	0.062	0.19	0.71	1.41	122	301	0.05	0.071
21	Glass	29.3	2.6	69	0.0014	0.3	1.004	3.4	21	0.106	0.0063	0.024	0.49	0.12	8.62	732	700	0.0013	0.011
	Glass	25.17	2.6	69	0.0014	0.3	1.004	3.4	21	0.101	0.0048	0.024	0.49	0.14	7.4	629	602	0.0015	0.011
23	Glass	29.3	2.6	65.1	0.002	0.377	1.004	3.4	21	0.151	0.0064	0.03	0.39	0.12	8.62	732	870	0.0019	0.017

Table1: The CSU Experiments Database (Cont'd)

Run	Type	d_s (mm)	G	y (mm)	S_f	u_f (m/s)	ν 10^{-6} (m^2/s)	k_s (mm)	N	V_{pobs} (m/s)	σ (m/s)	u_* (m/s)	δ (mm)	k_s/d_s	d_s/k_s	d_*	Re_*	τ_{*ds}	τ_{*ks}
(1)	(2)	(3)	(4)	(5)	(6)	(7)	(8)	(9)	(10)	(11)	(12)	(13)	(14)	(15)	(16)	(17)	(18)	(19)	(20)
23	Glass	25.17	2.6	65.1	0.002	0.377	1.004	3.4	21	0.143	0.007	0.03	0.39	0.14	7.4	629	747	0.0023	0.017
	Glass	21.7	2.6	65.1	0.002	0.377	1.004	3.4	21	0.13	0.0065	0.03	0.39	0.16	6.38	542	644	0.0026	0.017
	Glass	15.97	2.6	65.1	0.002	0.377	1.004	3.4	21	0.119	0.0067	0.03	0.39	0.21	4.7	399	474	0.0035	0.017
	Glass	14.48	2.6	65.1	0.002	0.377	1.004	3.4	21	0.113	0.0067	0.03	0.39	0.23	4.26	362	430	0.0039	0.017
24	Glass	29.3	2.6	66.67	0.003	0.513	1.004	3.4	21	0.237	0.0136	0.036	0.32	0.12	8.62	732	1056	0.0028	0.025
	Glass	25.17	2.6	66.67	0.003	0.513	1.004	3.4	21	0.234	0.0157	0.036	0.32	0.14	7.4	629	908	0.0033	0.025
	Glass	21.7	2.6	66.67	0.003	0.513	1.004	3.4	21	0.221	0.0166	0.036	0.32	0.16	6.38	542	782	0.0039	0.025
	Glass	15.97	2.6	66.67	0.003	0.513	1.004	3.4	21	0.216	0.0162	0.036	0.32	0.21	4.7	399	576	0.0053	0.025
	Glass	14.48	2.6	66.67	0.003	0.513	1.004	3.4	21	0.213	0.0163	0.036	0.32	0.23	4.26	362	522	0.0058	0.025
	Natural	13.6	2.65	66.67	0.003	0.513	1.004	3.4	21	0.189	0.0253	0.036	0.32	0.25	4	343	490	0.006	0.024
	Natural	9.6	2.65	66.67	0.003	0.513	1.004	3.4	21	0.202	0.0293	0.036	0.32	0.35	2.82	242	346	0.0084	0.024
	Natural	6.8	2.65	66.67	0.003	0.513	1.004	3.4	21	0.195	0.0236	0.036	0.32	0.5	2	172	245	0.0119	0.024
25	Glass	29.3	2.6	65.03	0.0041	0.64	1.004	3.4	21	0.363	0.0258	0.044	0.27	0.12	8.62	732	1278	0.0042	0.036
	Glass	25.17	2.6	65.03	0.0041	0.64	1.004	3.4	21	0.36	0.027	0.044	0.27	0.14	7.4	629	1098	0.0049	0.036
	Glass	21.7	2.6	65.03	0.0041	0.64	1.004	3.4	21	0.34	0.037	0.044	0.27	0.16	6.38	542	947	0.0056	0.036
	Glass	15.97	2.6	65.03	0.0041	0.64	1.004	3.4	21	0.34	0.0283	0.044	0.27	0.21	4.7	399	697	0.0077	0.036
	Glass	14.48	2.6	65.03	0.0041	0.64	1.004	3.4	21	0.341	0.0264	0.044	0.27	0.23	4.26	362	632	0.0085	0.036
	Natural	13.6	2.65	65.03	0.0041	0.64	1.004	3.4	21	0.298	0.0287	0.044	0.27	0.25	4	343	593	0.0087	0.035
	Natural	9.6	2.65	65.03	0.0041	0.64	1.004	3.4	21	0.301	0.0426	0.044	0.27	0.35	2.82	242	419	0.0123	0.035
	Natural	6.8	2.65	65.03	0.0041	0.64	1.004	3.4	21	0.277	0.035	0.044	0.27	0.5	2	172	297	0.0174	0.035
	Natural	4.8	2.65	65.03	0.0041	0.64	1.004	3.4	21	0.275	0.0332	0.044	0.27	0.71	1.41	121	209	0.0247	0.035
	Natural	3.4	2.65	65.03	0.0041	0.64	1.004	3.4	21	0.273	0.029	0.044	0.27	1	1	86	148	0.0349	0.035
26	Glass	29.3	2.6	50.32	0.0067	0.656	0.992	3.4	21	0.472	0.0405	0.05	0.23	0.12	8.62	738	1480	0.0055	0.047
	Glass	25.17	2.6	50.32	0.0067	0.656	0.992	3.4	21	0.464	0.0275	0.05	0.23	0.14	7.4	634	1271	0.0064	0.047
	Glass	21.7	2.6	50.32	0.0067	0.656	0.992	3.4	21	0.441	0.0323	0.05	0.23	0.16	6.38	546	1096	0.0074	0.047
	Glass	15.97	2.6	50.32	0.0067	0.656	0.992	3.4	21	0.441	0.0205	0.05	0.23	0.21	4.7	402	807	0.01	0.047
	Glass	14.48	2.6	50.32	0.0067	0.656	0.992	3.4	21	0.438	0.0294	0.05	0.23	0.23	4.26	365	731	0.0111	0.047
	Natural	13.6	2.65	50.32	0.0067	0.656	0.992	3.4	21	0.351	0.0253	0.05	0.23	0.25	4	346	687	0.0114	0.046
	Natural	9.6	2.65	50.32	0.0067	0.656	0.992	3.4	21	0.376	0.0513	0.05	0.23	0.35	2.82	244	485	0.0162	0.046
	Natural	6.8	2.65	50.32	0.0067	0.656	0.992	3.4	21	0.343	0.0398	0.05	0.23	0.5	2	173	343	0.0228	0.046
	Natural	4.8	2.65	50.32	0.0067	0.656	0.992	3.4	21	0.335	0.0266	0.05	0.23	0.71	1.41	122	242	0.0323	0.046
	Natural	3.4	2.65	50.32	0.0067	0.656	0.992	3.4	21	0.326	0.0294	0.05	0.23	1	1	86	172	0.0456	0.046

Table1: The CSU Experiments Database (Cont'd)

Run	Type	d_s (mm)	G	y (mm)	S_f	u_f (m/s)	ν 10^{-6} (m^2/s)	k_s (mm)	n	V_{pobs} (m/s)	σ (m/s)	u_* (m/s)	δ (mm)	k_s/d_s	d_s/k_s	d_*	Re_*	τ_{*ds}	τ_{*ks}
(1)	(2)	(3)	(4)	(5)	(6)	(7)	(8)	(9)	(10)	(11)	(12)	(13)	(14)	(15)	(16)	(17)	(18)	(19)	(20)
27	Steel	19.04	8.02	53.1	0.0084	0.774	0.992	3.4	21	0.175	0.0094	0.055	0.21	0.18	5.6	785	1056	0.0023	0.013
	Steel	15.88	8.02	53.1	0.0084	0.774	0.992	3.4	21	0.156	0.0065	0.055	0.21	0.21	4.67	654	880	0.0028	0.013
	Steel	14.28	8.02	53.1	0.0084	0.774	0.992	3.4	21	0.151	0.0077	0.055	0.21	0.24	4.2	588	792	0.0031	0.013
	Glass	29.3	2.6	53.1	0.0084	0.774	0.992	3.4	21	0.602	0.0328	0.055	0.21	0.12	8.62	738	1625	0.0066	0.057
	Glass	25.17	2.6	53.1	0.0084	0.774	0.992	3.4	21	0.599	0.035	0.055	0.21	0.14	7.4	634	1396	0.0077	0.057
	Glass	21.7	2.6	53.1	0.0084	0.774	0.992	3.4	21	0.593	0.0327	0.055	0.21	0.16	6.38	546	1203	0.0089	0.057
	Glass	15.97	2.6	53.1	0.0084	0.774	0.992	3.4	21	0.577	0.0342	0.055	0.21	0.21	4.7	402	885	0.0121	0.057
	Glass	14.48	2.6	53.1	0.0084	0.774	0.992	3.4	21	0.579	0.0363	0.055	0.21	0.23	4.26	365	803	0.0133	0.057
	Natural	13.6	2.65	53.1	0.0084	0.774	0.992	3.4	21	0.493	0.0307	0.055	0.21	0.25	4	346	754	0.0137	0.055
	Natural	9.6	2.65	53.1	0.0084	0.774	0.992	3.4	21	0.504	0.0534	0.055	0.21	0.35	2.82	244	532	0.0195	0.055
	Natural	6.8	2.65	53.1	0.0084	0.774	0.992	3.4	21	0.498	0.0461	0.055	0.21	0.5	2	173	377	0.0275	0.055
	Natural	4.8	2.65	53.1	0.0084	0.774	0.992	3.4	21	0.433	0.0584	0.055	0.21	0.71	1.41	122	266	0.0389	0.055
	Natural	3.4	2.65	53.1	0.0084	0.774	0.992	3.4	21	0.443	0.0387	0.055	0.21	1	1	86	189	0.055	0.055